NAS CR 72493

MATERIALS FOR ELECTROCHEMICAL CELL SEPARATORS

FINAL REPORT
15 December 1968

Prepared for:

NATIONAL AERONAUTICS and SPACE ADMINISTRATION
LEWIS RESEARCH CENTER

Under Contract NAS 3-8522

...VT LABORATORIES
CLEVELAND, OHIO

NAS CR-72493

Final Report

MATERIALS FOR ELECTROCHEMICAL CELL SEPARATORS

Prepared by

J. W. Vogt

for

National Aeronautics and Space Administration

December 1968

Contract No. NAS 3-8522

Technical Management

NASA - Lewis Research Center
Electrochemistry Branch
Daniel G. Soltis

Materials Technology
TRW Equipment Laboratories
TRW Inc.
23555 Euclid Avenue
Cleveland, Ohio 44117

I FOREWORD

This is the final report on Contract NAS 3-8522 initiated June 16, 1966. A First Summary Report NAS-CR-72148 was issued December 28, 1966, and a Second Summary Report NAS-CR-72267 was issued July 3, 1967.

The purpose of the work was to develop improved matrices for electrochemical cells. Chrysotile paper and millboard were first studied and characterized in terms of properties related to the function of matrix in alkaline electrochemical cells. The study was then extended to other natural fibrous materials, to synthetic inorganics, and finally to synthetic inorganics bonded by organic fibers. The best composites emerging from this study were processed into full size matrices and delivered to NASA for subsequent performance evaluation in electrochemical cells.

This work was carried out in The Materials Technology Laboratory of The TRW Equipment Group. The principal investigator for this program was Dr. J. W. Vogt, and Dr. D. P. Laverty served as the program manager. The bulk of the specific process development work was carried out by R. A. Prosek.

Daniel G. Soltis and Meyer R. Unger of Lewis Research Center were the NASA technical directors.

For internal TRW distribution, this report has been assigned the number ER-7055-4.

II ABSTRACT

A two-year, five-part program has been carried out to determine the properties of Fuel Cell Grade Asbestos and of alternate materials for application in alkaline-electrolyte electrochemical cell separators.

The first part of the program consisted of examining 20-mil thick and 60-mil thick chrysotile asbestos mats produced by Johns Manville especially for fuel cell application. The tests were designed to assess those attributes of the mats particularly pertinent to cell separator application, and they included physical properties, chemical and electrochemical compatibility, electrolyte absorption and retention, bubble pressure, and electrolytic resistance. The chrysotile asbestos mats were excellent in most of these properties. Their main shortcoming was lack of chemical compatibility with the KOH electrolyte at temperatures over 100°C.

The second part of the program studied other types of asbestoses and alternate fibrous inorganic materials in a search for improved cell separators. Of the dozen or so materials studied in this part of the program, none yielded a significant improvement over the chrysotile asbestos mats in overall properties. However, potassium titanate (PKT) and fibrous zirconia were identified as showing marked improvements in chemical compatibility.

The third part of the program was aimed at exploiting the good chemical resistance of PKT, zirconia (both in fiber and powder form), and ceria (available as powder and known to be compatible with KOH) by forming mats of these materials using organic binders. The organic binders examined included Teflon and polypropylene. The most promising separator mats developed in this phase of the program consisted of the base materials (either PKT, ceria powder, or zirconia powder) composited with a small percentage of Teflon powder which was formed into a fibrous network by repeated rolling treatments during the processing of the mat.

The fourth part of the program consisted of preparing and testing full-size (8-inch square) mats of 20, 30, and 60-mil thicknesses made by this fibrilated-Teflon-bonded approach. Three mat compositions (95% PKT + 5% Teflon, 99% ceria + 1% Teflon, and 99% zirconia + 1% Teflon) were examined to determine the best one for use in the last phase of the program.

Since all three mat compositions appeared promising and there was no clear choice of the best one, the final part of the program consisted of producing, for delivery to NASA, 100 each of the three types of mats. A selected number of each thickness

(20, 30, and 60 mils) were included to provide mats of each material for evaluation in the various types of electrochemical cells of possible application.

III. TABLE OF CONTENTS

TABLE OF CONTENTS (Cont'd)

TABLE OF CONTENTS (Cont'd)

IV. LIST OF FIGURES

LIST OF FIGURES (Cont'd)

IV. LIST OF TABLES

LIST OF TABLES (Cont'd)

VI INTRODUCTION

Development of alkaline fuel cells and electrolytic cells has depended to a considerable degree on the use of pure chrysotile paper as the electrolyte matrix and electrode separator. Chrysotile is a natural asbestos, a hydrated magnesium silicate, and with the exception of incidental impurities, it is electrochemically inert in an aqueous alkaline medium. The chrysotile paper is manufactured as a special product by specially refined commercial equipment, and consequently, its physical properties are quite uniform. Most of these properties - dry strength, fibrous structure, porosity, wettability, pore size are eminently appropriate for service as an electrolyte matrix.

Unfortunately, the chrysotile, being a magnesium silicate, reacts with alkali to form a soluble silicate and the gelatinous magnesium hydroxide. At moderate alkali concentrations and low operating temperatures, the chrysotile matrices will survive several thousands of hours in service. But in very concentrated alkali, and at 150 or 200°C, the chrysotile is rapidly degraded, and the service life is drastically shortened.

The purpose of this project is to improve the chrysotile matrices or develop alternative matrices with better service capabilities. Commercially available chrysotile paper was taken as the reference material, and selected physical and chemical properties were measured.

Prospective new materials and material composites were evaluated then by comparison of the selected properties with those of chrysotile. In order, the materials tested were, natural asbestos other than chrysotile, synthetic inorganics, blends of synthetic inorganics with chrysotile, blends of synthetic inorganics with synthetic organic binders, and finally, synthetic inorganics bonded by fibrilated Teflon. Matrices of the latter type were prepared in full matrix size and in quantity for performance testing in electrochemical cells.

VII WORK PLAN OF THE PROJECT

Task 1. Evaluation of Fuel Cell Asbestos Board

Fuel Cell Paper (0.02 inch thick) and Millboard (0.06 inch thick) were procured from Johns Manville and subjected to the following tests:

A. Asbestos Properties
   1. Chemical composition
   2. Fiber structure
   3. Surface area (per unit weight)

B. Dry Mat Properties
   1. Strength
   2. Porosity
   3. Density
   4. Thickness variation
   5. Pore size distribution

C. Wet Mat Properties (wet with 30% KOH)
   1. Electrolyte absorption
   2. Electrolyte retention
   3. Electrolytic resistance
   4. Gas permeability

D. Chemical Degradation in KOH Solutions

E. Electrochemical Reactivity

Task 2. Investigation of Other Asbestos Forms

Other asbestos fibers and selected synthetic inorganics were tested as was the chrysotile. Those materials with satisfactory resistance to chemical attack by KOH solution and satisfactory physical properties were to be incorporated in matrices and tested for matrix properties. Those synthetic inorganics of non-fibrous structure were to be blended with sufficient chrysotile fiber to provide the necessary matrix strength.

The asbestoses to be tested were:

1. Chrysotile
2. Tremolite
3. Anthophylite
4. Amosite
5. Crocidolite

The synthetic inorganics specified for test were:

1. Zirconia paper
2. Hydrated magnesia
3. Potassium titanate
4. Beryllium oxide
5. Zirconium silicate
6. Titanium oxide
7. Boron nitride

Project Extension

The work described above in Tasks 1 and 2 comprised the work to be performed in the original one-year contract. When it became evident that useful matrices could not be prepared from synthetic inorganics alone, the project was extended for a second year's work, as follows, to include the use of organic binders.

Task 2a. Matrices Incorporating Organic Binders

The following materials, alone, and in the specified combinations were tested.

1. Potassium titanate - Teflon emulsion
2. Ceria - Teflon emulsion
3. Potassium titanate - Teflon fiber
4. Zirconia E fiber - Teflon emulsion
5. Zirconia E fiber - Teflon fiber
6. Zirconia powder - Polypropylene fiber
7. Zirconia powder - Teflon fiber
8. Potassium titanate - zirconia E fiber - Teflon fiber.

On the basis of partial testing, the three most promising matrices were to be selected for complete property tests.

Task 3. Preparation and Evaluation of Full-Sized Matrices

The three best compositions were to be selected, and 8-inch square matrices were to be made in accordance with the following schedule. Six matrices of each composition were to be made in each of the thicknesses.

0.020 ± 0.002 inch
0.030 ± 0.003 inch
0.060 ± 0.004 inch

From the 9 composition-thickness groups, three matrices of each type were selected for testing. The full-size matrices were tested for density, electrolyte absorption, and gas permeability (or bubble pressure). On the basis of these properties tests, the best matrix composition was to be selected for Task 4.

Task 4. Matrix Fabrication

Two hundred matrices in 8-inch square size were to be made of the best matrix composition as follows:

a. 100 matrices of 0.03 inch thickness
b. 50 matrices of 0.02 inch thickness
c. 50 matrices of 0.06 inch thickness

When the property tests of Task 3 demonstrated that three matrix compositions were reasonably similar, the provisions of Task 4 were modified to specify the manufacture of matrices as follows:

Compositions
a) Potassium titanate (PKT) 95% - Teflon 5%
b) Ceria 99% - Teflon 1%
c) Zirconia 99% - Teflon 1%

One hundred matrices of each composition in 8-inch square size.

a) 25 matrices 0.020 inch thick ± 0.002 inch
b) 25 matrices 0.030 inch thick ± 0.003 inch
c) 50 matrices 0.060 inch thick ± 0.004 inch

The matrix weights, according to the original specifications, were to deviate no more than ± 2.5% from the average of the compositions - thickness group. This was subsequently changed to prohibit deviations of matrix density greater than ± 5% of the average for the composition thickness group.

The finished matrices were also to be free of visually detectable surface defects and pinholes. These finished mats were to be delivered to NASA-Lewis for subsequent evaluation including actual operation in electrochemical cells.

VIII TASK 1 PROPERTIES OF FUEL CELL ASBESTOS

A. Procurement and Preparation of Specimens

The chrysotile sheet stock to be tested was selected from the warehouse stocks on hand at the Johns Manville Tilton plant. One 25-sheet lot was cut from the leading end of a roll of 20-mil paper; another similar lot, from the trailing end. One 25-sheet lot of 60-mil millboard was cut from the start of a production run; another lot from the end of the same run. These four lots were given special care in handling and were specially packaged to prevent damage during shipping.

Upon receipt at TRW, the four lots were identified numerically as follows:

1000 series - 60 mil millboard-start of run
2000 series - 60 mil millboard-end of run
3000 series - 20 mil paper - start of run
4000 series - 20 mil paper - end of run

From each of the lots, 5 sheets were selected at random and identified numerically, for example, 1100, 1200, 1300, 1400, 1500. Each sheet was then cut into sections and identified for testing (1101, 1102, etc.). In each case, a one-inch margin was trimmed from each edge of the sheet in order to remove material that may have suffered physical damage. These trimmed edges were then used for some of the tests of properties that are independent of fiber packing.

B. Tests and Results

1. Asbestos Properties

a. Chemical analysis. - Two oven-dried chrysotile specimens were analyzed by standard wet methods. The specimens were digested for several hours with hydrochloric acid and filtered. The residue was ignited, weighed, and heated with HF to volatilize the silica. After weighing, the non-volatile residue was dissolved in HCl and added to the filtrate containing the acid solubles. The iron group ions were double-precipitated with NH_4 OH-NH_4 Cl and ignited. From the filtrate, calcium was precipitated as oxalate and ignited, and magnesium was precipitated as the ammonium phosphate and ignited. No attempt was made to resolve the R_2O_3 group into the usual constituents Fe, Al, etc.

Following are the results of this analysis:

	Specimen No. 1	Specimen No. 2
SiO_2	41.86%	42.14%
MgO	42.78	42.80
CaO	2.19	1.70
Fe_2O_3	0.85	0.87

The remainder (about 12%) is water which can be driven off by high temperature treatment.

b. Photographic and electronmicrographic examination. A piece of black vinyl "Electricians" tape was pressed lightly against the surface of a piece of the 60-mil millboard, and the fibers adhering to the surface were photographed at 10X (Figure 1). There are visible many very fine fiber bundles, several evident stalks of unresolved fibers, and several wads of very fine fibers.

The electron micrographic specimen was prepared by impressing the plastic replica material against an asbestos sheet. Fibers of the asbestos were retained by the plastic. The replica sheet was shadowed with chromium on carbon at about 20° angle. The photographs (Figure 2) made at 20,000X reveal that fibers of 0.01 mil diameter are bundles of many smaller fibers. These photographs do not permit an estimate of ultimate fiber diameter, but they do suggest the enormous porosity potential of the natural material.

c. Surface area. - These measurements were made with the Perkin Elmer Sorptometer, Model 212B. The instrument was standardized against materials obtained from American Instrument Co. and standardized by the Bone Char Research Project, Inc. (originated by The National Bureau of Standards). Following are the average surface areas reported by the Bone Char Project and the values obtained by TRW Inc.

	Bone Char Project	TRW
Reference Absorbent No. 2	10.3 m^2/gm	10.38 m^2/gm
Reference Absorbent No. 6	69.2	75.6
Reference Absorbent No. 8	560	515

The TRW values compare favorably with the span of values upon which the Bone Char Project averages are based.

One specimen of each of the asbestos stocks yielded the following values:

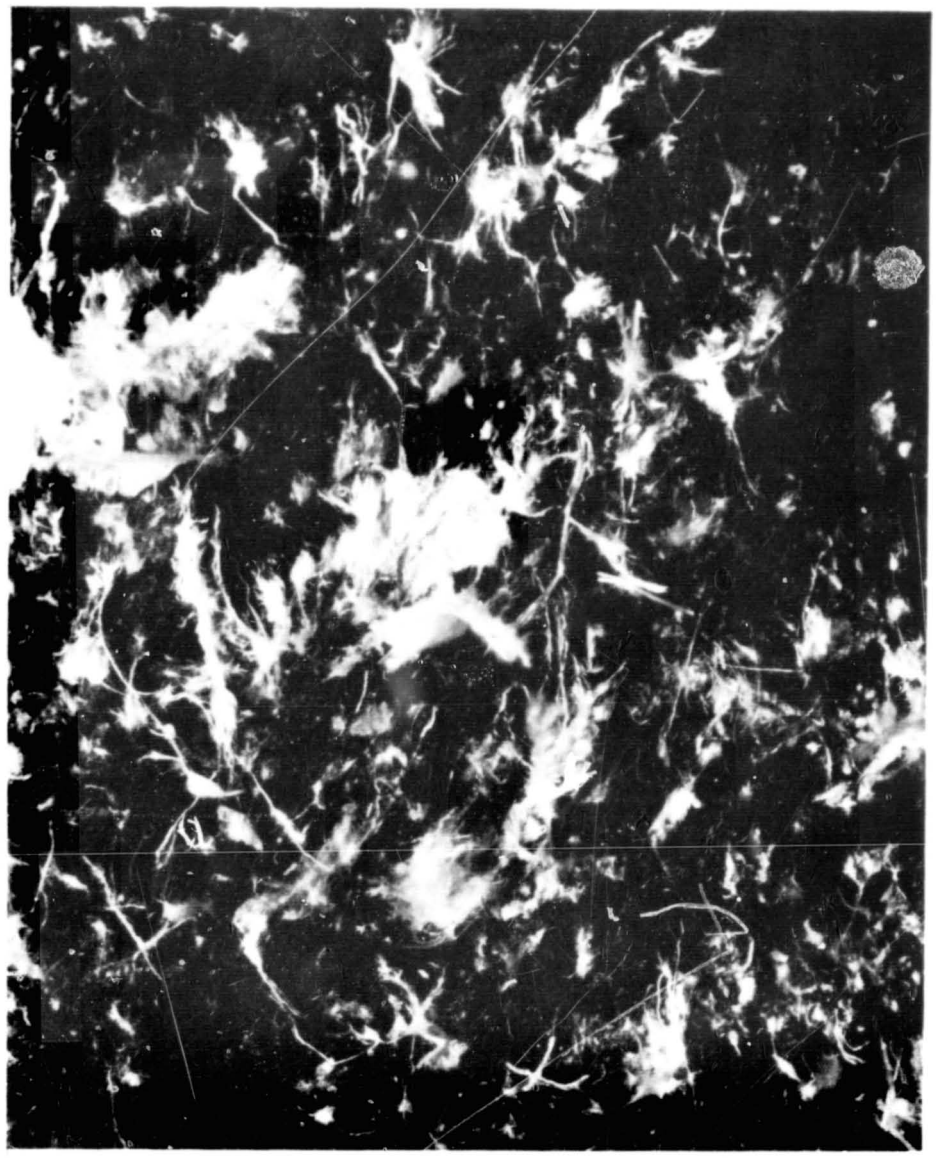

Figure 1. Chrysotile Asbestos Fibers: 10X

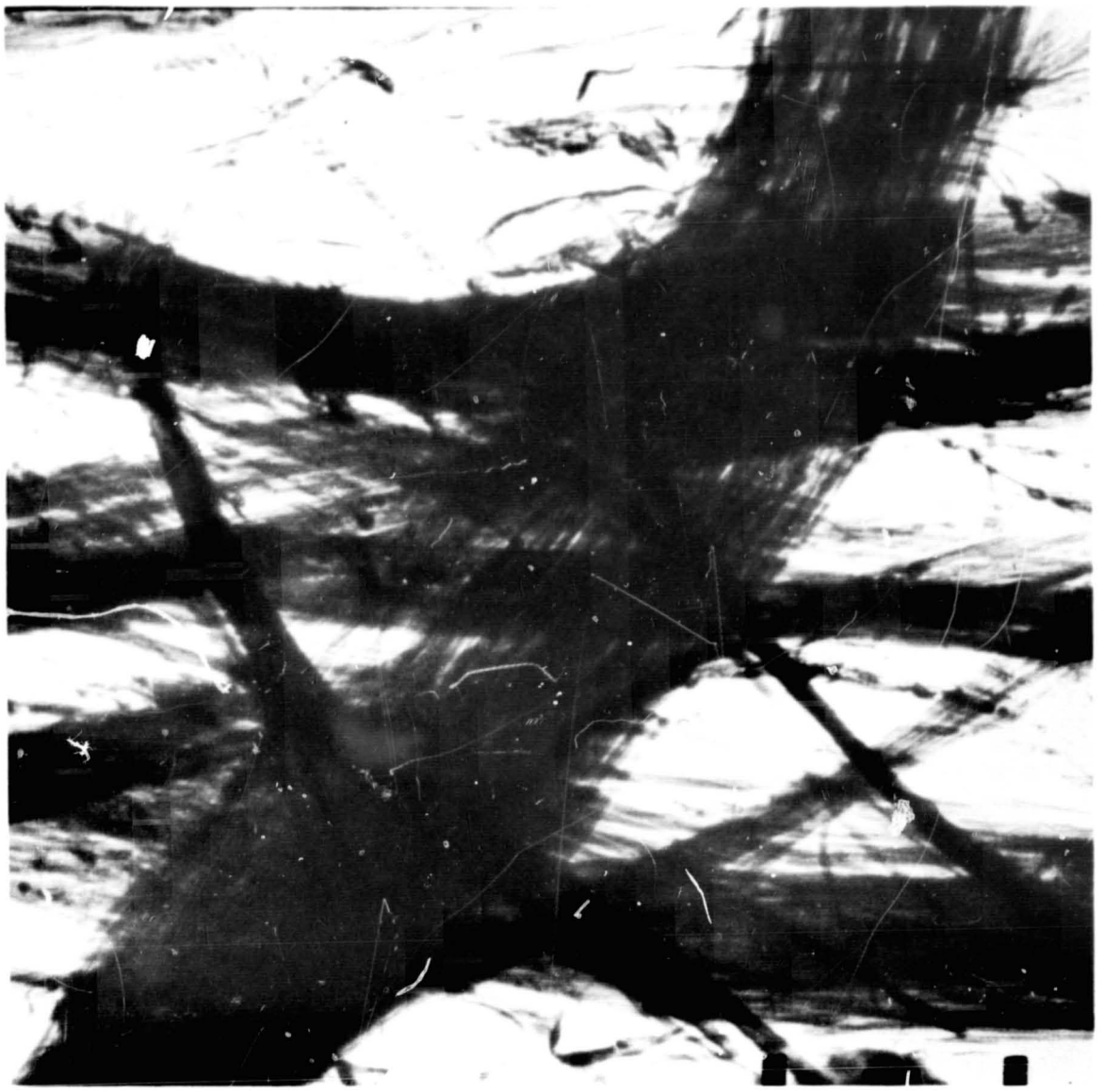

Figure 2. Electronmicrograph of Chrysotile Fibers; 20,000X

Specimen Number	Surface Area
1200	50.7 m^2/gm
2400	48.5
3100	55.5
4100	48.3

These values are in very close agreement, and they indicate that the property is not significantly dependent on the variables in the processes of converting suspended chrysotile pulp into paper and millboard.

2. Dry Mat Properties

a. Tensile tests. - Tensile tests were performed on an Instron Tensile Tester. The specimens were die-cut rectangles (2 x 3 inches) mounted to provide a gage length of 1 inch. Cross-head speed was 0.50 inch per minute.

In one set of tests, one specimen was taken from each of twenty test sheets. There were five sheets each of the material designated as 1000, 2000, 3000, and 4000 series. The tensile specimen were cut at random angles with respect to the processing direction of the material. The results are summarized in Table I and the load-elongation curves are presented, superimposed, in Figures 3, 4, 5, and 6. For the 20-mil paper, the values of load at failure and the curve shapes are reasonably similar. For the 60-mil millboard, however, the values of load-at-failure differ widely, and the elongation curves reveal different modes of failure. Some specimens failed after moderate extension while others stretched much more before failure. These tests did not reveal a clear relationship between mode of failure and angle of loading relative to processing direction.

A second set of tests was conducted to clarify the influence of direction of loading on the shape of the elongation curves. Two presumably similar sheets of the same stock (2000 series) were cut into specimens. One sheet (2701) furnished nine specimens, all with the loading direction parallel to the processing direction. The other sheet furnished six specimens parallel (2702A) and four specimens transverse (2702B) to the processing direction. The elongation curves for these tests are presented in superimposed groups in Figures 7, 8, and 9.

The curves reveal that loading in the transverse direction causes about 0.07 inch extension before abrupt failure. Loading in the parallel direction causes about 0.15 inch extension at a much lower stress level. This probably reflects a preferential orientation of the asbestos fibers parallel to the processing direction. Parallel loading apparently involves considerable slippage between the parallel oriented fibers. In transverse loading, less slippage of the fibers occurs. It is interesting

Table 1

Tensile Tests of Fuel Cell Asbestos

Specimen No.	Loading Angle	Load (lbs.)*
1100	45°	21.675
1200	0	18.975
1300	30	19.675
1400	50	16.575
1500	20	19.80
2100	60°	10.05
2200	30	9.475
2300	45	16.95
2400	90	10.75
2500	0	10.75
3100	0	6.625
3200	0	6.325
3300	45	6.650
3400	45	7.25
3500	90	8.90
4100	0	6.05
4200	45	6.725
4300	45	7.35
4400	90	6.95
4500	0	6.175

* This is maximum load for specimens with a cross-sectional area of 2 inches times the thickness of the asbestos mat (0.055" for the 1000 and 2000 series specimens and 0.020" for the 3000 and 4000 series).

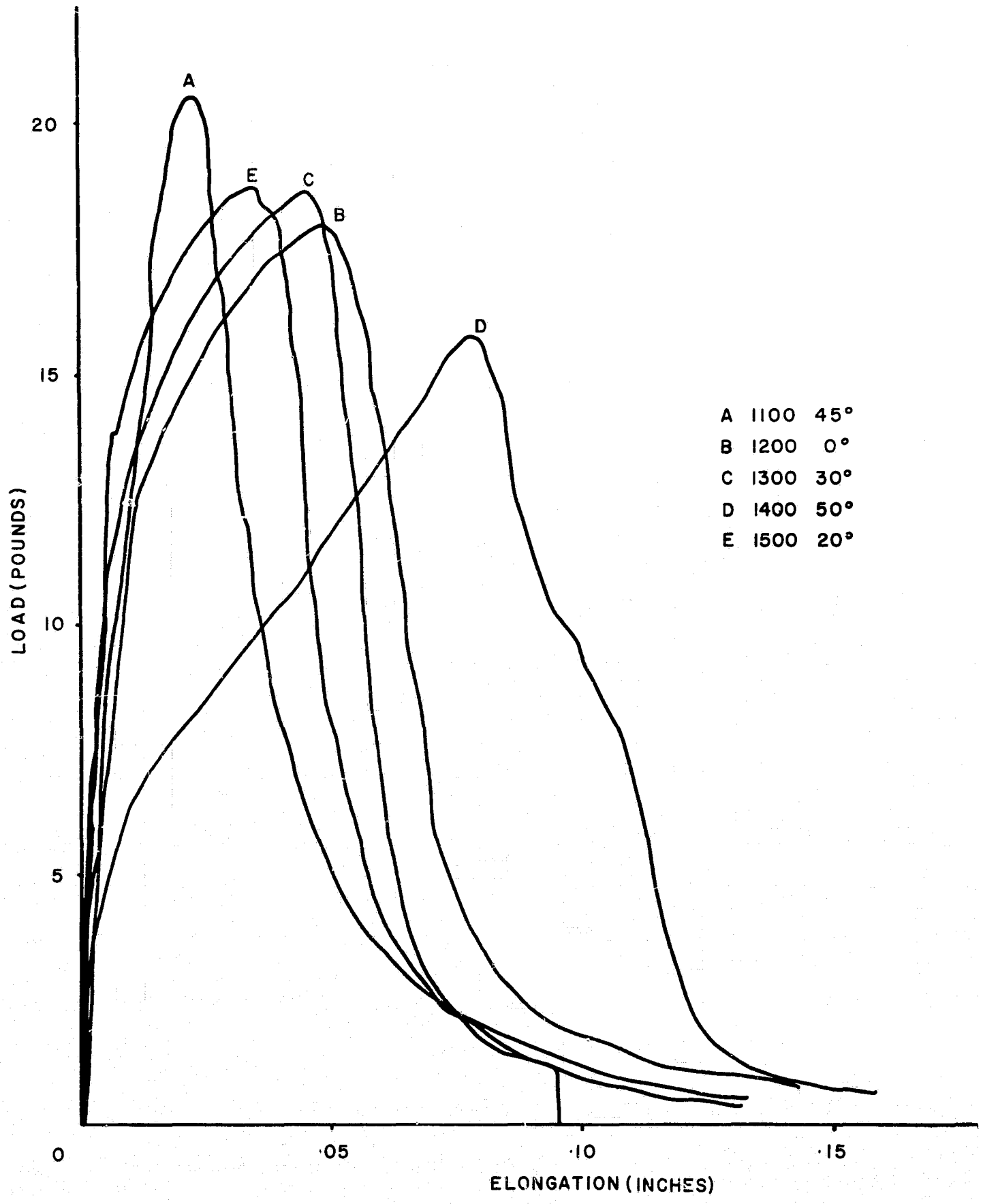

Figure 3. Tensile-Elongation Curves for 60 Mil Fuel Cell Asbestos Board (1000 series)

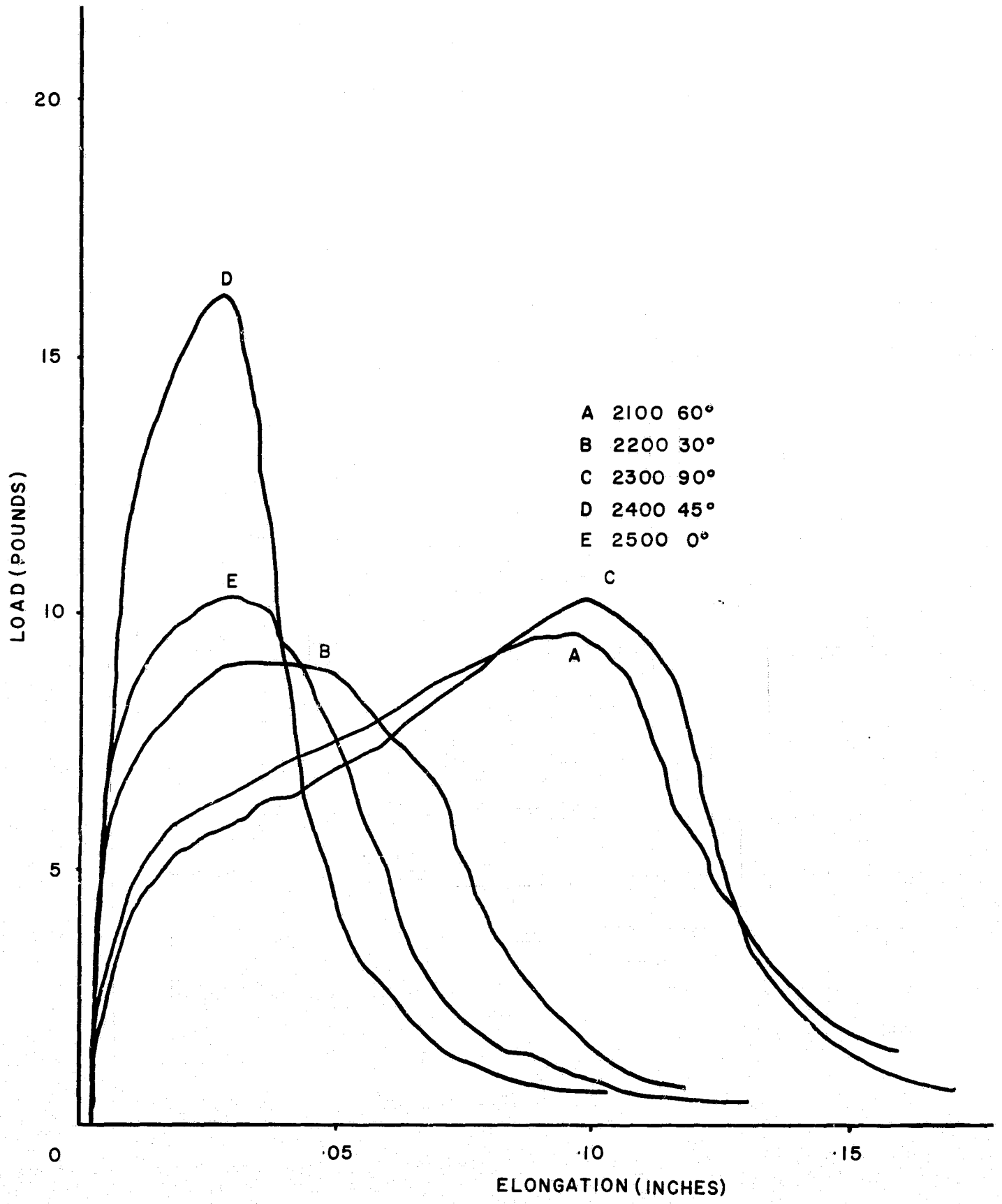

Figure 4. Tensile-Elongation Curves for 60 Mil Fuel Cell Asbestos Board (2000 series)

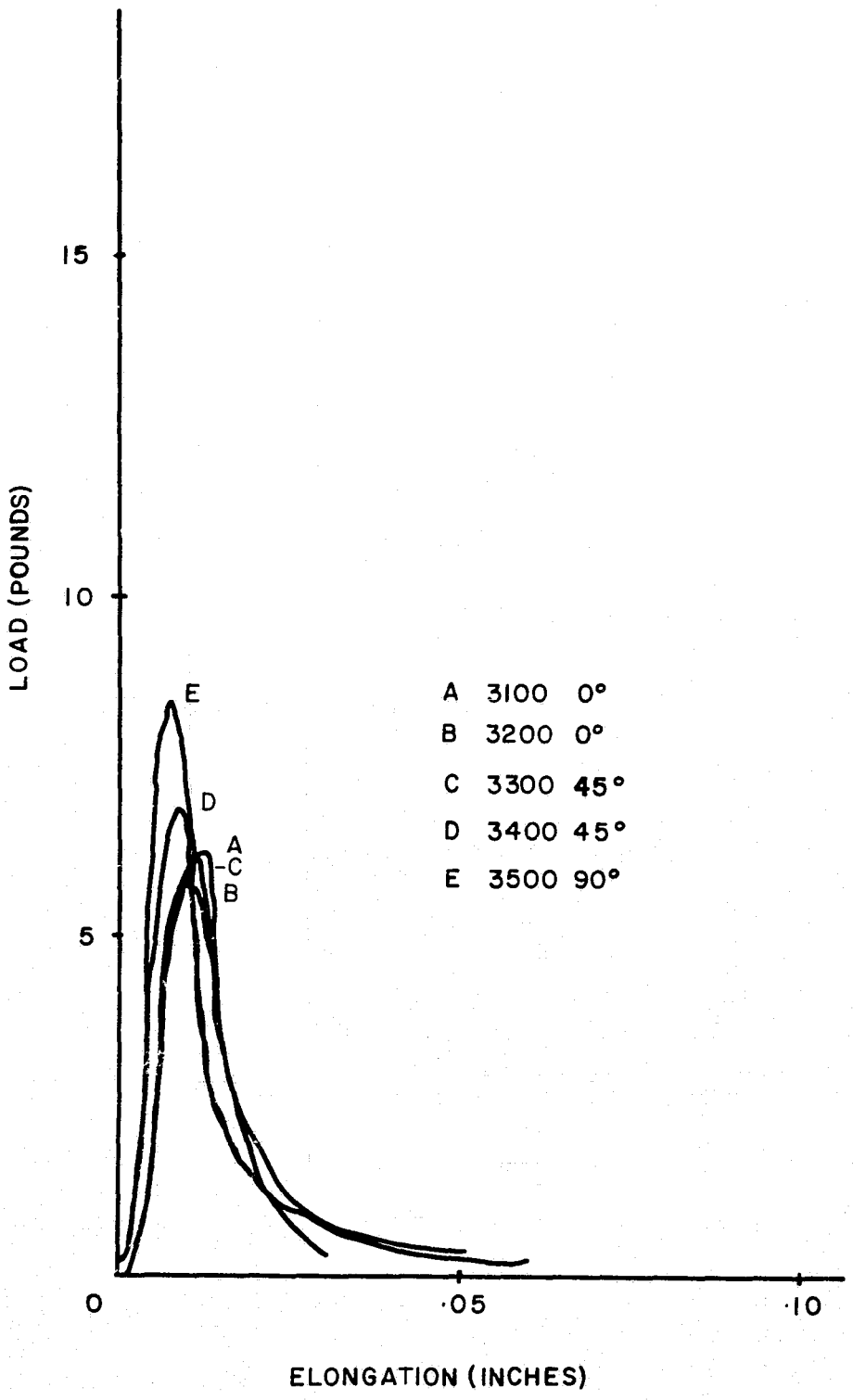

Figure 5. Tensile-Elongation Curves for 20 Mil Fuel Cell Asbestos Paper (3000 series)

4303A

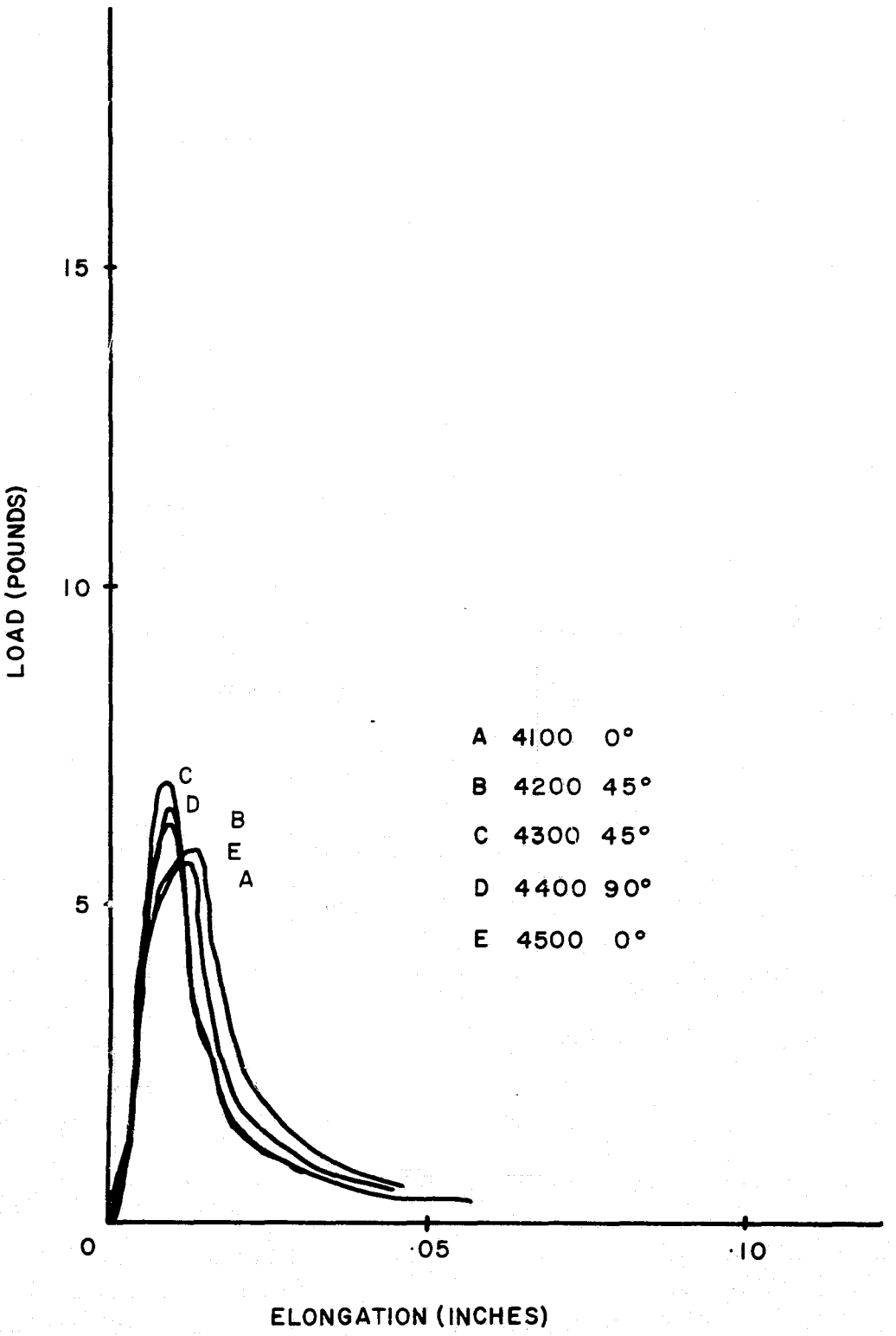

Figure 6. Tensile-Elongation Curves for 20 Mil Fuel Cell Asbestos Paper (4000 series)

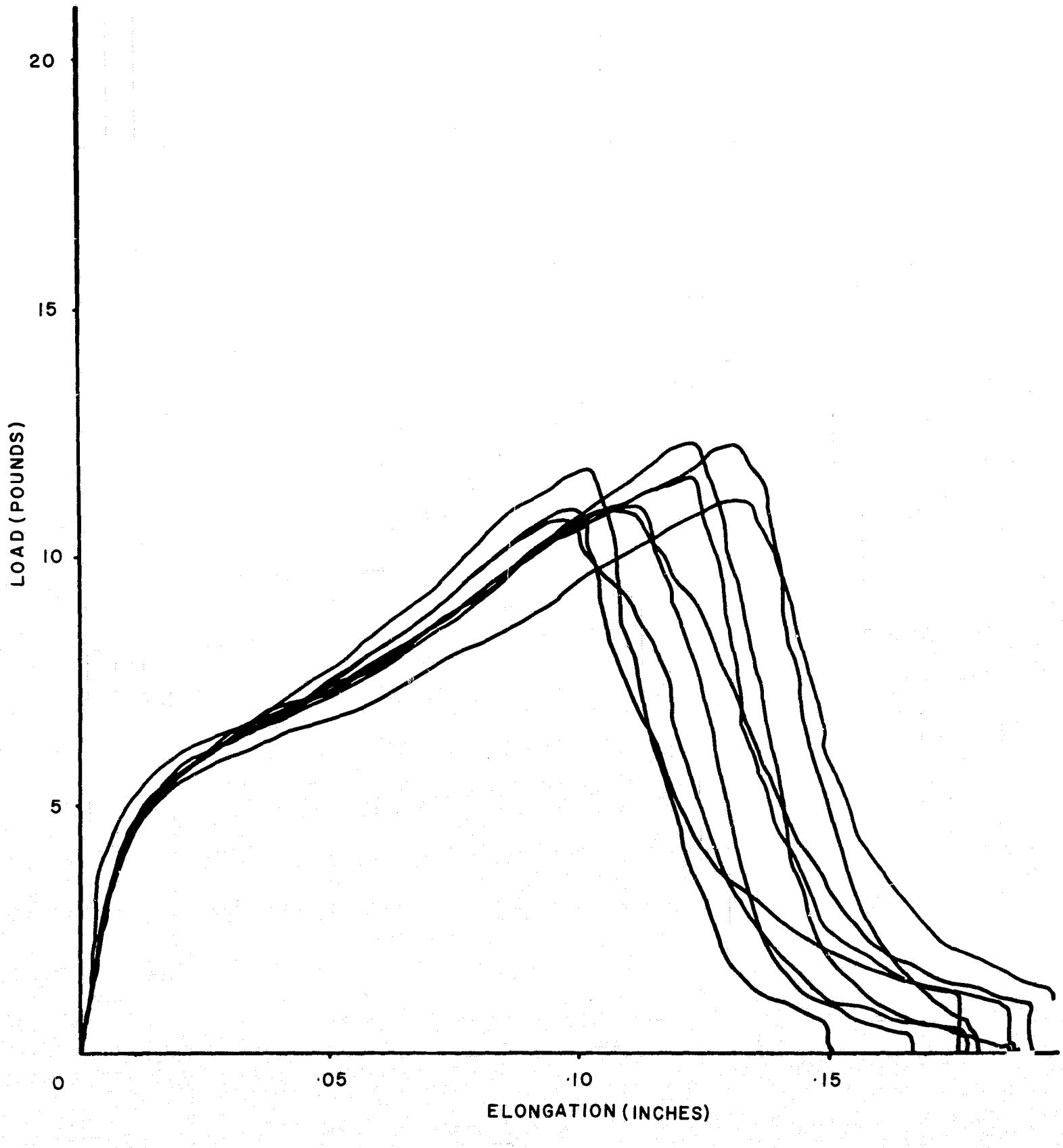

Figure 7. Tensile-Elongation Curves for 60 Mil Fuel Cell Asbestos Board (no. 2701) Stress Applied Parallel to Processing Direction.

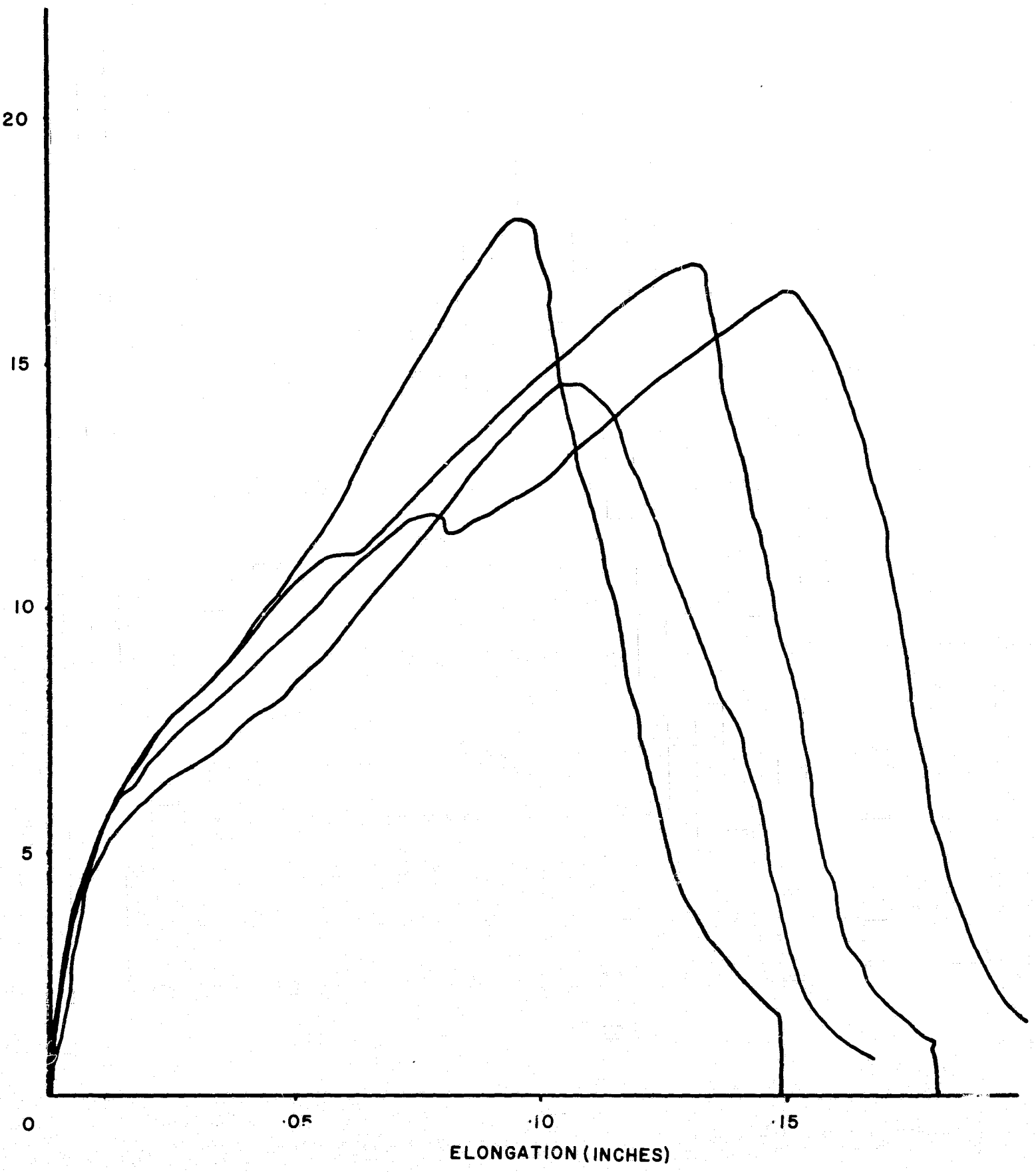

Figure 8. Tensile-Elongation Curves for 60 Mil Fuel Cell Asbestos Board (no. 2702) Stress Applied Parallel to Processing Direction.

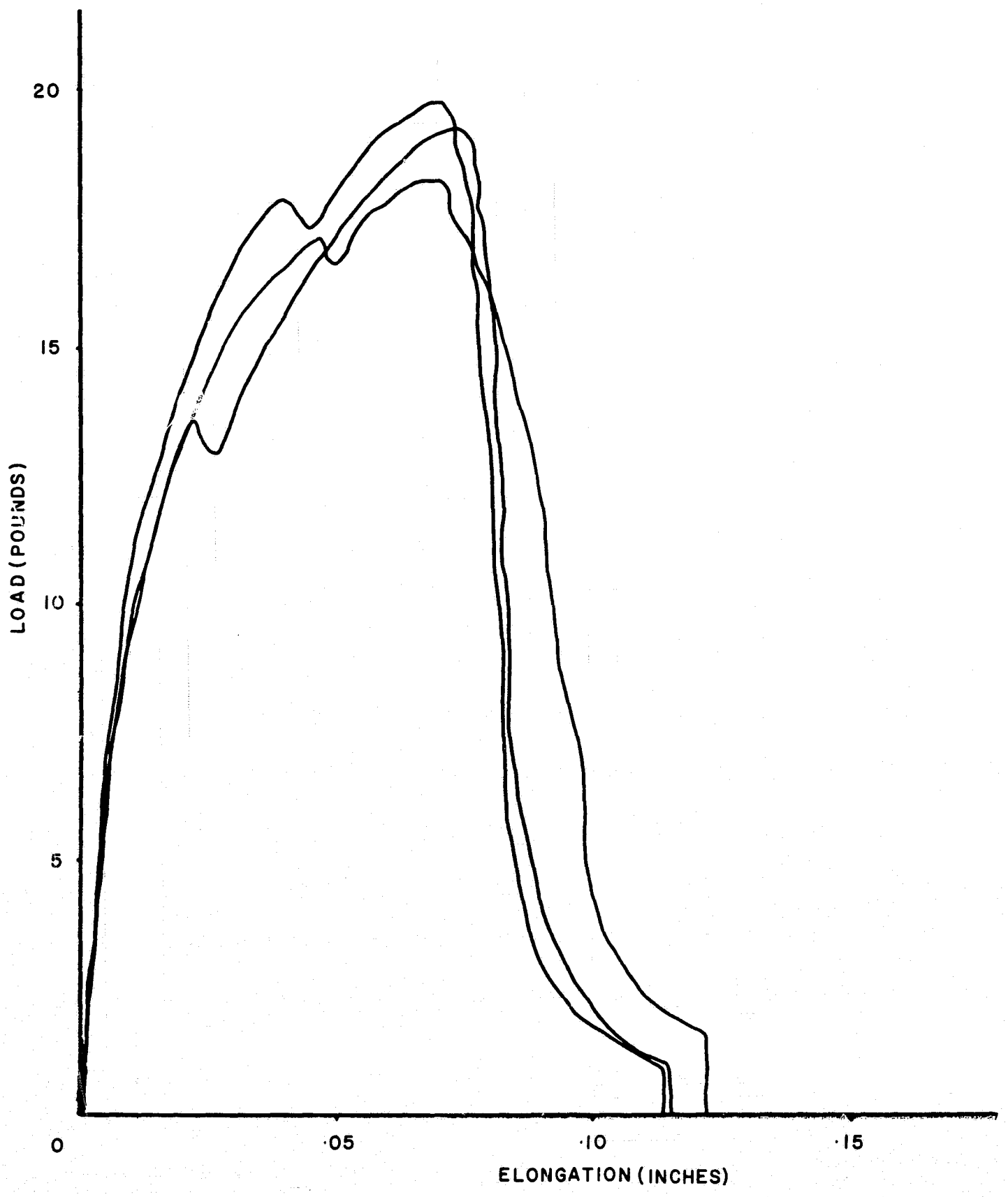

Figure 9. Tensile-Elongation Curves for 60 Mil Fuel Cell Asbestos Board (no. 2702) Stress Applied Transverse to Processing Direction.

that in tearing of the 20-mil paper, which is roll-compressed, there is not a similar dependence of failure mode on angle of loading.

b. Density and porosity. - True volume of the specimens was measured with the Beckmann Air-Comparison Pycnometer. The technique employed by this instrument intrudes air into all the open porosity of the specimen and, thereby, determines the density of the asbestos fibers. The instrument was standardized against the two steel balls furnished by the manufacturer, and the zero error was determined immediately prior to measurement of each specimen.

One large specimen of each sample lot of asbestos was measured, and the data are recorded below.

Specimen	Weight, gm	Volume (Corrected), cc	Density g/cc	
1000	25.2270	9.26	2.724	
2000	20.4995	7.55	2.715	2.732
3000	15.0466	5.51	2.731	Average
4000	14.6849	5.32	2.760	

Thus, the asbestos used to make the millboard (1000 and 2000 series) appear to be slightly less dense than that used in the paper (3000 and 4000 series).

For estimation of the percentages of theoretical density of the dry sheet material, several sheets of each specimen series were weighed, and the densities were calculated from the geometric volume. The data tabulated below reveal that the paper is slightly more dense than the millboard, probably as a result of the rolling operation experienced by the paper in its manufacture.

	60-mil millboard		20-mil paper	
	Specimen Series			
	1000	2000	3000	4000
Average sheet thickness (in.)	0.0550	0.0480	0.0205	0.0196
Number of sheets weighed	3	3	5	5
Total weight (g)	214.0	181.3	145.8	141.1
Geometric volume (cm^3)	253	221	157.2	150.4
Density (g/cm^3)	0.847	0.820	0.928	0.939
Density (air pyc.) g/cm^3	2.724	2.715	2.731	2.760
% Density	31.1	30.2	34.0	34.1

These data show that the 20-mil paper is about 66% porous in the dry mat state whereas the 60-mil material is about 70% porous. In the electrolyte-saturated state, however, the mats expand considerably, so the porosity of the asbestos mats in the cell environment will be considerably higher than that measured in the dry state.

c. Gas permeability. - Permeability of the dry specimens was measured as an incidental part of testing the wet specimens for gas permeability. This test, and the apparatus, is described in more detail later.

Generally, air flow through the dry specimen, as indicated by a bubbler, began when the pressure gradient was less than 1 inch of water. In several instances, the flow rate was measured at increasing pressures until the bubbler became unreliable as a rate indicator. These data are plotted in Figure 10.

The porosity of the specimen can be described satisfactorily, within the effective range of use of the bubbler in terms of the slope of the rate-versus-pressure curve. The slopes of these curves for the dry specimens are given in Table 2.

Note that where measurements were made over a small pressure range on specimens 2100 and 2500, the calculated flow range/pressure ratios were fairly constant. On the contrary, the ratios for the 4200, 4300, and 4400 series increase markedly with slight increase in pressure. Thus, the millboard gas permeability can be described by a single ratio value at low pressure, whereas the ratio for the 20-mil paper cannot.

d. Thickness variation. - Measurements of thickness were made with a Federal Dial gage instrument, equipped with a 0.5inch diameter foot and deadweighted for a pressure of 5 lbs./ sq. inch. This pressure seemed adequate to prevent arching of the specimen. In making a measurement, the gage foot was lowered gently to the specimen surface to prevent crushing the mat by impact. Each specimen piece was measured at four different locations chosen at random. The results are presented graphically in Figure 11.

It is evident that the paper is more uniform than the millboard. This probably reflects the fact that the paper is compressed whereas the millboard is not. Also, the actual thickness of the paper is quite near the nominal value, while the millboard, which is nominally 1/16" thick (or 0.0626 inch), is actually about 0.055 inch.

One may reasonably assume that the data for the paper are representative, but no such interpretation may be accepted for

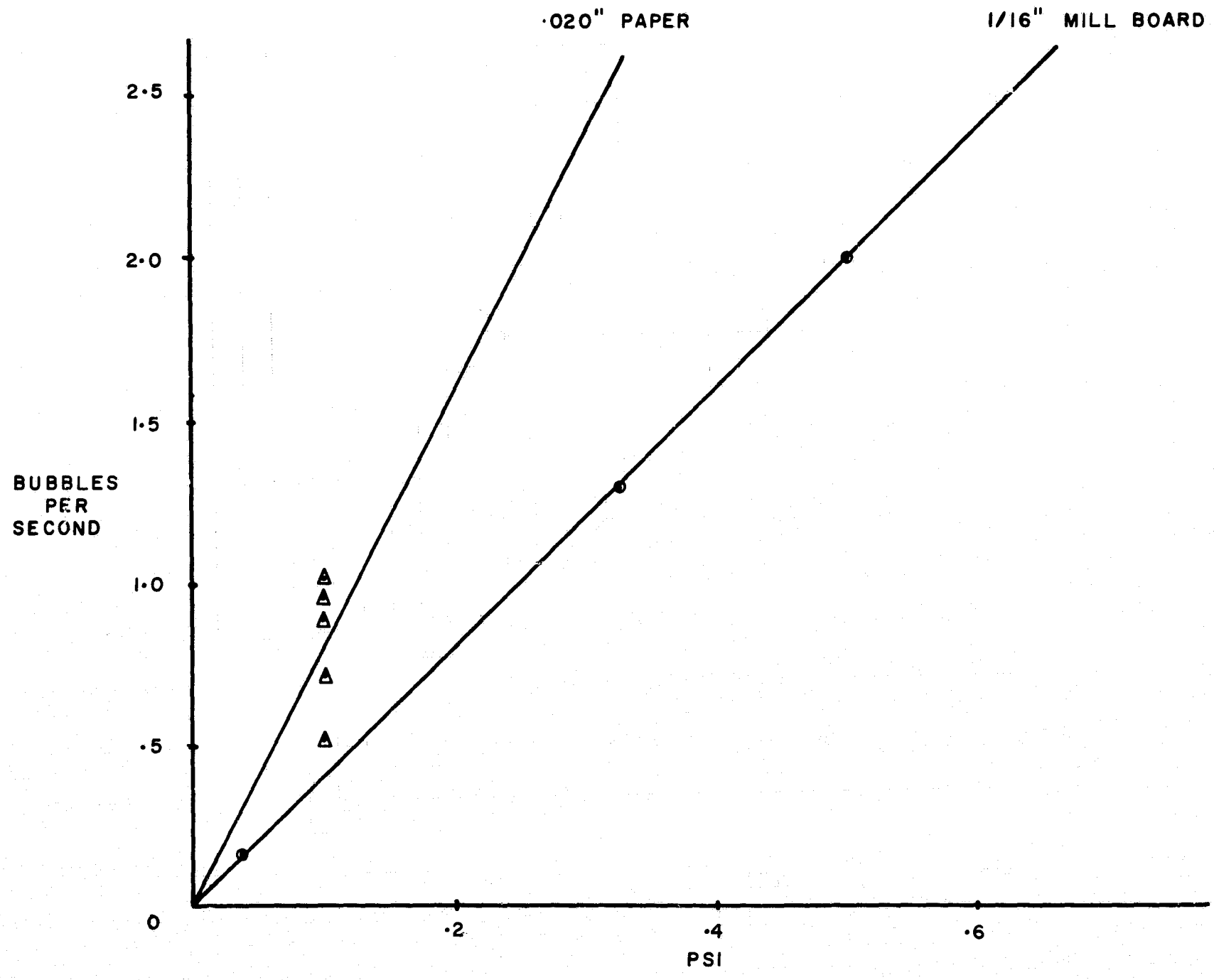

Figure 10. Relationship of Air Permeation Rate and Pressure Differential Across 20 Mil and 60 Mil Dry Fuel Cell Asbestos Mat.

Table 2

Gas Permeability of Dry Fuel Cell Asbestos

Specimen No.	Net Pressure (psi)	Flow Rate* (Bubbles/Second)	Ratio Flow Rate / psi
1200a	.040	.053	1.32
1200b	.140	.333	2.36
1300	.068	.100	1.47
1400	.061	.043	.71
1500	3.577	.714	.20
2100a	.036	.167	4.64
	.324	1.250	3.86
	.504	2.000	3.97
2100b	3.528	1.111	.31
2500	.032	.040	1.25
	.140	.625	4.46
	.324	1.250	3.86
	.504	2.000	3.97
3400	.047	.500	10.63
4200a	.036	.167	4.64
4200b	.036	.200	5.56
	.144	2.000	13.90
4300	.032	.909	28.41
	.036	1.428	39.65
	.054	3.333	61.72
4400a	.050	.312	6.24
	.144	1.667	11.58
4400b	.032	.007	.22
	.144	2.000	13.90
4500	.032	.167	5.22

* This is an arbitrary relative flow rate through a 1-1/4 inch diameter circular area of the mat.

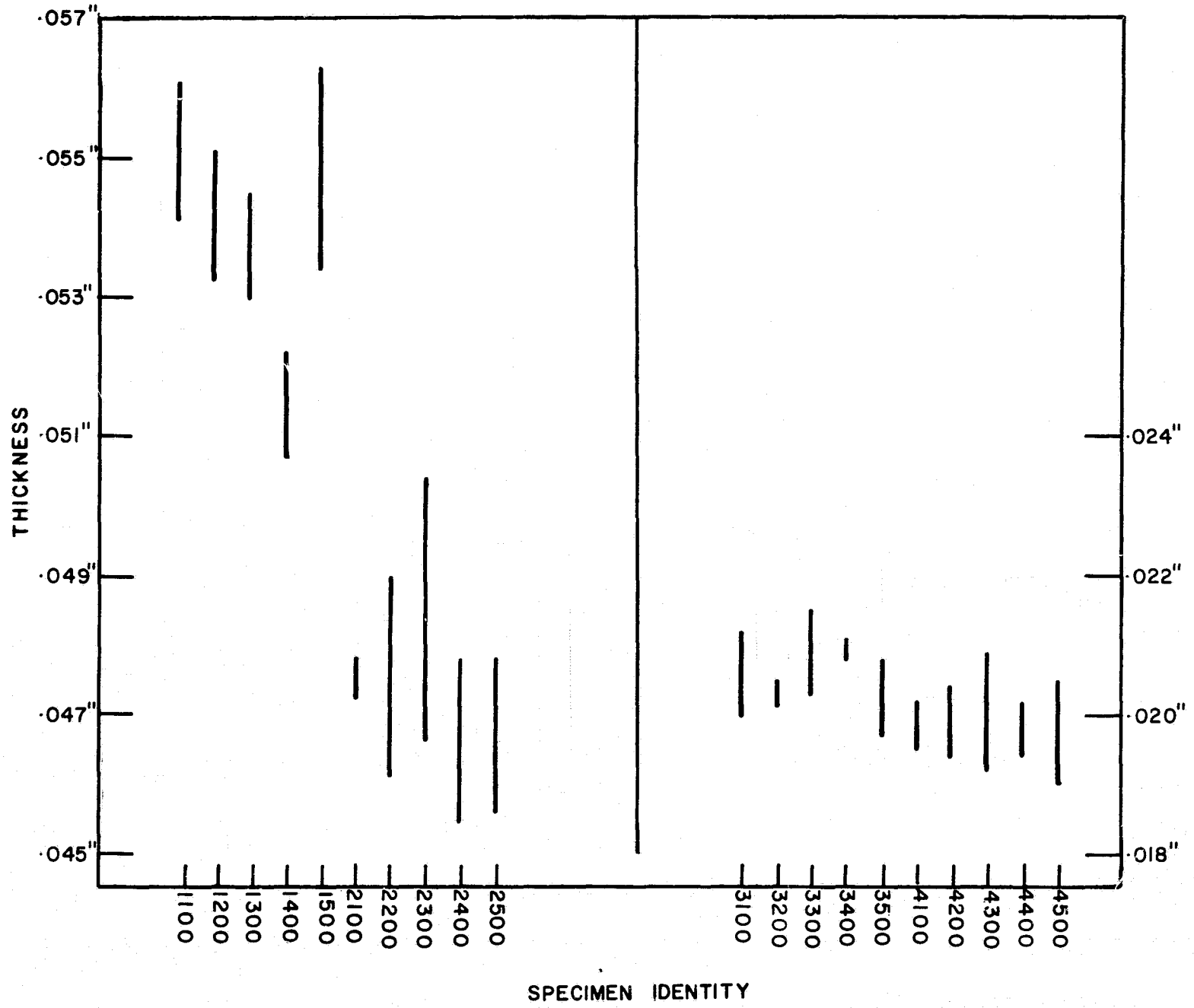

Figure 11. Thickness Distribution of 60 Mil Fuel Cell Asbestos Board and 20 Mil Paper.

the millboard. The millboard thickness depends mainly on the quantity of fiber accumulated on the drum surface for each sheet. These observations may justify the postulation that the measured thickness of asbestos is not pertinent to fuel cell application, but rather the weight per unit area may be a preferable index of the quantity of fiber being provided between the electrodes.

3. Mat Properties - Wet with KOH

a. Electrolytic absorption and retention. - This test calls for a measurement of the ratio by weight of 40% KOH solution required to saturate the chrysotile specimen. The saturated specimen is then subjected to an acceleration of 25g for 2 minutes, and the loss of KOH solution is determined. We learned immediately that the saturated chrysotile paper or millboard is much too fragile to survive the manipulations specified by Cooper and Fleischer*. They recommend that the oversaturated specimen be carefully drawn across the clean surface of a glass plate until it ceases leaving a trail of droplets of solution. However, the saturated chrysotile has not sufficient coherence and too much adherence to the plate, and it invariably tears.

In the procedure we adopted, the dry specimen is placed on a rectangle of nichrome screen slightly longer and wider than the specimen. Both are than weighed in a previously weighed plastic cup, to the cover of which is fastened a folded disk of filter paper. The specimen, on the screen, is then placed in a shallow puddle of KOH solution and permitted to become saturated by upward capillarity. We hope, by this procedure, to prevent entrapment of air pockets within the specimen. When the upper surface appears saturated, several drops of additional KOH solution are placed on the specimen, and after the surface excess is absorbed, the specimen (still on the wire screen) is placed on a sheet of dry filter paper and moved repeatedly to a new dry location until the free excess of electrolyte has been transferred. With careful handling, the filter paper touches only the lower surface of the supporting screen, and therefore presumably absorbs only the free liquid.

The saturated specimen, with its support screen, is weighed again inside the covered plastic cup (Figure 12). It is then subjected to acceleration of 25g for two minutes and returned to the weighing cup. A piece of the weighted filter paper is used to swab out the specimen holder and recover any KOH solution adhering to the specimen chamber walls; this piece of filter paper is placed in the cup and weighed with the specimen. From the several weighings, we derive the weight of the dry specimen, the saturated specimen, and the liquid retained during the centrifuge treatment.

A low speed centrifuge was built from a motor, speed reducer, and standard Unistrut channel and brackets. Based on the nominal speed of the motor reducer unit, the beam, specimen support bracket, and counter weights were mounted. Then the rotary speed was measured at 358 rpm. The specimen bracket was then adjusted to place the specimen at the proper distance (71.42 cm) from center. The centrifuge, without its protective shield, is shown in Figure 13.

*J.L. Cooper and A. Fleischer, editors, Characteristics of Separators for Alkaline Silver Oxide Zinc Secondary Batteries, Air Force Aero Propulsion Laboratory, 1964, ASTA N64-30013.

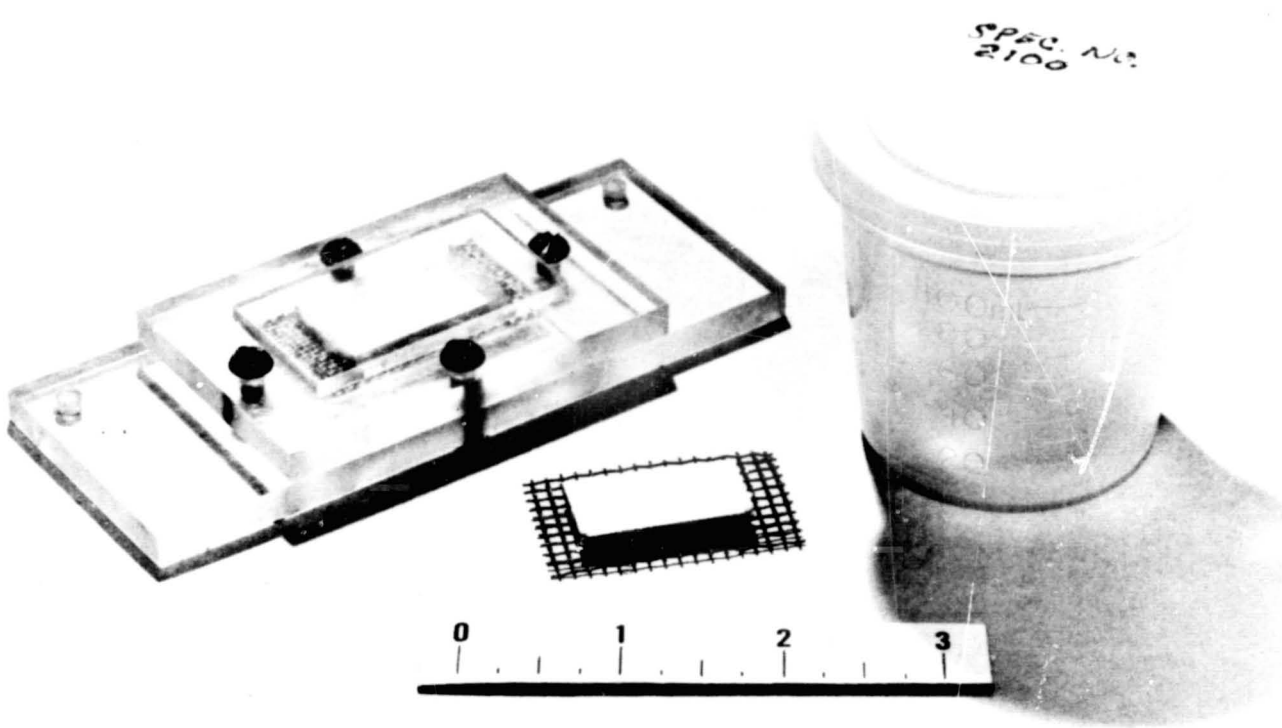

Figure 12. Specimen and Holder for Electrolyte Absorption and Retention Tests.

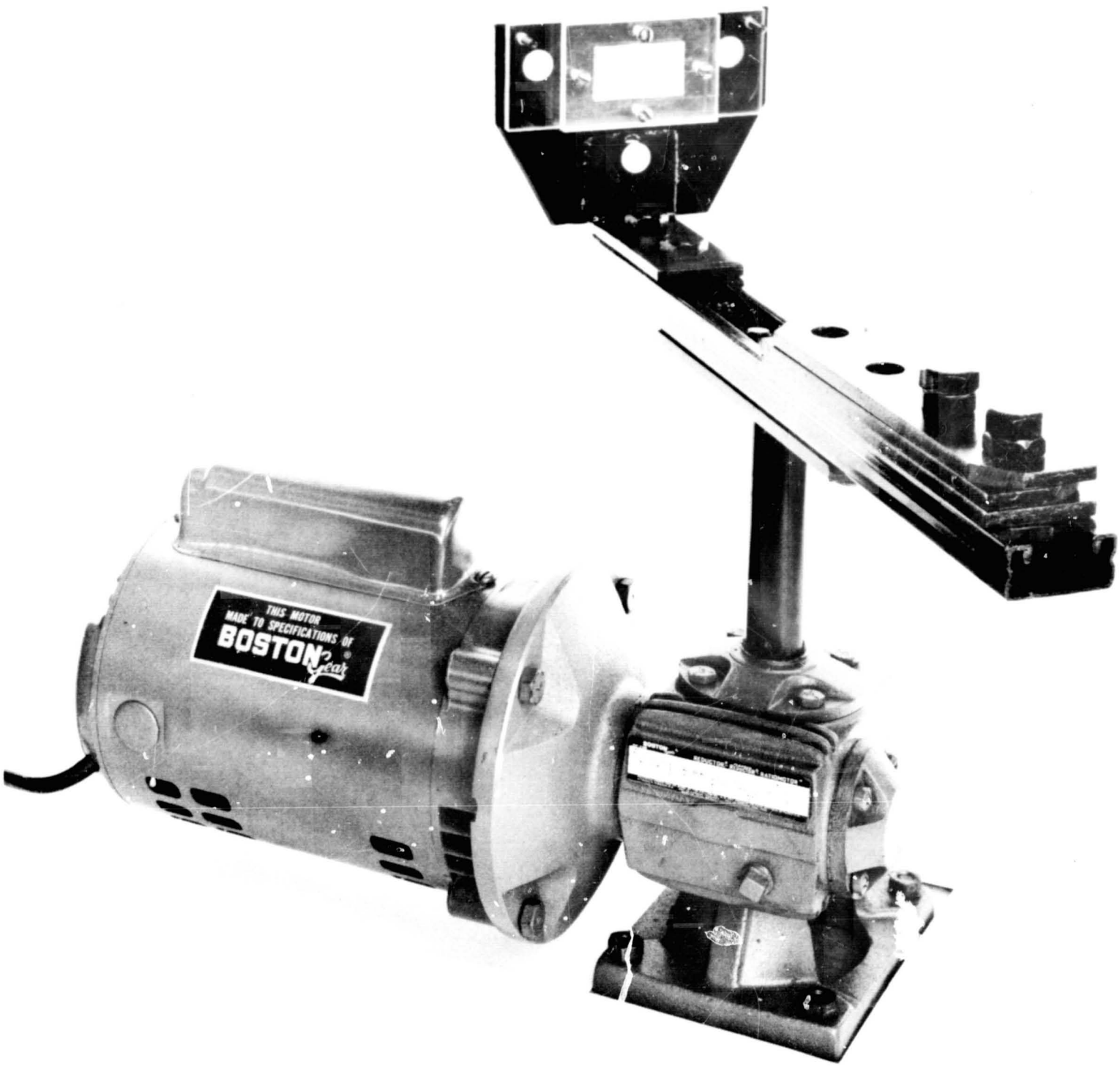

Figure 13. Centrifuge for Electrolyte Retention Test.

4306A

The data from these tests is summarized in Table 3. Despite the fact that specimens from each series were picked at random, the data are reasonably coherent. The ratio of electrolyte required to saturate the 60-mil millboard is significantly greater than that required for the 20-mil paper. However, the saturated millboard consistently loses a small amount of the electrolyte under 25g acceleration, where the loss by the paper is practically zero.

Perhaps the most interesting aspect of these results is that the millboard absorbs about 5.7 times its weight; the paper, only 3.8 times its weight. This difference is probably attributable to the fact that the paper is compressed by rolling whereas the millboard is not. The millboard swells freely upon absorption of the KOH solution whereas the paper is apparently restrained by the closer interlocking of fibers induced by pressure rolling.

b. Liquid permeability. - This test procedure was based on the description by Cooper and Fleischer with several modifications. The test consists in measuring the rate of water flow through a known face area of the specimen under a known pressure differential. The specimen is mounted against a supporting screen, and a circular area (1/2 inch diameter) is exposed to the water. From the chamber behind the specimen, a glass tube extends vertically about 4 feet. Near its top are two reference marks 10 cm apart and containing 1.120 ml of water between them. These features are presented schematically in Figure 14.

The specimen of sheet or millboard is cut about 1 inch in diameter to provide a rim area for mounting. This rim was saturated with melted paraffin wax to effect a positive seal to prevent liquid leakage through the edges. The specimen was mounted loosely in the holder and then saturated with water, after which the clamping ring was secured tightly. The holder was then filled with water, coupled to the vertical glass column, and immersed to a pre-determined depth in a beaker filled to overflowing with water. The two reference marks on the column were thus 114.4 cm and 124.4 cm (average = 119.4 cm) above the level of water in the filled beaker.

The vertical column was then filled with water, and the time required for the surface level to fall between the reference marks was measured. All the dimensions in the test are arbitrary, therefore, the method can serve only as a means of comparing specimens.

Table 3

Electrolyte Absorption and Retention

Spec. No.	Wt. of Spec. gm	Wt. of Absorbed Soln., gm	Wt. Ratio Absorbed	Wt. of Retained Soln., gm	Wt. Ratio Retained
1100	0.5674	3.3970	5.98	2.9034	5.12
1200	0.5250	3.1424	5.99	2.7855	5.31
1300	0.5491	3.0519	5.56	2.6844	4.89
1400	0.5371	2.7296	5.09	2.5925	4.83
1500	0.5470	3.0531	5.57	2.5955	4.74
		Average	5.64		4.98
2100	0.4611	2.5515	5.53	2.2699	4.93
2200	0.4411	2.4119	5.46	2.2976	5.22
2300	0.4499	2.6325	5.84	2.3367	5.20
2400	0.4535	2.6473	5.84	2.3108	5.09
2500	0.4148	2.3924	5.76	2.1640	5.22
		Average	5.69		5.13
3100	0.2245	0.8534	3.80	0.8534	3.80
3200	0.2280	0.8980	3.94	0.8633	3.79
3300	0.2207	0.7999	3.63	0.7852	3.56
3400	0.2186	0.8520	3.90	0.8512	3.89
3500	0.2301	0.8978	3.90	0.8978	3.90
		Average	3.83		3.79
4100	0.2187	0.8425	3.86	0.8443	3.86
4200	0.2153	0.8013	3.73	0.8015	3.73
4300	0.2229	0.8526	3.82	0.8327	3.74
4400	0.2163	0.8035	3.71	0.7957	3.68
4500	0.2138	0.8452	3.95	0.8076	3.77
		Average	3.81		3.76

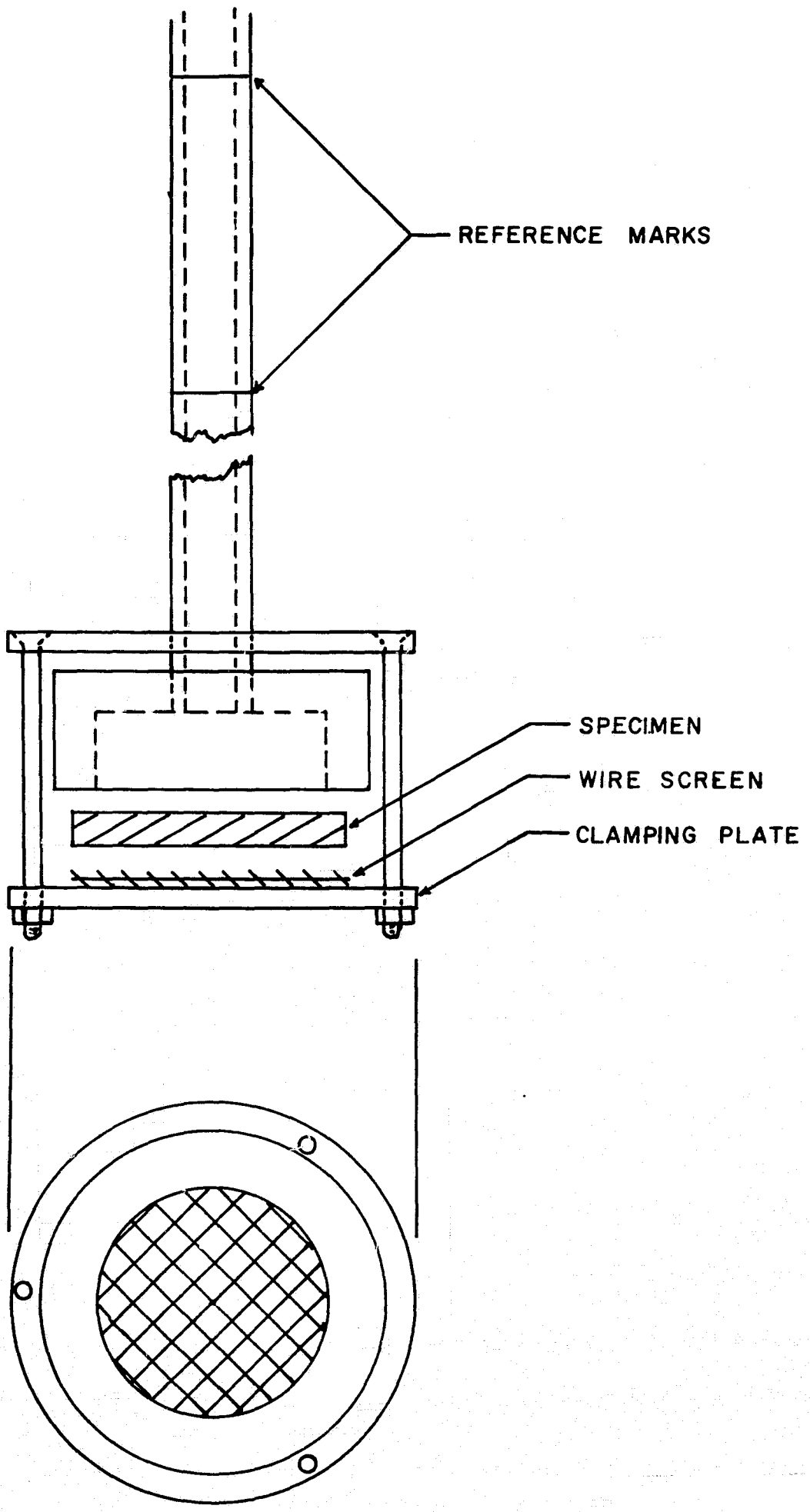

Figure 14. Schematic of Specimen Holder for Liquid Permeability Tests.

As described by Cooper and Fleischer, if one assumes that asbestos mat is essentially a packing of cylindrical tubes with axes all transverse to the plane of the mat, then, with incorporation of additional data, one may compute a numerical value of porosity of the specimen. However, this computation involves several idealizing assumptions that are not even remotely realized in asbestos mat, and consequently the porosity value so derived is fictitious. Since the liquid permeability test is being surveyed in this program merely as a convenient means of comparing specimens of asbestos for service as a matrix, we believe that the computation of porosity values is an unwarrented elaboration, and we report only the raw data.

The first tests with asbestos specimens yielded grossly erratic results, evidently because of entrapment of air pockets. When the specimens were permitted to saturate by capillary absorption upward from the lower surface, the data became much more coherent.

The data (Table 4) reveal that the specimens of the 1000 series (production start) are much less permeable and much more variable than the specimens of the 2000 series (production end). Roughly, the measured times of permeation correlate with the measured thickness of the dry specimens, although in the case of the 1000-series specimens, the permeability variations seem disproportionately great. Moreover, the slight difference in general thickness of the 2000 and 1000-series specimens cannot account for the notable difference between the permeabilities of the two groups.

For comparison, three sheets (8.5 x 11 inches) each of the 1000-series and the 2000-series material were weighed, and the following results were obtained:

1000 series	214.0g
2000 series	181.3g
Difference	32.7g (or about 15%)

Thus, the weight difference corresponds roughly with the difference in thickness between the two lots of millboard. However, the variation in water permeation rates is greater than that predicted from an exponential dependence on mat thickness. Evidently, the water permeation rate does reveal mat differences more significantly than simple thickness or geometric density differences.

c. Electrolytic resistance. - Electrolytic resistance of the saturated mat was measured with a cell similar to that described by Cooper and Fleischer. The cell (diagrammed in Figure 15) splits into two identical halves. Each of these pieces was machined from a Teflon block. When the specimen, with edges

Table 4

Liquid Permeability Tests

Specimen	Specimen Thkns. (inch)	Flow Time (sec.)*
1100	0.0565	978
1200	0.0538	719
1300	0.0537	586
1400	0.0532	732
1500	0.0550	795
2100	0.0494	362
2200	0.0470	317
2300	0.0506	352
2400	0.0478	365
2500	0.0483	323
3100	0.0208	42.5
3200	0.0208	39.7
3300	0.0201	39.4
3400	0.0206	40.7
3500	0.0203	41.3
4100	0.0198	43.8
4200	0.0194	41.0
4300	0.0195	38.8
4400	0.0205	39.1
4500	0.0192	39.2

* Time required to flow 1.12 ml. of water through a 1/2 inch diameter circular area of asbestos mat under an average head of 119.4 cm. of water.

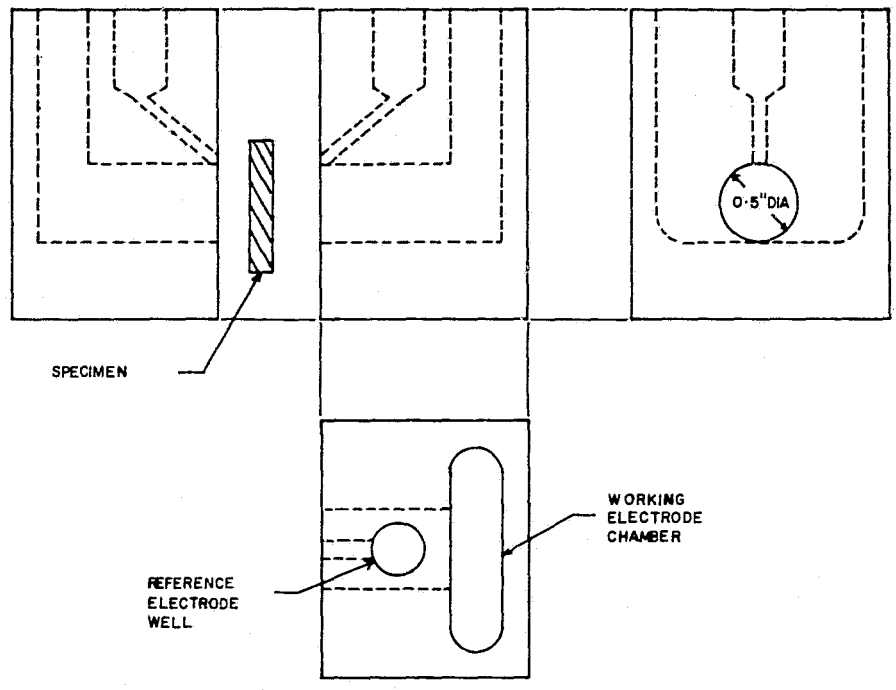

(a)

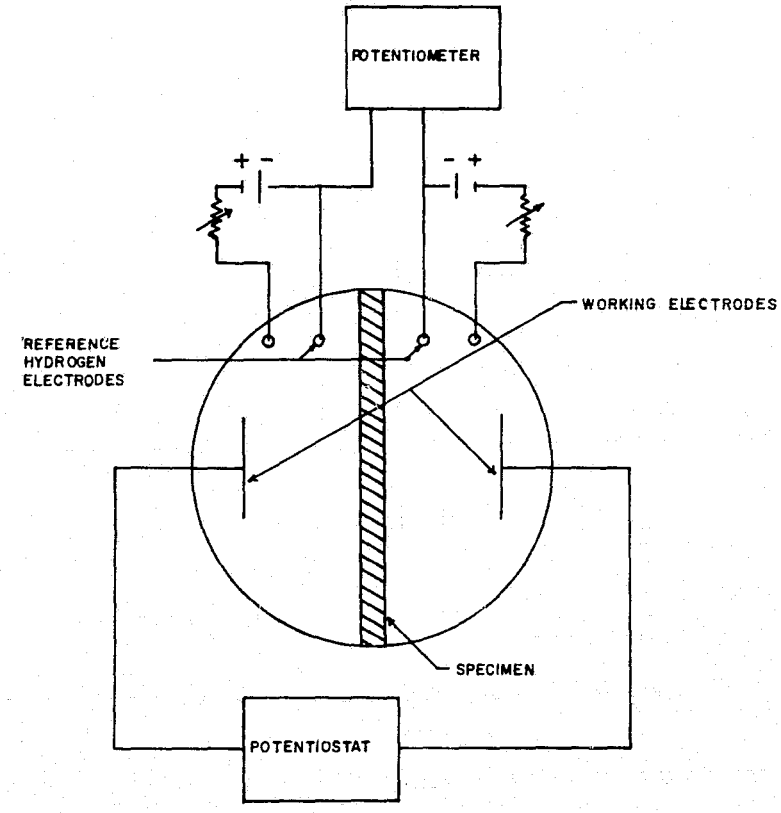

(b)

Figure 15 a) Diagram of Cell Used for Electrolytic Resistance Measurements.

b) Electrical Schematic of Resistance Apparatus.

sealed by melted paraffin, is clamped between the halves, it presents a circular area of 1/2 inch diameter to the electrolyte.

The reference electrodes in these tests were hydrogen-generating electrodes operating in the same electrolyte that filled the working cell. A Sorensen potentiostat furnished current controlled at 141 ma (which is equivalent to 100 amp./sq. ft. at the specimen surface.)

The test procedure follows: with zero current between the working electrodes, the rheostats in the reference electrode supply circuits were adjusted for gentle production of hydrogen and for zero potential difference between the two reference electrodes. Then, with 141 ma passing through the specimen, the potential difference between the reference electrodes was measured.

Finally, the electrolyte was removed, the specimen was flushed out of the cell by a stream of water, the electrolyte was replaced, and the resistance of the electrolyte alone was measured. The latter constitutes a blank measurement, but its relationship to the specimen measurement is very dubious. The distance of separation between the two Luggin capillary orifices is determined by the thickness of the compressed rim of the specimen, whereas the rest of the specimen mat expands freely to several times its dry thickness. Therefore, the mat resistance measured in this apparatus pertains strictly only to this particular condition of the mat and may not be applied unchanged to different situations. For that reason, the "blank" values are reported in Table 5, but are not incorporated in the measured values for the specimens. Since the current density is regulated at 100 ASF, the potential across the specimen is converted to ohms per square foot by applying the factor 10^{-2}.

The difference in resistance of the 1000 and 2000-series correlates qualitatively with the measured thicknesses of the dry mat, and also with the measured weights of the dry mats (cf. thickness measurement and liquid permeability tests).

d. Gas permeability of wet mat. - The air permeability was measured for specimens of the asbestos mats containing absorbed 40% KOH solution in the weight ratio 1:1 and increasing to saturation. For this purpose, the apparatus at hand was modified to improve its sensitivity. The specimen, with edges sealed by melted paraffin, was mounted in a holder which supplied air under measured pressure to the lower surface of the specimen. A 1-1/4 inch diameter circular area of the specimen was exposed to the test gas. The gas permeating the specimen was contained by an upper chamber of the holder and conducted to a water bubbler, which served to indicate and measure the gas flow. In the holder, the specimen was restrained against the pressure differential by a metal screen directly above it.

Table 5

Electrolytic Resistance of Fuel Cell Asbestos

Specimen	Δ E, Volts	R, ohm/ft
1103	0.1081	10.81×10^{-4}
1203	0.1083	10.83
1303	0.1081	10.81
1403	0.0835	8.35
1503	0.1088	10.88
2103	0.0891	8.91
2203	0.0843	8.43
2303	0.0905	9.05
2403	0.0917	9.17
2503	0.0874	8.74
3103	0.0466	4.66
3203	0.0695	6.95
3303	0.0541	5.41
3403	0.0667	6.67
3503	0.0508	5.08
4103	0.0400	4.00
4203	0.0574	5.74
4303	0.0445	4.45
4403	0.0659	6.59
4503	0.0561	5.61
Blank	0.0355	
Blank	0.0350	
Blank	0.0373	

Preliminary experiments with bubbler design to achieve maximum sensitivity as a gas flow meter revealed several interesting considerations. With decreasing orifice size, the bubble becomes smaller, but the capillary forces within the bubbler tube makes necessary greater gas pressures to expel a bubble of gas. In fact, with a very small diameter tube, the gas is released as a burst of bubbles. The optimum condition was attained by using a tapered polypropylene tube to minimize capillary effects and trimming off the tapered end to obtain the optimum orifice diameter.

Pressure of the air supplied to the specimen was measured by either a water manometer, a mercury manometer, or a Bourdon gage, depending on the pressure. This provided accurate pressure measurements ranging from a fraction of an inch of water to 30 psig. Very low pressures were corrected for the depth of immersion of the bubbler tip (about 1 inch).

The data are recorded in Table 6. Probably the most significant yield from these tests is the gross difference between the paper and millboard. The 20-mil paper specimens consistently leaked gas at low pressure differentials (about 10 inches of mercury) even when saturated with KOH solution. On the other hand, the 60-mil millboard usually was impermeable at 30 psi even at the minimum (1:1 weight ratio) content of KOH solution.

We observed that in all cases the gas pressure forced KOH solution out onto the top surface of the specimen. When the pressure differential was relaxed, the free solution was quickly reabsorbed into the specimen.

We suggest the following tentative interpretation. At the 1:1 weight ratio of asbestos to KOH solution, the paper contains only one-fourth the saturating quantity of solution, the millboard contains only one-sixth. Evidently, the millboard structure is such that the pressure induced migration of some liquid produces a saturated and sealed zone near the low pressure side. For some reason, the structure of the 20-mil paper or its lack of sufficient thickness does not permit a sealed zone to develop.

Table 6

Gas Permeability of Wet Asbestos

Specimen Identity and Electrolyte Ratio		Net Pressure (psi)	Flow Rate * (Bubbles/Sec)
1201	1:1	6.958	.023
		8.526	.025
		9.065	.028
		9.408	.045
	2:1	11.270	.019
		14.308	.014
		15.500	.018
		16.000	.014
	3:1	25.000	.032
		30.000	.008
1202	1:1	1.421	.071
		1.667	.100
		1.764	.100
	2:1	7.105	.038
		9.898	.043
		14.700	.067
		15.000	.062
		17.500	.067
		20.000	.071
		22.500	.083
		25.000	.091
		27.500	.100
		30.000	.111
1301	1:1	1.863	.020
		2.891	.028
		3.675	.037
		4.116	.037
		4.214	.040
		4.214	.042
	2:1	30.000	0.000
1401	1:1	30.000	0.000
1501	1:1	3.773	.048
		2.646	.333
		3.773	.500
		3.822	.083
	2:1	6.223	.143
		10.535	.125
		18.500	.143
		21.000	.143
3401	4:1	3.381	.067
	5:1	3.185	.056
		3.675	.056
		4.018	.056
4201	1:1	.378	.067
		.400	.067
		.428	.071

Specimen Identification		Net Pressure (psi)	Flow Rate * (Bubbles/Sec)
1501	2:1	25.0	.143
		25.0	.125
		25.0	.111
2101	1:1	3.283	.059
		4.949	.083
		7.448	.125
		12.005	.250
	2:1	10.241	.050
		12.225	.071
		14.700	.091
		17.500	.143
		20.000	.167
	3:1	17.500	.033
		20.000	.040
		25.000	.071
	4:1	17.500	.016
		20.000	.023
		25.000	.045
2102	1:1	21.500	.167
		18.000	.333
	2:1	19.000	.077
	3:1	30.000	0.000
2501	1:1	3.283	.100
		2.009	.250
		1.911	.250
	2:1	5.047	.050
		25.500	.023
3401	1:1	.418	.036
		.526	.034
		.814	.050
		.900	.040
	2:1	1.176	.048
		1.372	.056
		1.372	.050
	3:1	1.519	.050
		1.813	.053
		2.107	.059
	4:1	2.597	.059
		2.989	.062
4402	2:1	12.250	.143
	3:1	7.840	.071
		12.250	.143
	4:1	12.000	.100
		12.000	.100
		20.000	.333
4403	1:1	.407	.024

Table 6 (Cont'd)

Specimen Identity and Electrolyte Ratio		Net Pressure (psi)	Flow Rate * (Bubbles/Sec)
4201	2:1	.875	.031
		1.001	.029
		1.372	.031
	3:1	1.667	.033
		2.156	.034
		2.500	.034
	4:1	3.234	.032
		3.578	.028
		4.655	.031
4301	1:1	.119	.031
		.328	.042
		.911	.043
		5.635	.200
		9.800	.500
	2:1	.846	.013
		3.773	.040
		7.350	.125
		12.495	.200
4401	1:1	2.009	.011
		4.900	.021
		7.350	.033
		9.800	.050
		12.250	.071
	2:1	30.000	0.000
	3:1	18.000	.143
		18.000	.125
		.684	.037
		.864	.043
4403	1:1	2.450	.143
		7.350	.454
		12.250	.833
	2:1	2.646	.100
		7.399	.333
		12.225	.556
	3:1	4.753	.043
		7.350	.077
		12.225	.167
	4:1	5.978	.053
		7.350	.071
		12.225	.200
4501	1:1	.040	.167
		.043	.333
	2:1	.302	.091
		.367	.100
		.608	.143
	3:1	.504	1.667
4402	1:1	.972	.016
		2.450	.040
		4.900	.083
		10.045	.250
	2:1	2.205	.020
		4.900	.043

* This is an arbitrary relative flow rate through a 1-1/4 inch diameter circular area of the mat.

4. Chemical Degradation

These degradation tests consist in maintaining specimens in KOH solution of 30, 40, 50, and 60 weight percent concentration for 100 and 1000-hour periods at temperatures of 50, 100, 150, and 200°C. Tests at 50°C in 50 and 60% KOH and at 200°C in 30 and 40% KOH are not required.

The tests were performed in ordinary laboratory ovens which incorporate thermostat controls. As containers, we used 4 ounce Teflon FEP bottles with screw caps. These were satisfactory at the two lower temperatures, but would not retain the water at 150 and 200°F. We then sealed each bottle individually in a capsule made from standard 2 inch threaded pipe nipples, closed with the threaded caps (Figure 16). We used Teflon pipe tape for a thread sealant, and learned that only certain premium brands of Teflon tape are effective, and only when seven or eight laps of the tape are applied to the thread. The caps were then tightened with a large pipe wrench, the handle of which was lengthened with a four-foot pipe.

The Teflon bottles were weighed empty and with the specimens of asbestos. A polonium-activated dust brush was placed in the balance case to speed the equalization of static charges which are specially troublesome with this plastic. A volume of 50 ml of the KOH solution was placed in the bottle. Where 60% KOH was to be used, the appropriately weighed quantity of dry KOH pellets and volume of water were placed in the bottle. At the end of the test, the contents of the bottle were transferred quantitatively to a 600 ml beaker, diluted with much water and permitted to settle. The supernatant liquid was decanted through a sintered glass filter, and the washing was repeated. The final wash was very slightly acidified with HCl to facilitate complete removal of KOH, and the solid was transferred to the filter, dried, and weighed.

For the lower temperature tests, the bottles were capped tightly and placed in the oven. For the higher temperature tests, the bottles were capped lightly and placed in the pipe capsule, 1 ml of water was introduced to provide balancing vapor pressure, and the top cap was installed. Each capsule was then weighed to the nearest 0.1g and placed in the oven. After several days, the capsules were removed, allowed to cool, and weighed again. If there was any significant loss, the capsule was opened, a new sample was prepared and resealed in the capsule. Only those specimens that showed negligible weight loss were accepted as valid tests. The results of these tests are shown in Table 7.

As expected, the dissolution of specimens is greater with increasing time, temperature, and concentration of the KOH. However, with the exception of two tests and the results for the

Figure 16. View of Specimen Holder for High Temperature Chemical Degradation Tests.

Table 7

Chemical Degradation of Fuel Cell Asbestos

Tests at 50°C

Test Time (HR)	KOH Conc.	Specimen Identification	% Wt. Loss
100	30	1600	2.85
100	30	2600	1.14
100	30	4600	6.14
100	40	3600	4.70
100	40	3600	5.00
100	40	3600	5.33
1000	30	2600	3.00
1000	30	2600	2.00
1000	30	4600	5.31
1000	40	1600	3.52
1000	40	1600	5.56
1000	40	4600	5.61

Tests at 100°C

100	30	1600	7.50
100	30	2600	7.67
100	30	3600	5.30
100	40	1600	10.70
100	40	3600	9.75
100	40	4600	10.14
100	50	1600	16.55
100	50	2600	14.75
100	50	4600	16.35
100	60	2600	15.90
100	60	3600	32.85
100	60	4600	17.97
1000	30	1600	12.30
1000	30	1600	22.20
1000	30	4600	36.6
1000	40	2600	32.80
1000	40	3600	41.40
1000	40	3600	30.2
1000	50	2600	41.00
1000	50	3600	29.6
1000	50	4600	36.5
1000	60	1600	42.00
1000	60	2600	62.75
1000	60	4600	36.9

Table 7 (Cont'd)

Tests at 150°C

Test Time (Hr)	KOH Conc.	Specimen Identification	% Wt. Loss
100	30	1600	3.6
100	30	3600	16.9
100	30	4600	15.4
100	40	1600	2.0
100	40	2600	17.6
100	40	4600	22.4
100	50	1600	30.7
100	50	2600	31.5
100	50	3600	39.9
100	60	2600	32.4
100	60	3600	38.8
100	60	4600	51.4
1000	30	1600	19.8
1000	40	1600	30.6
1000	50	1600	59.5
1000	40	2600	25.1
1000	50	2600	38.0
1000	60	2600	38.8
1000	50	3600	37.2
1000	60	3600	39.9
1000	30	3600	7.4
1000	60	4600	39.5
1000	30	4600	19.5
1000	40	4600	22.5
		Tests at 200°C	
100	50	1600	36.2
100	50	2600	36.5
100	50	4600	36.6
100	60	2600	37.6
100	60	3600	38.6
100	60	4600	39.6

1000 hour, 200°F tests, the weight losses attain a limit of about 40%. This value corresponds quite well with the values predicted (44%) on the assumption that the chrysotile is converted completely to insoluble $Mg(OH)_2$ and soluble silicate. If this assumption is valid, the data indicate the conversion of chrysotile to $Mg(OH)_2$ or hydrated MgO is virtually completed in 1000 hours at 100°F and in 100 hours at 150°C.

Figure 17 shows the change in chrysotile caused by treatment with hot KOH solution. The residue from treatment retains some of the fibrous structure, but a large amount of granular material (dried $Mg(OH)_2$) appears scattered across the microscope field and also filling the remaining fiber clusters.

The data reveal that natural chrysotile is probably not a satisfactory matrix for long service at temperatures as high as 100°C. The tests suggest, however, that the insoluble residue, if it retains a satisfactory structure, may be superior to chrysotile.

5. Electrochemical Degradation

This test consisted essentially in subjecting the specimens to a current density of 40 ASF in 40% KOH electrolyte at 100°C for 72 hours. At 24 hour intervals, 1 ml samples were drawn of the anolyte and catholyte, and the electrodes were washed with nitric acid to remove any deposits. The electrolyte specimens and electrode washings were then analyzed spectrographically for identity and quantity of constituents of the asbestos mat.

These tests were performed in a V-shaped cell machined from a Teflon block (Figure 18). In one leg of the cell was a shoulder to support a platinum wire screen, on which the specimen rested. Since the specimen was located below the electrode level, the electrolytic gases escaped without entering the specimen.

The cell was placed in a laboratory drying oven at 100°C. Electrolytic hydrogen was vented through a tube to the exterior of the oven, and oxygen was vented into the oven. The requisite current (0.27 amp) was provided by a Sorenson potentiostat.

The 40% KOH solution purified electrolytically for these tests contained, as revealed by spectrography, very small concentrations of magnesium, calcium, and aluminum ions. These, of course, will not be removed by electrolysis. The several samples of used electrolyte analyzed were those taken at the ends of the 72 hour tests, when the soluble impurity concentrations were greatest. The concentrations of Mg, Ca, and Al ions were no greater than in the original electrolyte. Silicon was only barely detectable.

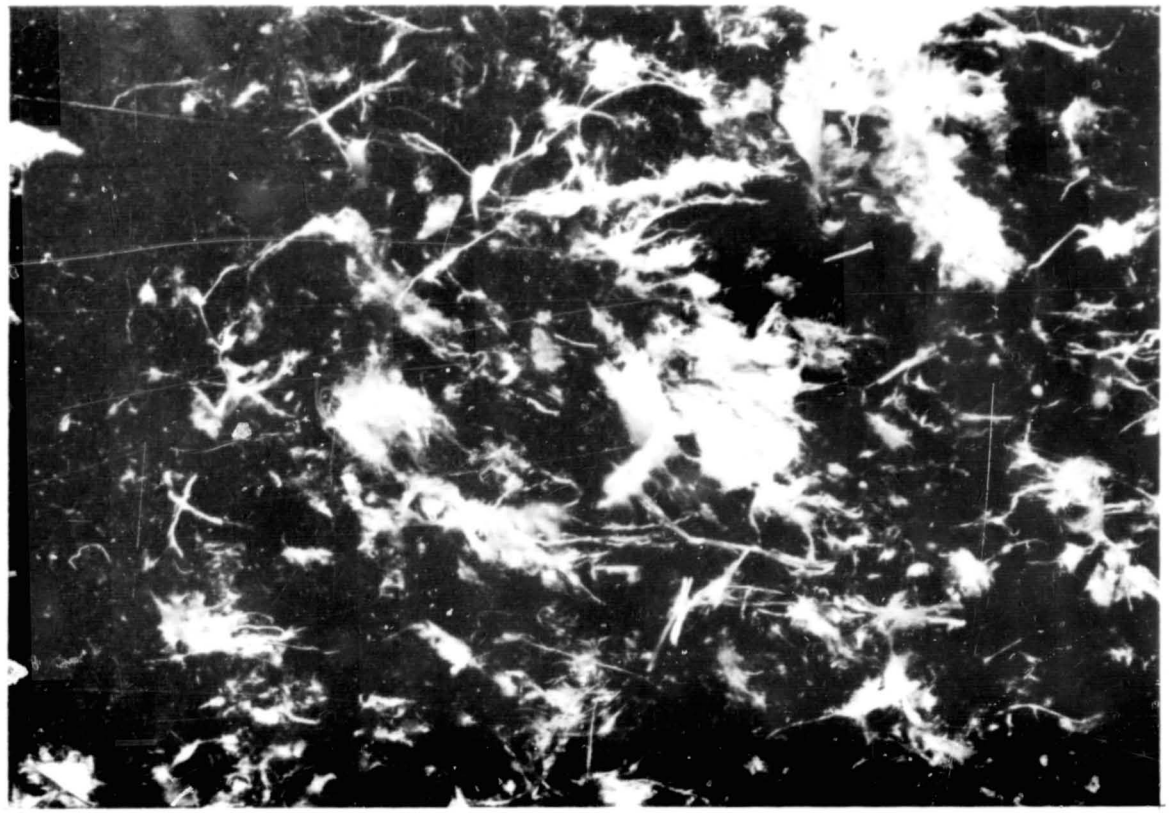

(a)

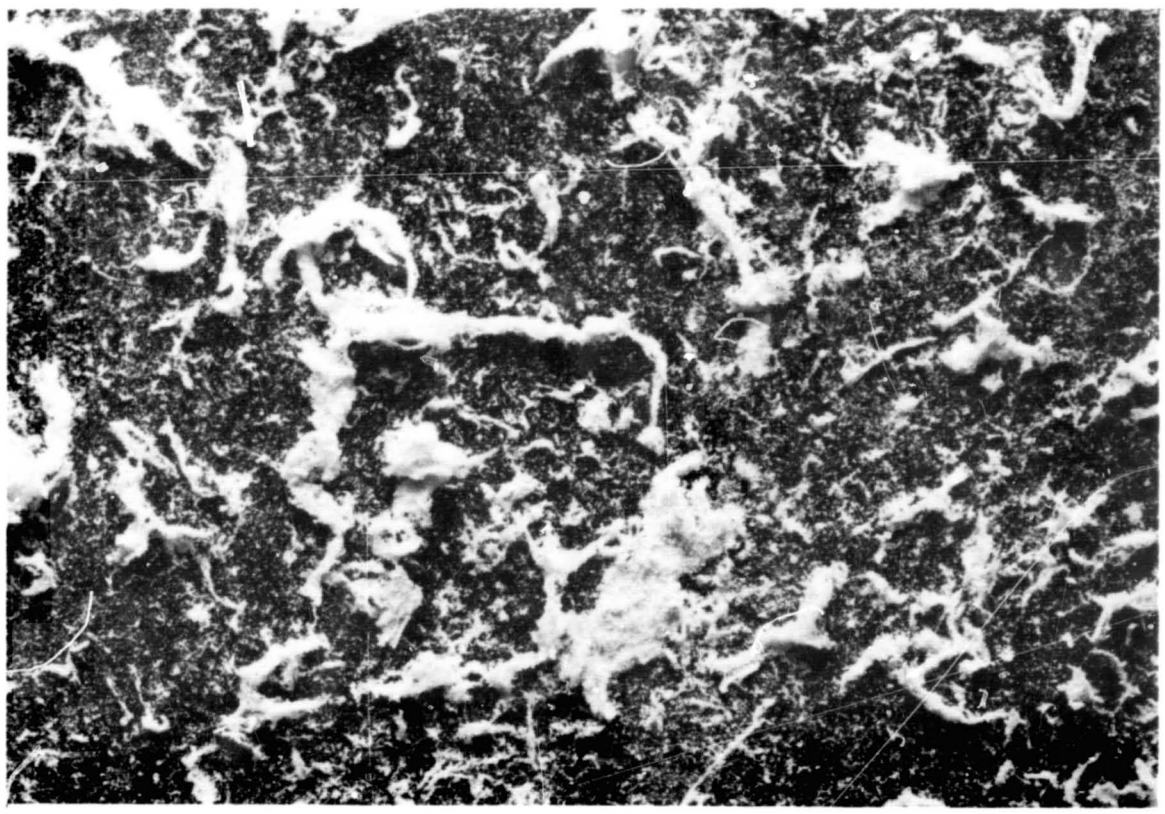

(b)

Figure 17. Chrysotile Before and After Chemical Degradation Test. (10X)

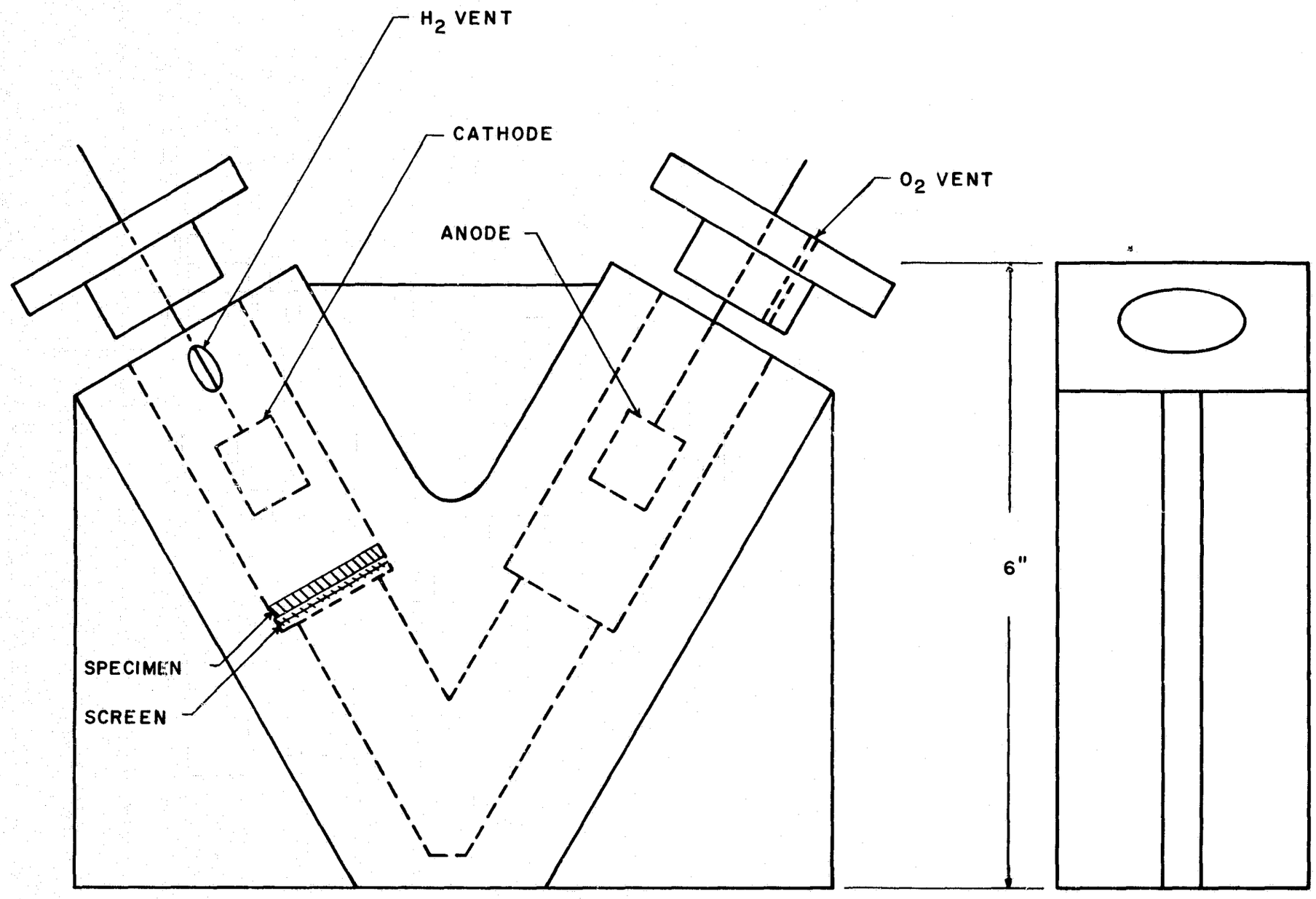

Figure 18. Schematic Diagram of V Cell for Electrochemical Degradation Tests.

In the first test, the specimen was the 20-mil chrysotile paper. At the end of the first 24 hours, there was a visible mottled grey deposit on the anode surface. The deposit did not dissolve in nitric acid. At the end of the test (72 hours) the deposit was apparently unchanged and still insoluble in nitric acid. After standing overnight in the KOH electrolyte, the grey material changed to a golden brown color which dissolved in nitric acid. Upon evaporation to dryness a very small quantity of brown residue appeared. It dissolved readily in a drop of hydrochloric acid, which was then analyzed and proved to contain iron.

Three subsequent tests were performed with 60-mil millboard specimens. During the first two of these tests, the electrodes remained bright and clean, and the electrolyte specimens revealed no significant concentrations of constituent elements of asbestos. During the last test (specimen 2600), very small amounts of brown deposit were formed on the anode. This material was readily soluble in nitric acid. Analysis of this also showed the presence of iron.

These data seem to indicate the deposition on the anode of the black Fe_3O_4 which, upon standing at room temperature for several hours, converts to the red Fe_2O_3. The appearance of iron at the anode is remarkable in view of our observation that iron is not present in the anolyte in spectrographically significant concentration.

C. Conclusions of Task 1 Work

The properties of chrysotile asbestos, already well known, are that it is fibrous, very porous, readily wettable, and moderately resistant to attack by alkaline solutions. It was well-chosen for matrix service in alkaline fuel cells. However, our tests revealed that some of the very small percentage of iron oxide normally present in chrysotile is transferred through the electrolyte and deposits on the anode in an electrolytic cell. It remains to be determined whether the deposited iron adversely affects the electrode operation.

The major deficiency of chrysotile revealed by these tests is its reactivity in alkaline electrolyte. The fibrous magnesium silicate is converted to a soluble silicate and geletinous magnesium hydroxide. The chemical compatibility tests demonstrated the degradation of chrysotile which occurs more rapidly with increasing temperature and KOH concentration. Evidently, 100°C is near the maximum temperature for 1000-hour survival of chrysotile in KOH solution.

The dry mat property tests did not produce any novel information.

When the chrysotile mat absorbs KOH solution, it swells appreciably and loses much of its dry strength. The retention of electrolyte under 25G acceleration is excellent, and the gas-sealing capabilities of the wet mat is adequate.

At sub-saturation proportions of absorbed electrolyte, the thicker mat seals more effectively against gas transfer, evidently because the electrolyte pushed toward the low-pressure side is able to develop a completely saturated layer. The 20 mil thick mat does not seal under a similar pressure differential.

In general, the wet mat properties, as measured in this project, cannot be applied quantitatively to the same material in an electrochemical cell. In a cell, the matrix is compressed between rigid electrodes, whereas, in the tests they were not confined. If the test data are to be related to the cell environment, the degree of restraint of the specimens must be specified for tests like gas permeability and electrolytic resistance.

The fundamental and inherent limitation of chrysotile asbestos is its chemical reactivity with alkaline solutions. At low temperatures and alkali concentrations, the low reaction rate may permit its use as matrix for a reasonable time. But at higher temperatures and electrolyte concentrations, the matrix life will be short.

IX TASK 2. TESTS OF ALTERNATE MATERIALS

A. Material Selection

The materials selected for test in this task of the program consisted of the following:

Asbestoses:

1. Leached chrysotile
2. Tremolite
3. Amosite
4. Anthophylite
5. Crocidolite

Other inorganic materials:

1. Zirconia E fiber (neodymia stabilized)
2. TX fiber - nemolite (Hydrated magnesia)
3. Potassium titanate fiber (PKT)
4. Boron nitride fiber
5. Beryllium oxide
6. Zirconium silicate
7. Titanium oxide

Several tests of leaching treatments of chrysotile demonstrated that chrysotile is not improved by a preliminary chemical treatment. Leaching with concentrated HCl dissolves the magnesium constituent, leaving fibers of nearly pure silica. The silica fibers are readily soluble in KOH solution. Leaching with sequestering agents has a similar effect. Pre-treatment with a surfactant converts the chrysotile fiber into an agglomerated, slimy, intractable mass having no apparent advantage over the original material.

Acid leaching of the other asbestoses - tremolite, amosite, anthophylite, and crocidolite - also dissolves the constituent cations, leaving a fibrous silica which dissolves readily in alkali.

As a result of these tests with leached asbestos, the long-time compatibility tests of leached material were omitted.

Examination of the reported reactivities of beryllium oxide showed that it will dissolve in hot KOH solutions. Chemical attack of KOH on zirconium silicate was also expected. Consequently, these two materials were omitted and the more promising materials, ceria and silicon carbide fiber were substituted. The following three proprietary matrices were also tested.

ACCO-1 (American Cyanamide Company)
Ace-Sil (Amerace Corporation)
Chrysotile-PKT-Neoprene (Pratt & Whitney Aircraft)

B. Chemical Degradation

The compatibility tests were conducted by the techniques described earlier. The test result was the quantity of insoluble solid, in terms of the percentage of the original sample weight, recovered from the KOH solution. Table 8 reports the test results. Many materials were submitted to only part of the specified testing schedule - sufficient to demonstrate failure of the material.

These test results can be summarized as follows:

1. The asbestoses, being silicates, are inherently rea active with KOH and are, therefore, unsuitable. Pretreatment of the asbestos with dilute acid or sequestering agent removes the metallic cations from the fiber, leaving silica, which is readily soluble in alkali.

2. TX fiber is superior in resistance to KOH, but its high iron content renders it unsuitable for matrix service.

3. The three proprietary mats are poor.

4. Boron nitride dissolves completely, and silicon carbide fiber is poor.

5. Zirconia E fiber and ceria powder are virtually unc changed.

6. PKT and titania change only slightly during the 100 hour test, but both gain weight significantly during the 1000 hours. The titania developed an insoluble, gelatinous film, which may be a hydrated titania, but we have not established a chemical identification.

The materials selected for further study on the basis of the initial chemical degradation tests were Zirconia E, PKT fiber, ceria, and titania. It should be noted that two forms of potassium titanate were tested. A long-fiber form, "Tipursul", is desirable for matrix application, but the production of Tipursul has been discontinued. The short-fiber form, "PKT", is being produced commercially for use principally as a paint pigment. The Tipursul tested initially was from a small quantity at hand in the laboratory. Later, the PKT was used exclusively.

Table 8

Chemical Degradation Tests

Specimen Identification	Test Time (Hr)	Test Temp (°C)	KOH Conc.	% Wt. Loss
ACE-SIL	100	100	30	27.9
ACE-SIL	100	100	50	27.7
ACE-SIL	100	150	30	27.7
ACE-SIL	100	150	50	25.3
Potassium Titanate with Asbestos and Neoprene Binder	100	100	30	7.2
"	100	100	50	8.4
"	100	150	30	10.7
"	100	150	50	17.1
ACCO No. 1	100	100	30	3.0
ACCO No. 1	100	100	50	11.2
ACCO No. 1	100	150	30	19.9
ACCO No. 1	100	150	50	45.5
ACCO No. 1	1000	150	30	35.4
ACCO No. 1	1000	150	30	33.2
ACCO No. 1	1000	150	50	71.0
ACCO No. 1	1000	150	50	76.9
Boron Nitride	100	100	30	93.4
Boron Nitride	100	100	50	98.3
Boron Nitride	100	150	30	99.8
Boron Nitride	100	150	50	99.9
Boron Nitride	1000	150	30	
Boron Nitride	1000	150	30	
Boron Nitride	1000	150	50	
Boron Nitride	1000	150	50	
Potassium Titanate (Tipersul Pulp)	1000	150	30	2.7
"	1000	150	30	8.6
"	1000	150	50	13.4
"	1000	150	50	7.2
"	100	100	30	4.0
"	100	100	50	8.2
"	100	150	30	0.4
"	100	150	50	0.6
Zirconia E	1000	150	30	0.2
Zirconia E	1000	150	30	0.3
Zirconia E	1000	150	50	0.7
Zirconia E	1000	150	50	0.6
Zirconia E	100	100	30	0.1
Zirconia E	100	100	50	0.1
Zirconia E	100	150	30	0.4
Zirconia E	100	150	50	0.3

Table 8 (Cont'd)

Specimen Identification	Test Time (Hr)	Test Temp (°C)	KOH Conc.	% Wt. Loss	
TX Fiber	1000	150	30	20.5	
TX Fiber	1000	150	50	3.6	
TX Fiber	1000	150	30	- -	Lost Sample
TX Fiber	1000	150	50	37.3	
TX Fiber	100	100	30	5.5	
TX Fiber	100	100	50	1.5	
TX Fiber	100	150	30	1.6	
TX Fiber	100	150	50	1.7	
Amosite	100	100	30	6.8	
Amosite	100	100	50	30.3	
Amosite	100	150	30	9.7	
Amosite	100	150	50	39.2	
Crocidolite	100	100	30	7.0	
Crocidolite	100	100	50	26.9	
Crocidolite	100	150	30	37.2	
Crocidolite	100	150	50	47.4	
Anthophyllite	100	100	30	3.0	
Anthophyllite	100	100	50	7.5	
Anthophyllite	100	150	30	9.0	
Anthophyllite	100	150	50	25.6	
Tremolite	100	100	30	4.6	
Tremolite	100	100	50	5.5	
Tremolite	100	150	30	7.5	
Tremolite	100	150	50	12.9	
Silicon Carbide (wool)	100	150	50	14.6	
Ceric Oxide	1000	150	30	1.9	
Ceric Oxide	1000	150	30	1.2	
Ceric Oxide	1000	150	50	0.6	
Ceric Oxide	1000	150	50	1.8	
Ceric Oxide	1000	100	30	1.5	
Ceric Oxide	1000	100	30	1.6	
Ceric Oxide	1000	100	50	1.8	
Ceric Oxide	1000	100	50	1.2	
Potassium Titanate PKT	1000	100	30	4.1	
Potassium Titanate PKT	1000	100	50	3.0	
Potassium Titanate PKT	1000	150	30	8.4	
Potassium Titanate PKT	1000	150	30	--	No Loss or Gain
Potassium Titanate PKT	1000	150	50	32.7	
Potassium Titanate PKT	1000	150	50	--	Lost Sample
Potassium Titanate PKT	1000	100	30	9.8	
Potassium Titanate PKT	1000	100	50	5.8	

Table 8 (Cont'd)

Speciment Identification	Test Time (Hr)	Test Temp (°C)	KOH Conc.	% Wt. Loss	
Titanium Oxide	1000	150	30	34.3	
Titanium Oxide	1000	150	30	30.4	
Titanium Oxide	1000	150	50	60.4	Both had a thin
Titanium Oxide	1000	150	50	87.7	film of transparent material present
Titanium Oxide	1000	100	30	6.8	
Titanium Oxide	1000	100	30	6.3	
Titanium Oxide	1000	100	50	41.3	
Titanium Oxide	1000	100	50	44.8	

C. Tests of Selected Compatible Materials

The four materials (zirconia fiber, PKT, ceria and titania) selected in the chemical compatibility tests were evaluated by the full complement of tests in this part of the program. This included a further study of the as-received fibers or powders, the preparation of 20-mil and 60-mil thick mats from these materials, the study of the dry mats, and an evaluation of the mats when wet with KOH. For the preparation of mats from these materials, 10% chrysotile fiber was added to the base constituent to help improve the structural integrity of the mats.

1. Starting Materials

a. Chemical composition. - The chemical composition of the four materials used in mat preparation are listed below. These analyses have been supplied by the vendors of the respective materials.

PKT (Pigmentary Potassium Titanate from duPont)

TiO_2	85%
K_2O	11
K_2SO_4	3.0
KCl	0.1
Fe	100 ppm

Titania (TiO_2) (Fisher Scientific Co., Certified Anhydrous)

Water soluble salts	0.05%
Arsenic (As)	0.00024
Iron (Fe)	0.01
Lead (Pb)	0.002
Zinc (Z)	0.01

Zirconia Fiber (H. I. Thomas Fiberglass Co.)

This material is basically zirconium oxide, stabilized by 10-15% neodymia. Semiquantitative spectrographic analysis by a commercial laboratory yielded the following results:

Zirconium	73%
Hafnium	0.74
Magnesium	0.012
Titanium	0.068
Silicon	0.13
Calcium	0.003

Ceria (ceric oxide - Fisher Scientific Co. Certified Grade)

CeO_2	99.5% min.
Fe_2O_3	0.003
P_2O_5	0.005
Rare Earth Oxides	0.05 max.

Our spectrographic analysis revealed appreciable calcium, but no quantitative estimate was attempted.

b. Fiber structure. - The natural asbestoses - amosite, anthophyllite, tremolite, and crocidolite - and TX fiber were photographed at 10X magnification (Figures 19, 20, 21, 22,and 23). Although these materials were not selected for the comprehensive testing program, the photographs reveal the wide difference in character of the material. The fiber length and degree of fiber separation are largely determined by the processing each one has received, but some inherent differences are evident. Tremolite is a very soft, "ropey" fiber, while TX fiber is fine, loose, and tends to be brittle. The anthophyllite fibers are short and poorly resolved.

The Zirconia E fiber is evidently a smooth surfaced fiber, tends to curl, but the fibers tend to remain separated (Figure 24). The potassium titanate (PKT) is a short straight fiber that tends stongly to clump together (Figures 25 and 26). The ceria and titania are not included here since they were purchased as powders and, therefore, have no fibrous structure..

c. Surface area. - Surface areas of the component materials selected for incorporation in mats were measured by the adsorption technique, with the Perkin Elmer Sorptometer, Model 212B.

Ceria	2.08 m^2/g
Chrysotile	50 m^2/g
Potassium Titanate	10.2 m^2/g
Titanium Oxide	8.16 m^2/g
Zirconia E	2.85 m^2/g

The manufacturer, H. I. Thompson Fiberglass Co., reports the value of 100m^2/g for Zirconia E fiber. The relatively smooth appearance of this fiber as shown in Figure 24, however, indicates that our experimental value of 2.85 m^2/g is more nearly the true value.

2. Preparation of Mats

Because mats composed individually of the four selected materials - PKT, ceria, zirconia, and titania - are too weak and brittle to be tested, these materials were blended with 10 weight percent of chrysotile asbestos fibers to add structural integrity

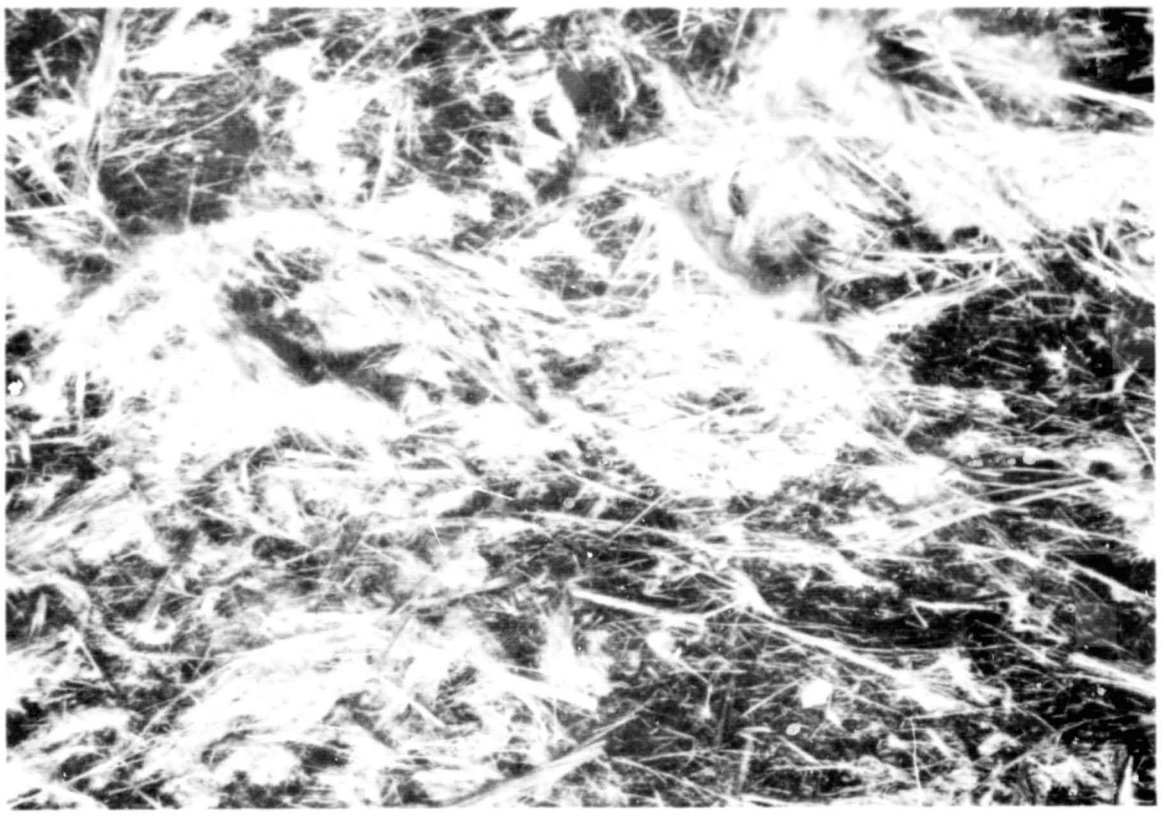

Figure 19. Amosite (10X)

Figure 20. Anthophylite (10X)

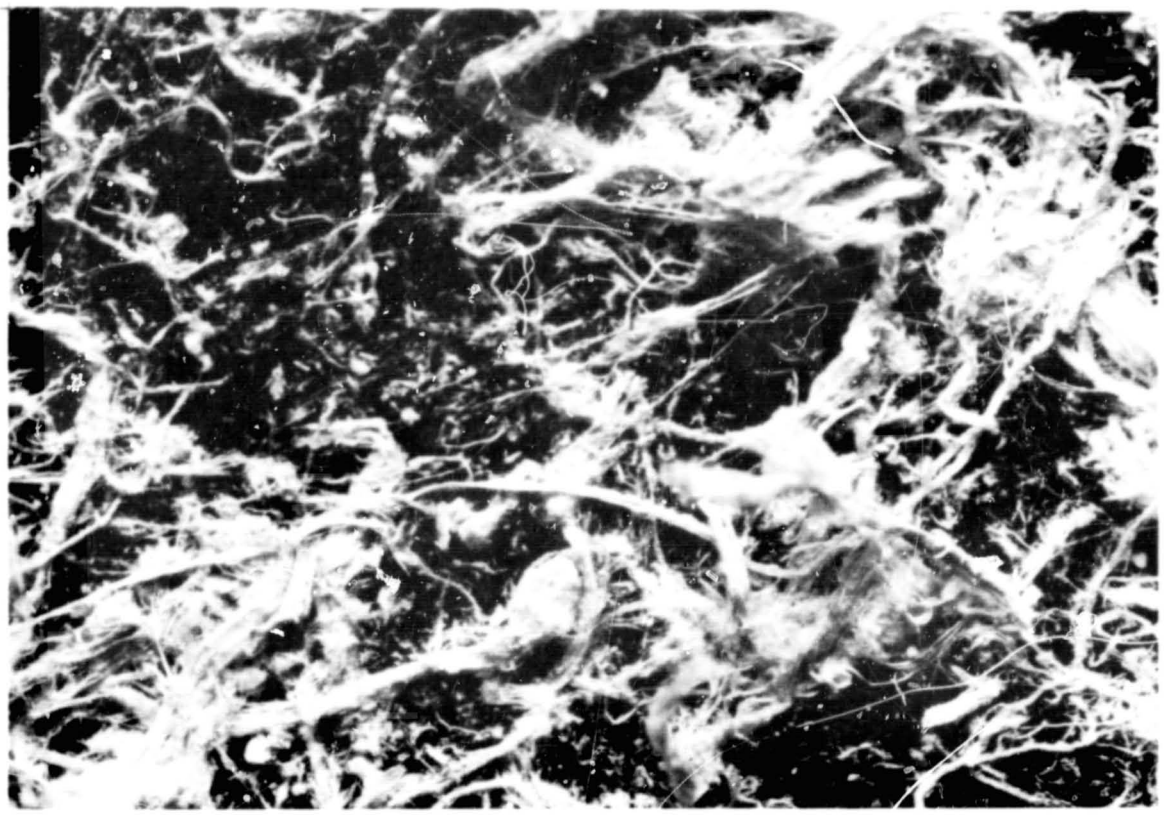

Figure 21. Tremolite (10X)

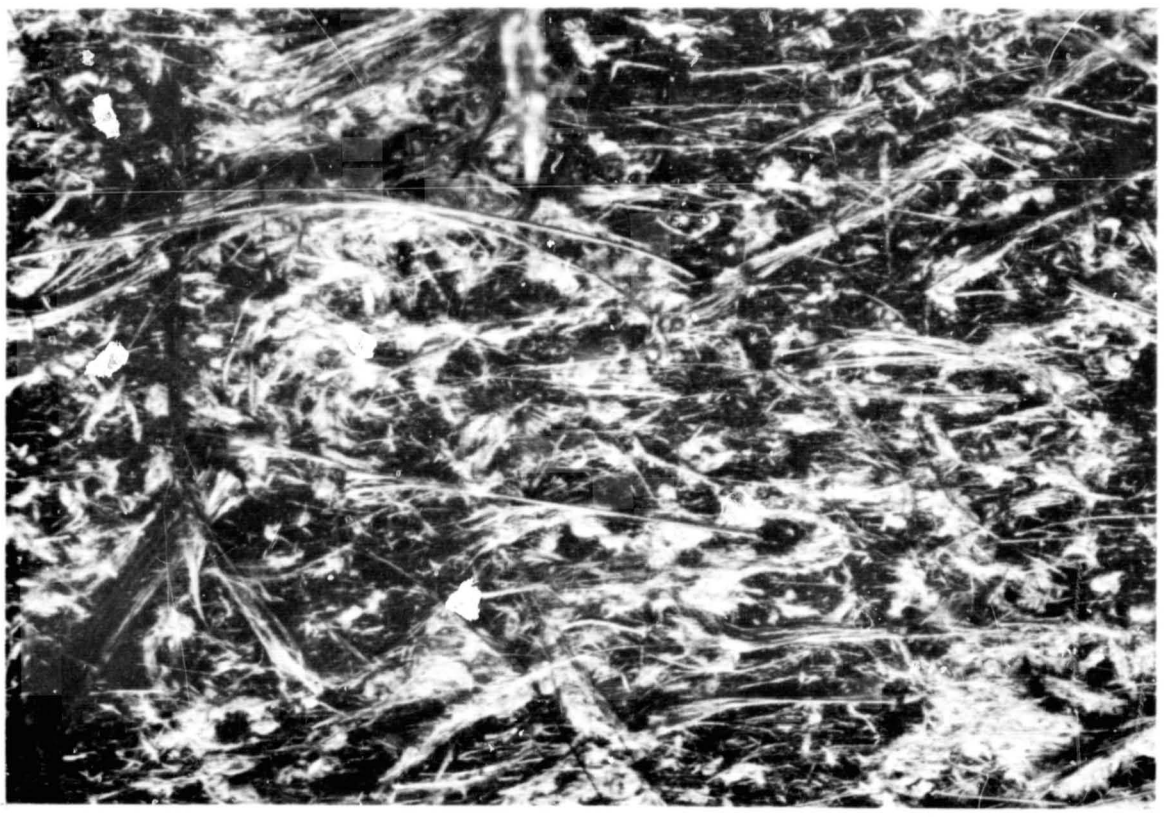

Figure 22. Crocidolite (10X)

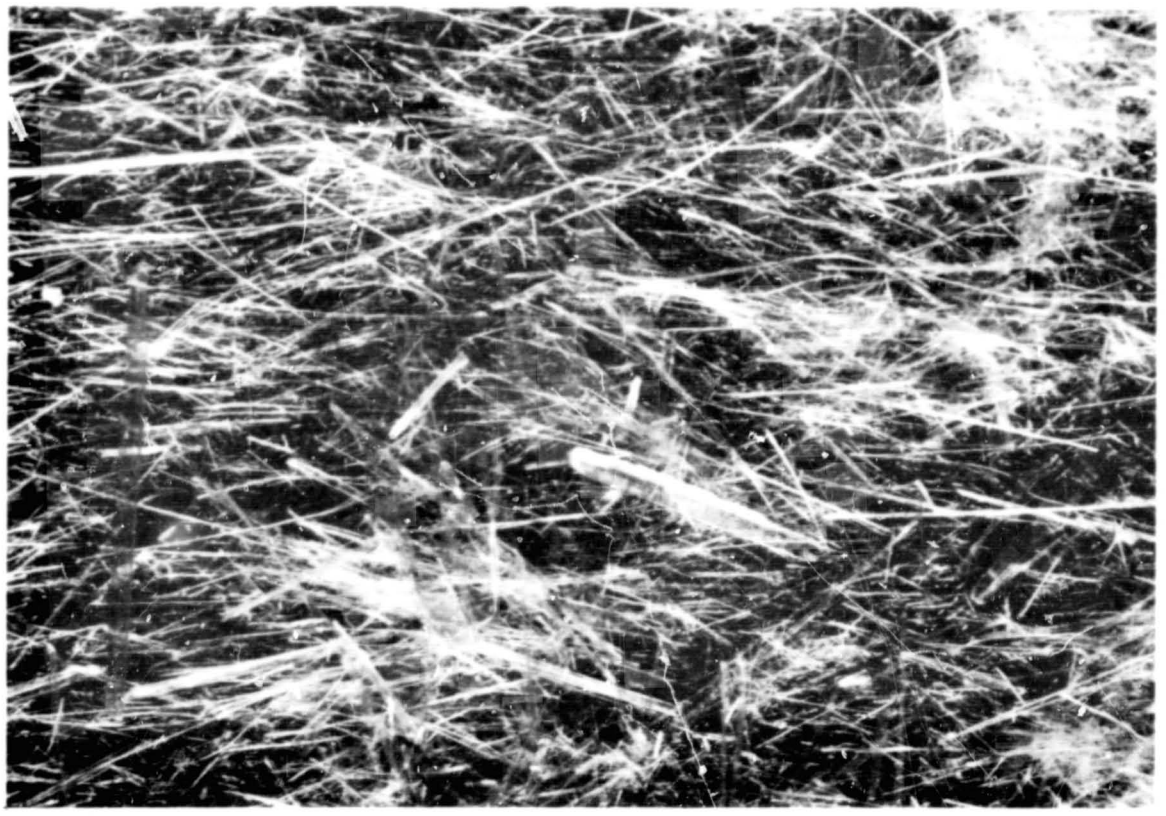

Figure 23. TX Fiber (10X)

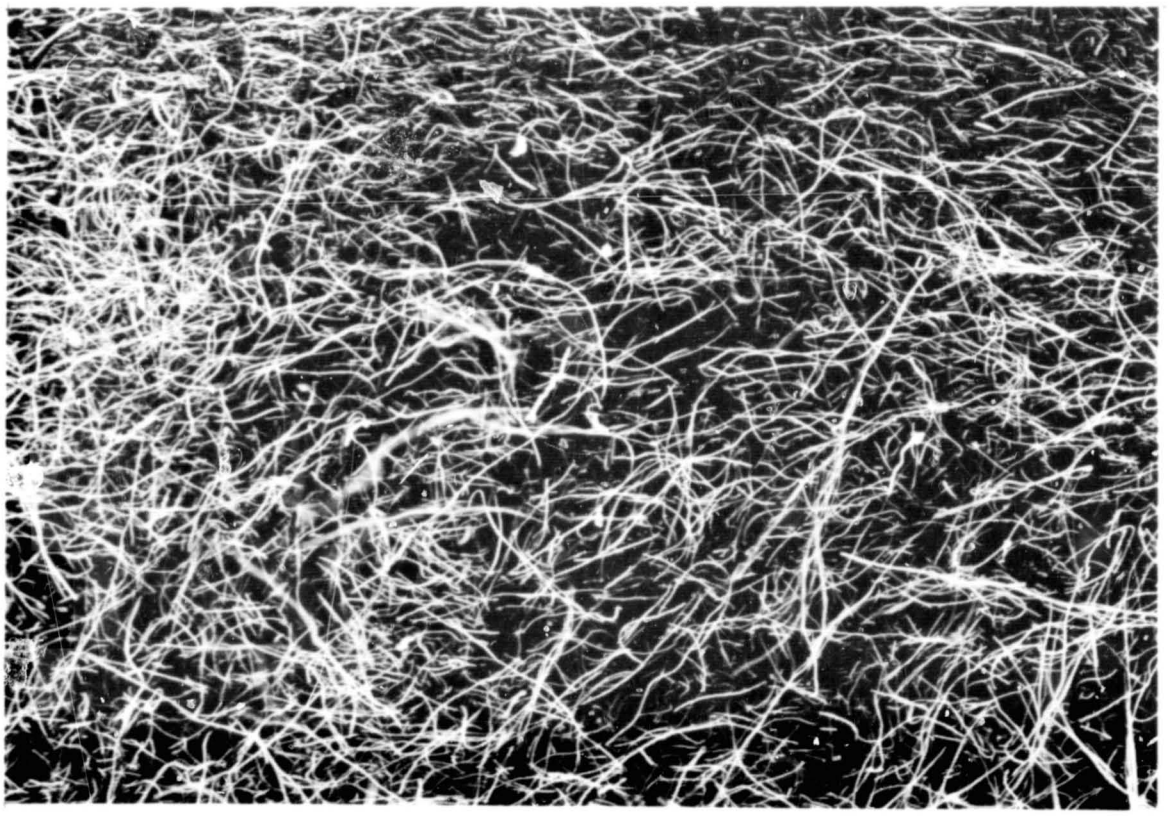

Figure 24. Zirconia E Fiber (10X)

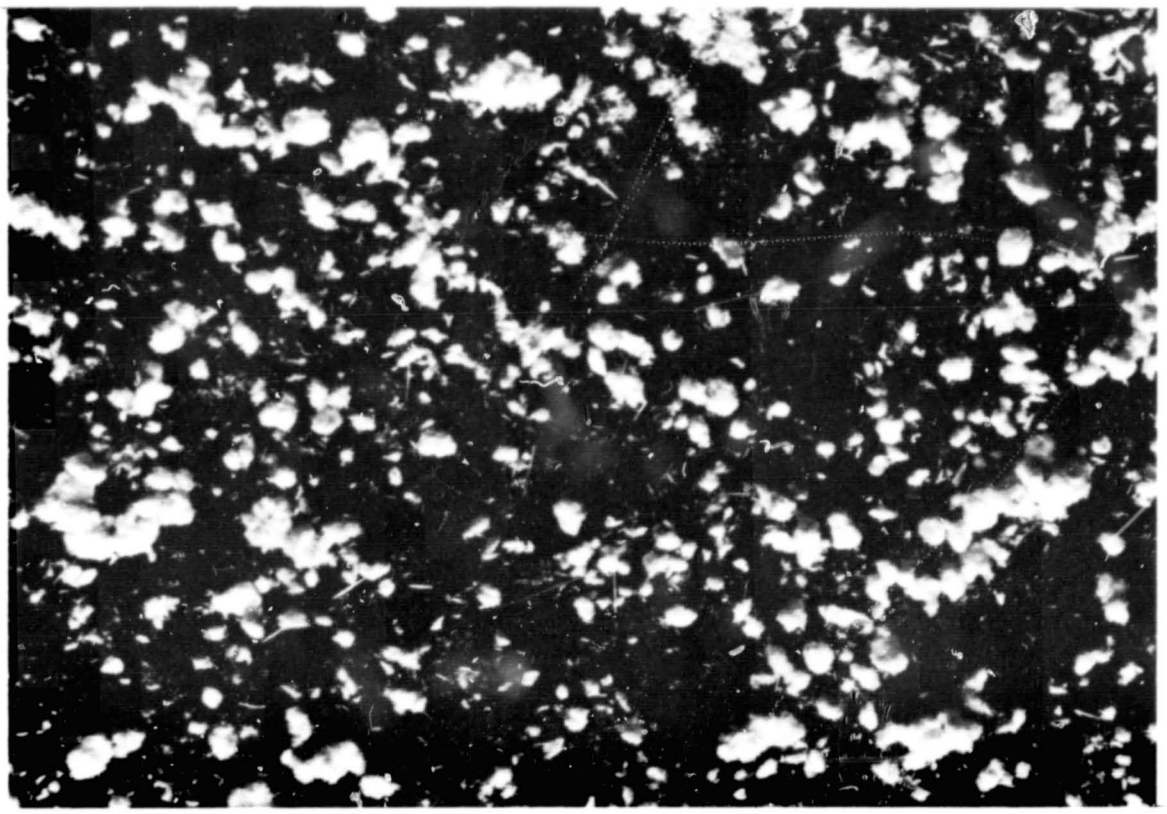

Figure 25. Potassium Titanate (PKT) 10X

Figure 26. Potassium Titanate (PKT) 10,000X

to the mats. The components for each mat were weighed separately and then blended together in water by prolonged gentle mechanical stirring.

Chrysotile fiber, when well dispersed, forms a very slowly-settling aqueous suspension. Mats are best prepared with a sheet mold which consists essentially of a reservoir equipped with a fine screen bottom and a water column drain to generate about 30 inches of hydrostatic pressure at the screen. The dilute suspension of fiber is poured into the reservoir, agitated, allowed to become quiescent, and then quickly sucked down against the screen. The mat is then lifted off the screen, pressed between absorbent paper, and dried.

A sheet mold was built in this laboratory to make mats of chrysotile and similar fibers (Figure 27). The reservoir was made unusually tall to contain, in one filling, the quantity of dilute suspension needed for a 60-mil thick mat. The screen was replaced by a layer of 1-inch thick, fine-pore polyurethane sponge on a perforated Plexiglass plate support. The sponge was an effective non-clogging filter bed, from which the mat could be cleanly separated. The wet mat was then sandwiched between layers of absorbent paper and plastic plates and compressed by rolling with a 20 lb. steel cylinder, after which it was dried in a laboratory oven.

The sheet mold cannot be used with the other selected materials. In contrast with chrysotile fiber, the other materials are more dense and settle much faster from a dilute suspension. When mixed with chrysotile in dilute suspension, the great disparity in settling rates causes gross stratification in the mat that is formed. In order to preserve the desired homogeneity in the mat, the suspension must be made quite concentrated and it must be cast quickly. The polyurethane sponge, which served so well as a bed for the casting of fibrous chrysotile, is unable to retain the small particle powders. Consequently, we used a standard laboratory Buchner funnel with filter paper for preparation of the composite mats. After being formed in the funnel, the mat was placed on paper towels to remove most of the water by capillarity. Finally, it was placed between paper towels, and compressed in a small manual hydraulic press.

Composites with zirconia fiber were completely crushed by the hydraulic pressing, and therefore required more gentle treatment. We compacted the zirconia composite mats by placing them between layers of absorbent paper sandwiched between Lucite plates (with metal shims to establish the final mat thickness) and rolling manually with a 20-lb. steel cylinder.

The mats prepared for testing were to be of two thicknesses: 0.020 ± 0.002 inch and 0.060 ± 0.004 inch. The mats containing PKT, ceria, and titania were made conforming to the thickness

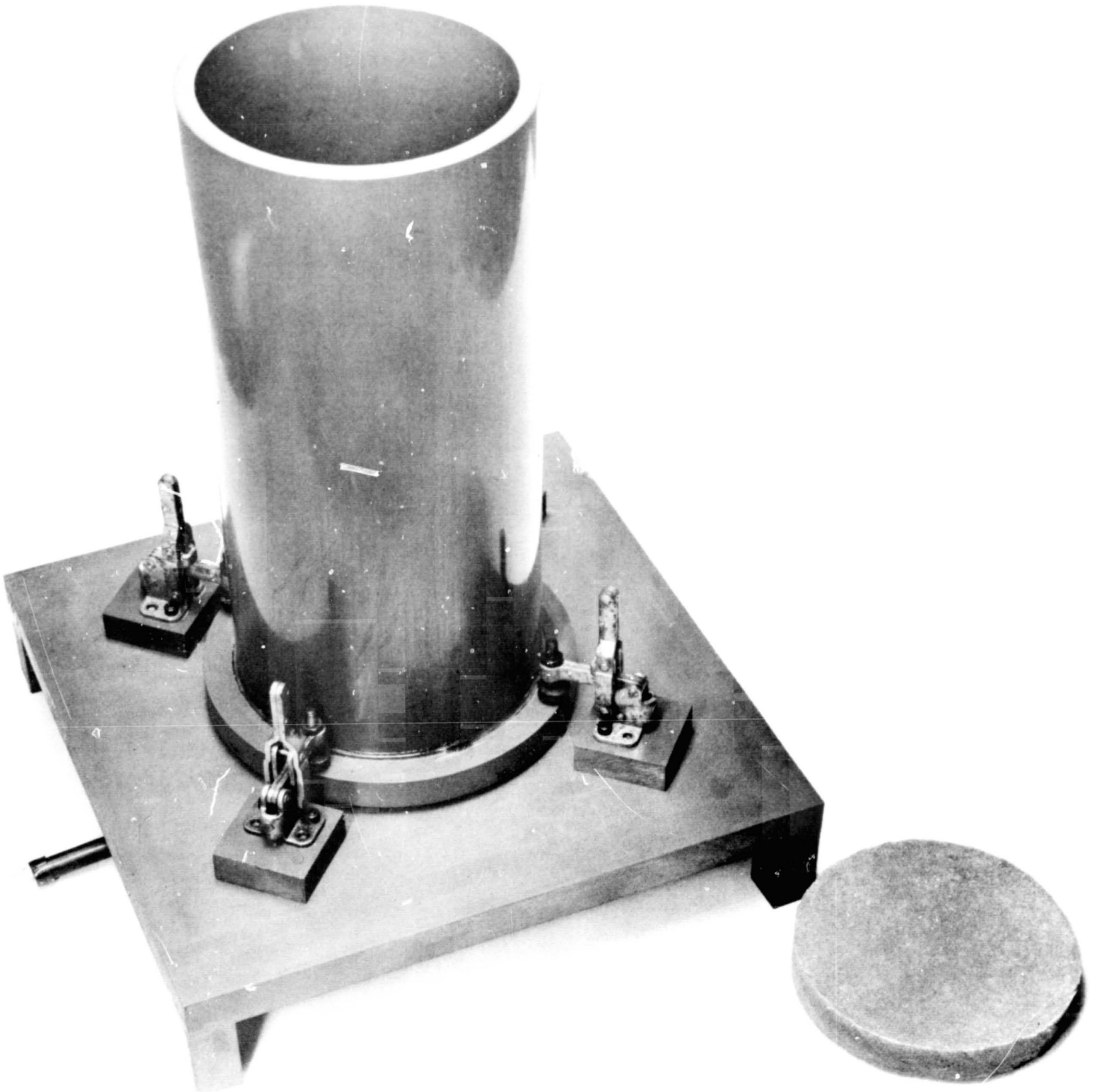

Figure 27. Mat Casting Apparatus

requirements by maintaining a constant molding technique and final compaction pressure, and by controlling the weight of material in a mat. In the case of the zirconia fiber composites, the weight of material per mat was adjusted to permit the final compaction without incurring undue destruction of the brittle fibers. In all cases, the mats of each composition produced for test were uniform in thickness and weight.

Dry Mat Properties

a. Tensile strength. - Tensile tests were performed on the Instron Tensile Tester. The specimens were die-cut rectangles, 2 x 3 inches, mounted to provide a gage length of 1 inch. Crosshead was 0.50 inch per minute.

Typical extension curves are presented in Figure 28, and the tensile strength results are recorded in Table 9. It is noted that these mats are approximately only 10-15% as strong as the Fuel Cell Asbestos mats. It is likely, therefore, that most of the strength of these mats can be attributed to the 10% chrysotile fibers added to the mat.

b. Density. - True densities were measured with the Beckmann Air Comparison Pycnometer. Values for the mat components separately are:

Ceria	6.93 g/cc
Chrysotile	2.73 g/cc
Potassium Titanate (PKT)	3.32 g/cc
Titania	4.03 g/cc
Zirconia E	4.70 g/cc

True densities of the finished mats were also determined, the results are recorded in Table 10. The mat porosity was also computed from a comparison of true density with the geometric density. Porosity in the 70-85% range was obtained in these mats. This appears favorable compared to the 70% porosity typical of the standard asbestos mats.

c. Thickness variations. - Thickness was measured with a dial gage instrument equipped with a 1/2-inch diameter foot and dead-weight loaded to 5 lb per square inch. Only those mats were retained for testing which fulfilled the thickness tolerance requirements, namely ± 0.002 inch for the 0.020-inch mats and ± 0.004 inch for the 0.060-inch mats.

d. Pore size distribution. - The pore size distribution of these mats was measured by the mercury intrusion method using an Aminco-Winslow Porosimeter. The intrusion curves are shown in Figure 29. These results show that the titania and the PKT mats contain pores mostly in the sub-micron range. The ceria mat has most of its pores in the 1-1.5 micron range, and the zirconia mat

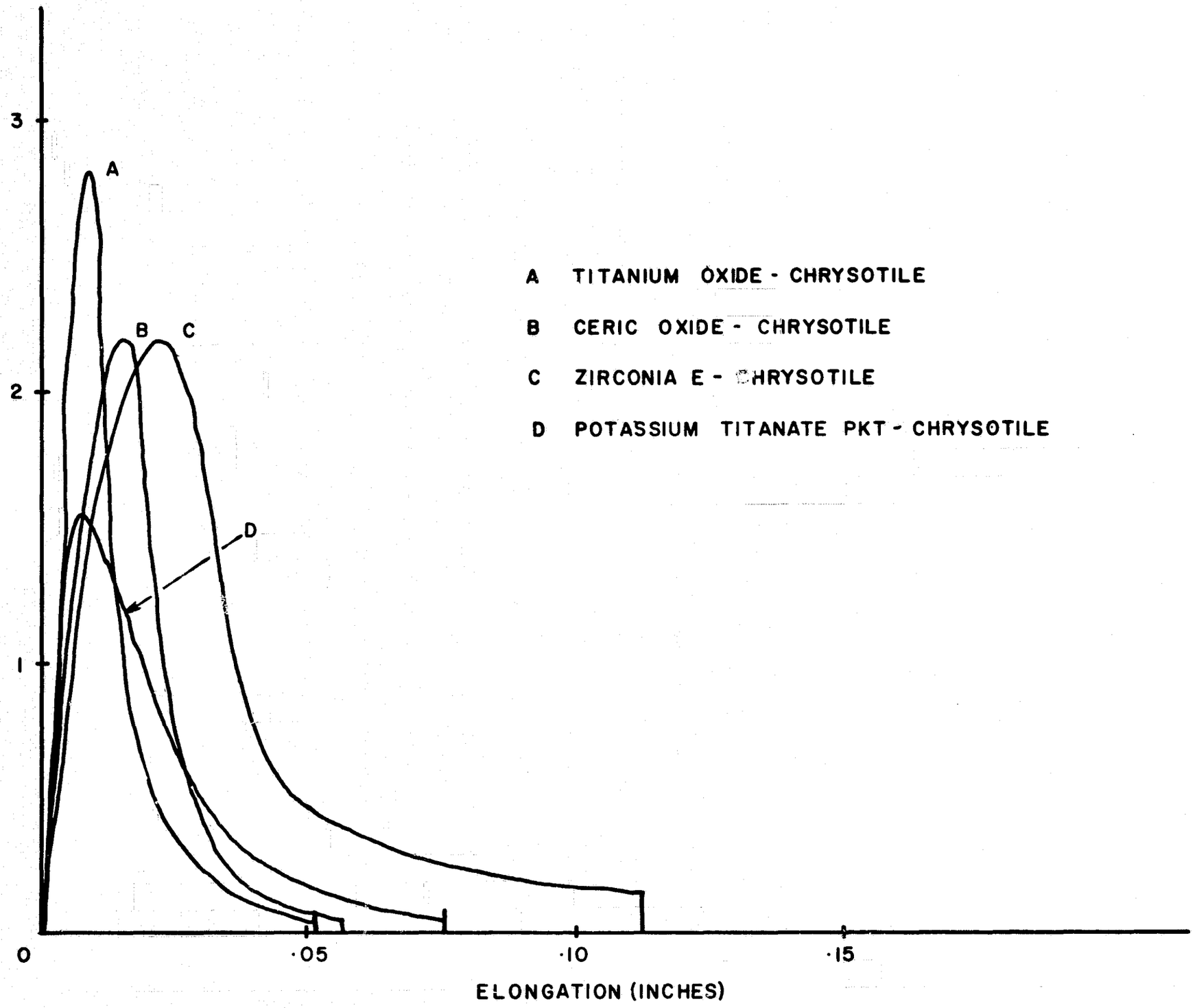

A TITANIUM OXIDE - CHRYSOTILE

B CERIC OXIDE - CHRYSOTILE

C ZIRCONIA E - CHRYSOTILE

D POTASSIUM TITANATE PKT - CHRYSOTILE

Figure 28. Tensile-Elongation Curves for Pressed Mats.

Table 9

Tensile Tests of Pressed Mats

Specimen	Thickness	Load (lbs.)*	Tensile Strength (psi)
Ceric Oxide-Chrysotile	.020"	.715	17.9
Ceric Oxide-Chrysotile	.020"	.895	22.4
Ceric Oxide-Chrysotile	.060"	4.06	33.8
Ceric Oxide-Chrysotile	.060"	2.295	19.2
Titanium Oxide-Chrysotile	.020"	.71	17.7
Titanium Oxide-Chrysotile	.020"	.54	13.5
Titanium Oxide-Chrysotile	.060"	3.18	25.6
Titanium Oxide-Chrysotile	.060"	2.89	24.1
Potassium Titanate PKT-Chrysotile	.020"	.550	13.7
Potassium Titanate PKT-Chrysotile	.020"	.505	12.6
Potassium Titanate PKT-Chrysotile	.060"	1.955	16.3
Potassium Titanate PKT-Chrysotile	.060"	1.615	13.5
Zirconia E-Chrysotile	.020"	.620	15.5
Zirconia E-Chrysotile	.020"	.725	18.1
Zirconia E-Chrysotile	.060"	2.305	19.3
Zirconia E-Chrysotile	.060"	2.20	18.4
Fuel Cell Asbestos **	.020"		150
Fuel Cell Asbestos **	.060"		80-170

* Load on a 2" wide cross-section of the listed mat thickness
** Results from Task 1 of the program.

Table 10

Density of Pressed Mats

Specimen Identification	Actual Density	Apparent Density	% Void Volume
Ceric Oxide-Chrysotile			
.020" Thickness	6.24 g/cc	1.64 g/cc	74
.060" Thickness	6.18 g/cc	1.80 g/cc	71
Zirconia E-Chrysotile			
.020" Thickness	4.97 g/cc	0.67 g/cc	86
.060" Thickness	5.39 g/cc	0.72 g/cc	87
Potassium Titanate PKT-Chrysotile			
.060" Thickness	3.59 g/cc	0.47 g/cc	87
Titanium Oxide-Chrysotile			
.020" Thickness	3.67 g/cc	0.98 g/cc	73
.060" Thickness	3.85 g/cc	1.16 g/cc	70

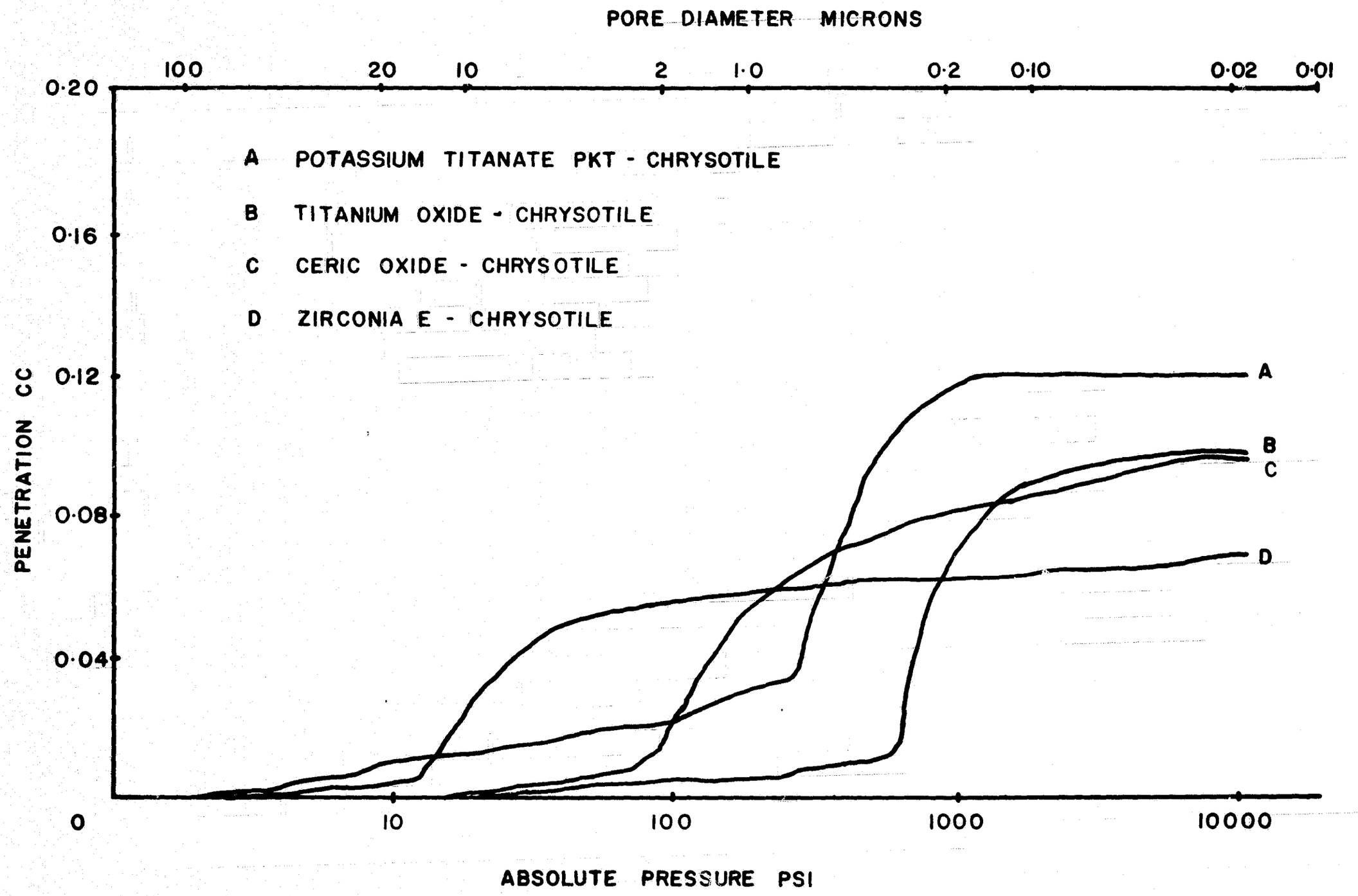

Figure 29. Pore Size Distribution Curves for Pressed Mats.

contains pores mostly in the 10-micron range. As will be seen later, this relatively large pore size of the zirconia mat results in poor gas-sealing behavior compared to the other mats.

Mercury intrusion curves could not be obtained on the new Fuel Cell Grade Asbestos mats studied in Task 1 because their flexibility caused them to collapse under the mercury pressure.

4. Electrolyte Absorption and Retention

The technique used for this test was essentially that described in the Task 1, except that in the recent tests all the manipulations - weighing, saturating centrifuging, etc. - have been performed without transferring the specimen from its supporting screen. The mats, when saturated with KOH electrolyte, are too fragile to permit such a transfer. The results from these tests are summarized in Table 11.

As a basis on which to compare these results, it is recalled that the 20-mil asbestos absorbed 3.8 times its weight in KOH, and the 60-mil mat absorbed 5.6 times its weight. On this basis, the zirconia mat and the PKT mat compare favorably with the standard asbestos in ability to abosrb electrolyte. The mats made from the powders (ceria and titania) do not compare as favorably with the asbestos. Part of this difference is due to the higher density of the powders compared with the chrysotile asbestos. If this density difference is corrected for, however, these mats still have only about one half the absorbancy of asbestos on a volume-to-volume basis.

The ability of the mats to retain electrolyte under the action of an acceleration force of 25g compares well with the asbestos mats. The mats made from the zirconia fiber lose significantly more than the others. However, the ability of the 60-mil zirconia mat to retain 78% of the electrolyte during the test is about the same as was experienced with the 60-mil asbestos mats.

5. Electrolytic Resistance

The measuring cell was changed to accommodate the pressed matrix specimens. When the chrysotile matrices were tested, the specimens were simply clamped between the cell halves and permitted to expand freely. However, these pressed matrices disintegrate when saturated with electrolyte, and consequently, a physical support was required for this test. The cell was modified by installing between the cell halves a Plexiglass sheet (1/8 inch thick) with a 5/8 inch hole bored coaxial with the 1/2" diameter hole that forms the electrolyte channel, Figure 30. This arrangement provides a chamber in which the specimen can be mounted between double layers of supporting metal screen. Under these conditions, the specimen can attain a maximum thickness of about 60 mils.

A question of data interpretation arises. The exposed diameter of the specimen is now 5/8 inch rather than 1/2 inch. This constitutes an area increase of 56%. However, this increased area is a rim 1/16 wide lying outside the region of rectilinear electrical flow lines. The degrees to which this rim area contributes to the total specimen conductivity is not known.

Table 11

Electrolytic Absorption and Retention

Specimen	Thick. Inches	Wt. of Spec. gm	Wt. of Absorb. Solution, gm	Weight Ratio Absorbed	Weight of Retained Soln. gm	Weight Ratio Retained	% Retained
Ceric Oxide-Chrysotile	.020	.4090	.4884	1.19	.4755	1.16	
Ceric Oxide-Chrysotile	.020	.3856	.5671	1.47	.5218	1.35	
			Average	1.33	Average	1.26	95
Ceric Oxide-Chrysotile	.060	1.5494	1.6199	1.04	1.4770	.95	
Ceric Oxide-Chrysotile	.060	1.3713	1.4249	1.04	1.3153	.96	
			Average	1.04	Average	.96	92
Titanium Oxide-Chrysotile	.020	.2351	.4189	1.78	.4088	1.74	
Titanium Oxide-Chrysotile	.020	.2215	.4172	1.88	.4055	1.83	
			Average	1.83	Average	1.78	97
Titanium Oxide-Chrysotile	.060	.7374	1.0564	1.43	1.0439	1.42	
Titanium Oxide-Chrysotile	.060	.7589	1.0930	1.44	1.0809	1.42	
			Average	1.44	Average	1.42	98
Zirconia E-Chrysotile	.020	.1273	.7966	6.26	.6295	4.94	
Zirconia E-Chrysotile	.020	.1702	.8589	5.05	.6525	3.88	
			Average	5.66	Average	4.38	77
Zirconia E-Chrysotile	.060	.4871	1.6911	3.47	1.3520	2.78	
Zirconia E-Chrysotile	.060	.4802	1.6374	3.41	1.2513	2.60	
			Average	3.44	Average	2.69	78
PKT-Chrysotile	.020	.0941	.6201	6.59	.5367	5.70	
PKT-Chrysotile	.020	.1029	.6639	6.45	.6171	6.00	
			Average	6.52	Average	5.85	90
PKT-Chrysotile	.060	.3546	1.6558	4.67	1.6310	4.60	
PKT-Chrysotile	.060	.3494	1.6310	4.67	1.5856	4.54	
			Average	4.67	Average	4.57	98

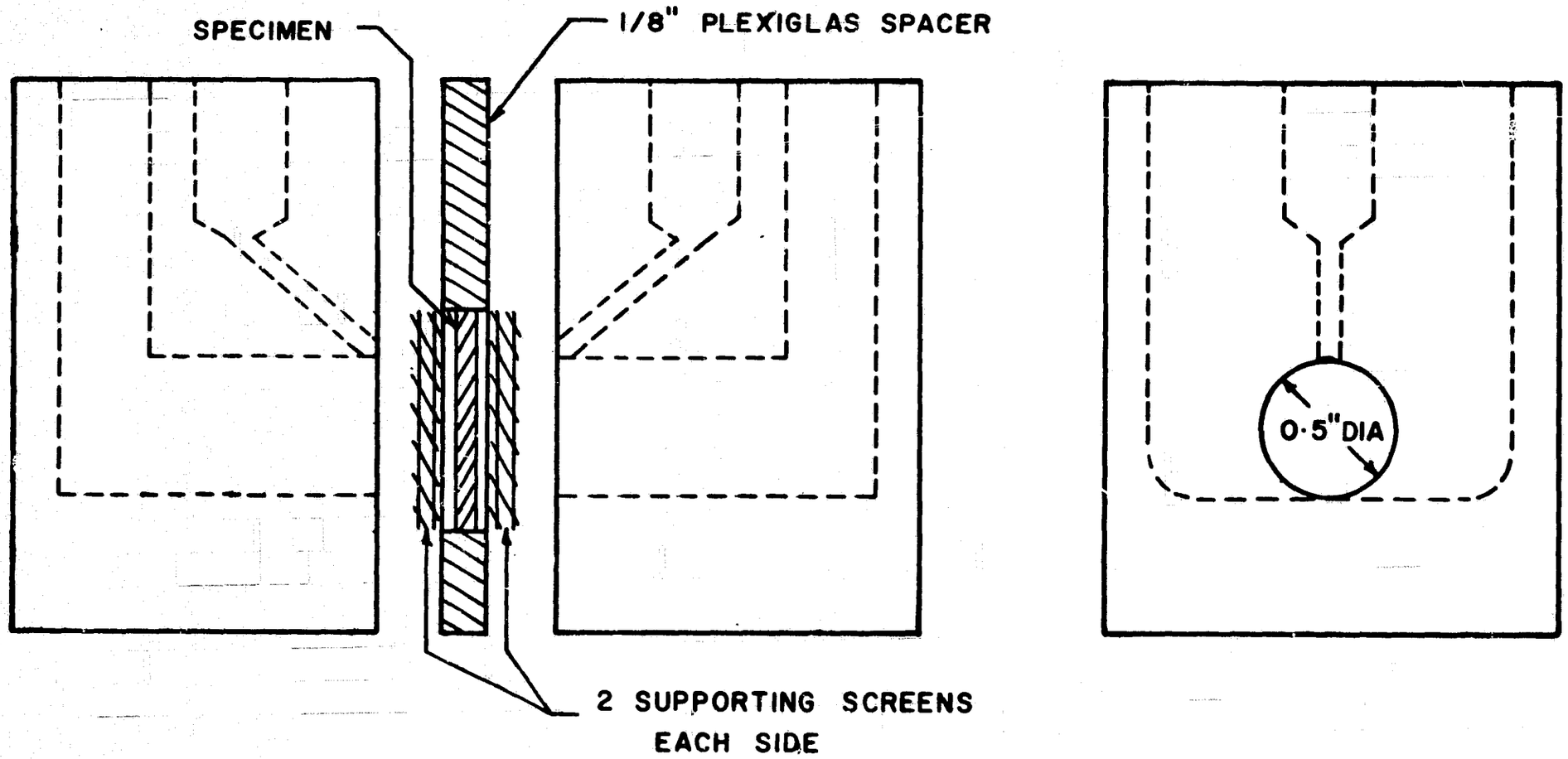

Figure 30. Electrolytic Resistance Cell - Modified.

Also, the degree to which the supporting screens reduce the effective specimen area is not known. A test was therefore performed to provide a factor of relationship between the total geometric area and the effective conducting area of the supported specimen.

For this test we selected Ace-Sil, a well-bonded non-swelling microporous rubber separator material of 27-mil thickness. A piece of this material was first tested without, and then with, the Plexiglass separator and supporting screens. First, the specimen was mounted directly between the test-cell halves so that a 1/2 inch diameter disk of surface was fully exposed to the electrolyte. Data from this test yielded the true electrolytic resistance of the specimen.

In the second test, the specimen, trimmed to 5/8" diameter, was mounted between the double layers of supporting screen in the Plexiglass recess between the test cell halves. The results of this test indicated just about four times the resistance of the unsupported specimen.

Accordingly, in the data reported for electrolytic resistance (Table 12), the computations are based on the full specimen area (1.98 cm^2) and the final value of resistance is reduced by the factor of four. In order to establish a basis of relationship, specimens of chrysotile were also measured and the data are included in Table 12.

Incidentally, inasmuch as the supporting screens are used in pairs on each side of the specimen, the question arose, whether the orientation of the contiguous screens influences the effective conducting area. Tests were, therefore, performed using the Ace-Sil membrane with the screens oriented wires-parallel and the wires-crossed 45°. The data were practically identical, and we conclude that screen orientation is not critical.

The data listed in Table 12, show several significant things. First, the resistance of the Fuel Cell Asbestos as measured by this modified test rig was about one-half of that determined by the original test rig in Task 1 of the program. This probably can be attributed to the restricted degree of swelling that can take place in the modified test rig. The second observation is that all the mats tested in this part of the program showed less resistance to ionic conduction than the Fuel Cell Grade Asbestos mats.

6. Gas Permeability

The gas that permeates the specimen under a pressure differential is measured by a water bubbler. As expected, all the dry mats are permeable (Table 13). The ratio of pressure

Table 12

Electrolytic Resistance of Pressed Mats

(Current 87 ma, Specimen Area 1.98 cm^2

Specimen	Thickness (inches)	R of Mat* (ohm-cm^2)	Specific Resistances (ohm-cm)
Potassium Titanate (PKT)	0.020	0.209	4.13
	0.020	0.218	4.30
Zirconia E	0.020	0.198	3.90
	0.020	0.181	3.58
	0.020	0.180	3.55
	0.060	0.228	1.50
	0.060	0.226	1.49
	0.060	0.226	1.49
Titanium Oxide	0.020	0.170	3.36
	0.020	0.176	3.47
	0.060	0.285	1.87
	0.060	0.260	1.71
Ceric Oxide	0.020	0.213	4.20
	0.020	0.202	3.98
	0.060	0.319	2.10
	0.060	0.306	2.01
Fuel Cell Asbestos	0.020	0.24	4.74**
	0.060	0.36	2.37**

* These derived values of resistance incorporate the assumption that all specimens swell to fill completely the 0.060-inch thick space between the supporting screens and, therefore, replace a 0.060-inch thick layer of KOH solution. This may account for the general difference between the computed values for the 0.020-inch and 0.060-inch thick mats.

** These values compare with values of 9 ohm-cm for the 20-mil paper and 5.5 ohm-cm for the 60-mil mat determined during Task 1 of the program on the unmodified test apparatus.

Table 13

Gas Permeability of Dry Pressed Mats

Specimen	Thick. (inch)	Net Pressure (psi)	Flow Rate (Bubbles/sec)
Zirconia E-Chrysotile	.060	.09	1.4
Zirconia E-Chrysotile	.060	.11	4.0
Zirconia E-Chrysotile	.060	.11	2.0
Zirconia E-Chrysotile	.060	.13	4.0
Zirconia E-Chrysotile	.060	.08	2.0
Zirconia E-Chrysotile	.060	.09	4.0
Zirconia E-Chrysotile	.020	.05	1.5
Zirconia E-Chrysotile	.020	.06	4.0
Zirconia E-Chrysotile	.020	.05	2.0
Zirconia E-Chrysotile	.020	.06	4.0
Zirconia E-Chrysotile	.020	.06	1.8
Zirconia E-Chrysotile	.020	.06	4.0
PKT-Chrysotile	.020	.07	3.0
PKT-Chrysotile	.020	.07	-
PKT-Chrysotile	.020	.07	3.0
PKT-Chrysotile	.060	.07	1.8
PKT-Chrysotile	.060	.07	1.6
PKT-Chrysotile	.060	.07	1.7
Titanium Oxide-Chrysotile	.060	.32	1.5
Titanium Oxide-Chrysotile	.060	.32	1.4
Titanium Oxide-Chrysotile	.020	.22	3.0
Titanium Oxide-Chrysotile	.020	.22	2.7
Ceric Oxide-Chrysotile	.060	.22	2.0
Ceric Oxide-Chrysotile	.060	.22	1.9
Ceric Oxide-Chrysotile	.020	.11	3.0
Ceric Oxide-Chrysotile	.020	.11	3.0

differential to flow ratio in terms of bubbles per second was calculated for each test. This ratio reveals a satisfactory consistency of the data for the potassium titanate, the titania, and the ceria mats. In each case, the thin mats are more permeable than the thick ones, and in the case of the powders (titania and ceria) the permeabilities are related inversely as the mat thicknesses. The more loosely-packed zirconia fiber mats reveal very little consistency of the test data.

Gas permeability data for the wet mats are recorded in Table 14. The net pressure recorded for each specimen is the pressure (with gradual increase) at which gas leakage was first detected. The ceria, titanate, and the PKT mats demonstrated good gas sealing characteristics (particularly in the 60-mil mats) when they contain electrolyte in the 1:1 weight ratio. At higher electrolyte loadings, these mats leak gas because of loss of structural integrity.

The zirconia-fiber mats generally did not have as high a bubble pressure as the others. However, they were ablt to hold more electrolyte and still retain their structural integrity, so that the best gas sealing properties were obtained at electrolyte loadings generally greater than the 1:1 ratio.

Although the gas sealing properties of these mats may be ample for cell application, they are generally inferior to fuel cell asbestos in this respect.

7. Liquid Permeability

Liquid permeabilities were measured by allowing water, under the pressure of a vertical column, to flow through the supported specimen. The average head of water pressure was 119.4 cm and the volume of water passed in a test was 1.12 ml. The results of these tests are shown in Table 15. Generally, these mats are considerably more permeable to liquid flow than the Fuel Cell Asbestos mats tested in Task 1.

In a general way, these data correlate with the gas permeabilities of the dry mats (Table 6). That is, the mat compositions that are the most permeable to gas also are the most permeable to liquid flow as indicated by short flow times in the liquid permeability tests. These data also have some correlation to the electrolytic resistance tests (Table 5) is that the asbestos has the highest resistance to both the liquid flow and electrolytic current flow, and the zirconia mats show the least resistance in these two tests.

8. Electrochemical Degradation

Electrochemical degradation tests have been performed on the four mat compositions studied in this program by the experimental

Table 14

Gas Permeability of Wet Pressed Mats

Specimen	Thick. (inch)	Electrolyte Ratio	Net* Pressure (psi)	Flow Rate (Bubbles/sec)
Ceric Oxide-Chrysotile	.060	1 : 1	12.2	2.0
" " "	.060	1 : 1	12.2	.6
" " "	.020	1 : 1	0	Ruptured
				4.0
Titanium Oxide-Chrysotile	.060	1 : 1	12.2	3.0
" " "	.060	1 : 1	9.3	4.0
" " "	.020	1 : 1	0	Ruptured
" " "	.020	1 : 1	1.9	3.0
PKT-Chrysotile	.060	1 : 1	6.1	2.4
" "	.060	1 : 1	6.9	3.0
" "	.060	1 : 1	11.5	2.3
" "	.020	1 : 1	0.1	3.0
" "	.020	1 : 1	0.3	Ruptured
" "	.020	1 : 1	0.6	1.8
Zirconia E-Chrysotile	.060	1 : 1	1.5	First Leakage
" "	.060	2 : 1	2.2	First Leakage
" "	.060	3 : 1	0	Ruptured
" "	.060	1 : 1	1.2	First Leakage
" "	.060	2 : 1	1.9	First Leakage
" "	.060	3 : 1	2.0	First Leakage
" "	.060	1 : 1	0.4	First Leakage
" "	.060	2 : 1	1.4	First Leakage
" "	.060	3 : 1	0	Ruptured
" "	.020	1 : 1	0.4	First Leakage
" "	.020	1 : 1	0.4	First Leakage
" "	.020	1 : 1	0.3	First Leakage

* This is the pressure at which bubbling first occured, so it may be considered the "bubble pressure" of the specimen.

Table 15

Liquid Permeability of Pressed Mats

Specimen	Thickness (inch)	Average Flow Time (sec)*
Zirconia E-Chrysotile	.020	Too rapid to measure
	.060	14.7
Potassium Titanate PKT-Chrysotile	.020	9.1
	.060	36.5
Titanium Oxide- Chrysotile	.020	52.9
	.060	168.7
Ceric Oxide-Chrysotile	.020	5.8
	.060	42.8

* Time required to flow 1.12 ml of water through a 1/2" diameter circular area of mat at an average head of 119.4 cm of water.

procedure described above under Task 1. None of these tests showed any obvious contamination of either the electrolyte or of the electrodes. The only indication noted was a light gray deposit on the cathode during the testing of the PKT mat. In all other tests, the electrodes remained clean and bright. The electrolyte specimens and electrode wash solutions were also free of contaminant detectable by spectrography.

D. Conclusions From Task 2 Results

1. All the natural asbestoses, being silicates, are inherently reactive with KOH and will not survive long immersion in hot concentrated KOH solutions. Chrysotile in the form of Fuel Cell Asbestos is superior to the other asbestoses in its resistance to KOH and in containing only traces of electrochemically reactive constituents or impurities.

2. TX fiber, a natural magnesia, is unsuitable because of its high content of iron, which is apparently an essential element of the fiber structure.

3. Boron nitride and silicon carbide fibers dissolve in KOH solution.

4. Zirconia fiber has excellent resistance to attack by KOH, but the fibers are extremely fragile.

5. Titania and PKT both react slowly with hot KOH to form insoluble products - probably hydrated titanates. The products may be useful as a matrix component.

6. Ceria is essentially unchanged by KOH under the most destructive test conditions.

7. The composites of chrysotile with zirconia, PKT, and ceria are essentially cakes of the granular material with somewhat improved dry strength due to the chrysotile fibers. When saturated with KOH solution, they lose almost all cohesion. The chrysotile fiber is still vulnerable to attack by the KOH, and consequently its influence on mat properties must be regarded as temporary.

It must be concluded that these composites incorporating chrysotile fail to show any significant advantages over Fuel Cell Asbestos paper in overall properties.

X TASK 2A. - MATRICES INCORPORATING ORGANIC BINDERS

Task 2a is an extension of the original project to include the testing of selected organic materials as binders for the inorganic powders that were previously shown to be good matrix materials. The requirement of resistance to chemical attack by hot KOH reduces the choice of materials to hydrocarbons and Teflon. Of the polymeric hydrocarbons, only polypropylene has the required temperature service range. Teflon is available as powder, emulsion, and fiber, and the temperature range for Teflon is more than adequate.

Both these organic materials are very hydrophobic and, therefore, in proportion to concentration in a matrix, tend to reduce the absorbancy of aqueous electrolyte. Therefore, a satisfactory matrix requires the proportion of inorganic powder and organic binder that has satisfactory strength and also satisfactory absorbancy and gas sealing capabilities.

A. Composition of Mat Components

Zirconia powder was tested in this Task and was a component of the best matrices. As reported by the manufacturer, Zirconium Corporation of America, the composition of zirconia is:

$ZrO_2 + HfO_2$	99.0%	Fe_2O_3	0.10%
SiO_2	0.18%	Al_2O_3	0.16%
CaO	0.22%	TiO_2	0.11%
MgO	0.15%		

The other inorganic materials studied in this task included PKT, ceria, magnesia, magnesium titanate, and titanium dioxide. The organic components used were Teflon and polypropylene. Teflon was used in the forms of chopped floc, which is pure Teflon, and Teflon emulsion - an aqueous suspension stabilized with Triton X-100. Ultimately Teflon 6 extrusion powder was used; this is a pure teflon powder. The polypropylene chopped floc and felted fiber are pure hydrocarbon.

B. Chemical Degradation Tests

The prospective matrix component materials individually and in the proposed mixtures, were tested as described previously. Those materials with better resistance to KOH were carried through the entire range of tests. Others were tested only sufficiently to demonstrate their inadequacy.

In view of the fact that Teflon is the material adopted for the matrices with the best promise, it should be noted that in most instances, the material under test was contained in a Teflon bottle. Therefore, the tests of materials individually are really tests of that material with Teflon.

Like the mat materials tested previously, mats formed from these materials disintegrated completely in the KOH. The insolubles were recovered by filtration, washed, dried and weighed. The weight change is reported in terms of percent of the original specimen weight.

Results of these tests are reported in Tables 16, 17, 18, 19, 20. Figures in the rectangles are the percent changes in weight. Data for the 100 hour tests are recorded above the slash lines: data for 1000 hour tests are below. Where tests were duplicated, the results are recorded individually.

Ceria and zirconia were virtually unchanged during these tests. PKT lost weight slightly in the more moderate tests, but then gained weight in the more severe tests. The gain suggests reaction with the KOH to form an insoluble higher titanate, or perhaps an insoluble hydrate. This change also seems to modify or destroy the short-fiber aspect of the PKT crystals.

Magnesia was converted completely to a gelatinous hydrate. Magnesium titanate reacted to form, probably, an insoluble potassium titanate and insoluble hydrated magnesia. Titanium dioxide apparently formed a potassium titanate.

Polypropylene felt was tested at temperatures including 150°C, which exceeds the recommended service limit. In all tests, the polypropylene seemed entirely unchanged.

C. Properties of Pressed Matrices

1. Mat Preparation

Our first attempts to prepare composite matrices with organic binders were adaptations of the "sheet casting" methods described previously. The components, with sufficient water to form a mobile slurry, were mixed in an electric blender. The slurry was then quickly suction filtered in a Buchner funnel, and the moist cake was finally compacted in a hydraulic press.

The organic binders specified for test were Teflon fiber, Teflon emulsion, and polypropylene fiber. Teflon fiber and polypropylene fiber were procured as floc, in 6.7 denier and 1.8 denier, respectively, and chopped to several lengths. The one-

Table 16. Chemical Degradation Tests of PKT

WEIGHT CHANGE OF SPECIMENS IN PERCENT

Specimens: Potassium Titanate (PKT)

100 Hr. / 1000 Hr.	50°C		100°C		150°C		200°C	
30% KOH	+28.1	+3.9	-4.0		-0.4			
40% KOH	+31.2	+3.5	+21.1	+27.3	+9.1	+11.4		
50% KOH	+47.2		-8.2		-0.6		+33.4	+ 0.4 +31.4
60% KOH	+113.6		-1.6	+38.4	+33.0	+32.1	+63.4	+58.3

Table 17. Chemical Degradation Tests of Ceria

WEIGHT CHANGE OF SPECIMENS IN PERCENT

Specimens: Ceric Oxide

100 Hr. / 1000 Hr.	50°C	100°C	150°C	200°C
30% KOH	-1.4 / -1.3	+0.1 /	-1.4 /	/
40% KOH	-0.7 / -1.9	-1.5 / - 0.1	-4.3 / -0.3	/
50% KOH	/	-0.5 /	-0.5 /	-1.6 / -3.0 -1.9
60% KOH	/	-0.8 / -1.1	-5.3 / -0.5	-1.0 / -2.0 -1.6

Table 18. Chemical Degradation Tests of Zirconia

WEIGHT CHANGE OF SPECIMENS IN PERCENT

Specimens: Zirconium Oxide Fiber

100 Hr. / 1000 Hr.	50°C	100°C	150°C	200°C
30% KOH	-0.3	-0.1		
40% KOH	-0.4	0 -0.2	-0.7 -0.4	
50% KOH		-0.1	-0.4 -0.3	-0.4 -5.6 -1.4
60% KOH		-0.3 -0.3	-1.5 -3.0	-0.9 -5.3 -3.3

Table 19. Chemical Degradation Tests of Titanium Oxide

WEIGHT CHANGE OF SPECIMENS IN PERCENT

Specimens: Titanium Oxide TiO_2

100 Hr. / 1000 Hr.	50°C	100°C	150°C	200°C
30% KOH	-0.3 / +1.9	+6.4 /	+11.7 /	/
40% KOH	+5.2 / +8.4	+8.2 / +25.7	+29.6 / +50.4	/
50% KOH	/	+77.7 /	+83.3 /	+47.2 / +31.0 +36.3
60% KOH	/	+67.8 / +77.7	+64.9 / +88.7	+113.6 / +5.6 +48.0

Table 20. Chemical Degradation Tests of Polypropylene Felt

WEIGHT CHANGE OF SPECIMENS IN PERCENT

Specimens: Polypropylene Felt

100 Hr. / 1000 Hr.	50°C	100°C	150°C	200°C
30% KOH		(0) -2.6	(0) -2.4	
40% KOH		(0) -2.7	(0) -0.2	
50% KOH		(0.2) -2.9	(0) -1.8	
60% KOH		(0.3) -3.2	(0) -2.3	

( ) insolubles in the KOH

eighth and one-sixteenth inch lengths seemed to be appropriate for this purpose.

When these organic fibers, both hydrophobic, were blended with hydrophyllic and more dense inorganic solids in a fluid slurry, upward segregation of the fibers began immediately upon cessation of vigorous mixing. Consequently, the organic fibers were invariably concentrated in the upper levels of the filter cake and the final pressed mat.

This effect could be somewhat moderated by adding suitable surfactants to the mixture. However, being hydrophobic and also less dense than water, polypropylene floc segregates almost completely from the slurry. The polypropylene floc was therefore quickly rejected as a useful matrix component.

In mixtures with PKT and ceria, the segregation of Teflon floc was only partial, a small amount of the Teflon remaining in the bottom layers. Several matrices were made by compressing two such filter cakes, face-to-face, so that the Teflon floc-rich layers formed the outer surfaces, supporting the fiber-deficient middle layer. As anticipated, these "sandwich" matrices had moderately good gas sealing properties when wetted with KOH electrolyte solutions, but they lacked the cohesion that is desired in an acceptable matrix. It should be expected that these matrices, having so much Teflon fiber in the surface, would establish a discontinuous, high resistance, electrolytic interface at an electrode surface. This effect was not tested.

It became evident that the smooth-surface hydrophobic fibers of Teflon and polypropylene were not suited for matrix bonding.

We made several attempts to produce a matrix by loading a polypropylene felt with inorganic powder. The felt is a random packed mat of fibers, cross-locked by transverse fibers drawn through by barbed felting needles. A polypropylene felt has excellent properties of strength and flexibility, but the needle punctures, and the transverse hydrophobic fibers form paths for gas leakage. We believed that, if such a fiber structure could be loaded with PKT or ceria, the composite might be sufficiently hydrophyllic to absorb electrolyte and seal against gas transfer. Several attempts to infiltrate a loose polypropylene felt with PKT were complete failures, and we desisted these efforts in favor of a completely different and more promising technique.

Teflon emulsion was tested as a binder for PKT, ceria, and zirconia fiber. Teflon 308 emulsion, sufficient to provide 5 weight percent of Teflon solids in the final composite, was dispersed in water and stirred vigorously in the blender until coagulation occurred. The inorganic powder or fiber was then added and blended. The slurry was quickly filtered with suction and the moist cake was compacted with a small hydraulic press.

These composites were completely unsatisfactory; they were weak and brittle when dry and disintegrated when wet.

The several composites containing zirconia E fiber proved to be entirely unsatisfactory because of the pronounced fragility of the fibers. Under very moderate compacting force, the zirconia fibers disintegrated to a fine powder, and matrix cohesion was lost. The vendor stated that the extreme fragility of the zirconia fiber is a problem without prospect of correction with current technology.

2. Selection of Matrices for Testing

In consultation with the NASA Project Manager, we selected six pressed matrices for the following preliminary tests: electrolyte absorption and retention bubble pressure, and electrolytic resistance. Two specimens of each matrix were tested. The identities of these matrices are listed below.

Specimen No.	Composition
1	75% PKT + 25% Teflon Emulsion (30B) (Filtered and pressed)
3	95% PKT + 5% Teflon floc (Filtered and pressed - two 0.030 cakes pressed face-to-face with Teflon fiber rich regions at surfaces.)
8	80% PKT + 18% zirconia fiber + 2% Teflon floc (Filtered and pressed)
9	85% PKT + 10% Pretreated PKT + 5% polypropylene floc (Filtered and Pressed) (PKT was pretreated in molten KOH for 5 minutes and washed free of KOH)
10	98% Ceria + 2% Polypropylene floc + $Mg(OH)_2$ (Filtered and Pressed - two cakes pressed face-to-face to form a matrix with floc concentrated in outer surfaces. $Mg(OH)_2$ amounting to 1% of ceria weight was added to aid in sealing against gas transfer.
11	Similar to (10) except that $Mg(OH)_2$ amounting to 10% of the ceria weight was added.

3. Electrolyte Absorption and Retention

The pressed matrices wet readily by capillarity, but lose practically all strength when saturated. Therefore, the specimens were supported on a metal screen and were handled with

special care to prevent accidental loss of the matrix material. The specimen was placed in a shallow pool of solution and permitted to become saturated by spontaneous absorption. A few drops of solution were placed on the top surface to ensure complete flooding of the specimen. The specimen, on its supporting screen, was then placed several times on dry filter paper to remove the visible excess of solution, and then weighed.

The saturated specimen was then subjected to 25g acceleration in the centrifuge and weighed again.

The results of these tests are recorded in Table 21.

4. Gas Permeability Tests (Bubble Pressure)

The pressed matrices were tested in accord with the original test specifications, namely, that each specimen is to be tested dry, and at specimen: electrolyte proportions of 1:1, 1:2, 1:3 etc. to saturation. The apparatus for test was designed to contain any effluent gas and permit escape to atmosphere through a sensitive bubbler which served as leakage detector. The specimen is mounted between two slabs of Plexiglass, each milled out to form a shallow gas chamber at each face of the specimen. Several layers of fine-mesh metal screen were installed in the gas chambers to provide physical support for the specimen. The influent side was connected to a compressed air source equipped with sensitive pressure gages and controls. The effluent side was connected to the bubbler, so that gas leakage through the specimen was detected quickly by reaction of the bubbler.

The specimen was weighed and installed, dry, in the mount. The required measured amount of electrolyte was then placed on the specimen surface and permitted to abosrb by capillarity. Because the rim region of the specimen is clamped in the mount, thus modifying its capacity to absorb electrolyte, one does not know the true proportion of specimen to electrolyte when the value is nominally 1:1 or 1:2. Only the saturated condition is known with any assurance. Also, because the specimens were composites of hydrophyllic with hydrophobic materials, the electrolyte is probably not uniformly distributed through the specimen. Consequently leakage is to be expected at the more prominently hydrophobic locations.

Gas permeability data for small specimens are recorded in Table 22.

5. Electrolyte Resistance

Like the pressed matrices tested previously, these matrices lose almost all structural cohesion when saturated with KOH. They were therefore mounted between double layers of supporting

Table 21

Electrolyte Absorption and Retention of Pressed Matrices

Spec. No.	Thick. (inch)	Wt. (g)	Absorption Electrolyte (g)	Ratio Electrolyte/ Spec	Electrolyte Retained (g)	% of Original
1a	0.06	0.3682	1.3369	3.6	1.2824	95.9
1b	.06	0.3607	1.3999	3.9	1.2939	92.4
3a	0.06	0.4449	1.5401	3.5	1.4755	95.8
3b	.06	0.4657	1.5855	3.4	1.5129	95.4
8a	0.062	0.3770	1.5999	4.2	1.5374	96.1
8b	.062	0.4399	1.7901	4.1	1.7300	96.6
9a	0.070	0.5538	1.3880	2.5	1.3364	96.6
9b	.070	0.4955	1.2907	2.6	1.2170	94.3
10a	0.070	2.4175	1.0260	0.4	0.6760	65.9
10b	.070	2.3040	0.9943	0.4	0.6706	67.4
11a	0.070	2.3036	0.7486	0.3	0.7163	95.7
11b	.070	2.1889	0.7472	0.3	0.7114	95.2

Table 22

Gas Permeability of Pressed Matrices

(Specimens 1-inch Diameter)

Spec. No.	Matrix Comp.	Thick. (inch)	Electrolyte Matrix Wt.	Spec. 1 Bubble Pressure (psi)	Spec. 2
1	PKT 75% Teflon Emulsion #41 25%		Dry 1:1 2:1	0.41 0.98 Ruptured	1.32 4.90 Ruptured
3	PKT 95% Teflon floc 5% (sandwich matrix)[1]	0.082	Dry 1:1 2:1	0.34 10.54 11.98	0.37 9.80 7.10
8	PKT 80% Zirconia fiber 18% Teflon floc 2%	0.062	Dry 1:1 2:1 3:1 4:1	0.14 0.16 1.03 6.96 Ruptured	 Disintegrated
9	PKT 85% PKT(pretreat)[2] 10% Polypropylene floc 5%	0.070	Dry 1:1 2:1 3:1	0.23 0.43 5.39 9.80	 14.70
10	Ceria 98% Polypropylene floc 2% (+ 1% $Mg(OH)_2$) (sandwich matrix)	0.070	Dry 1:1 1/2:1	0.90 would not absorb soln.	0.29 6.86
11	Ceria 98% Polypropylene floc 2% (+ 10% $Mg(OH)_2$) (sandwich matrix)	0.070	Dry 1/2:1	1.96 7.35	0.68 5.14

[1] Made by pressing together two cakes, face-to-face.

[2] Treated with molten KOH, rinsed, and dried.

screen in the specimen holder described earlier. The calculated values of electrolytic resistance are reported in Table 23.

6. Conclusions Pertaining to Pressed Mats

These pressed matrices lack the dry and wet strength required for practical use. They are brittle when dry and semi-fluid when wet. Evidently the preformed fibers of Teflon and polypropylene are too coarse to serve as effective binders of the composite when present at low concentration. Teflon emulsion is ineffective as a binder when the mixture is simply compacted by pressing.

Although a fiber reinforced matrix might be prepared by loading a preformed polypropylene felt with PKT, ceria, or zirconia, we believe that such a composite would be brittle when dry and mushy when saturated.

We conclude, therefore, that matrices of these types were poor prospects for continued development.

As an alternate and improved method of preparing mats, reinforcement by powdered Teflon was investigated. Teflon fibrils are produced from this powder during mat preparation and give the processed mat improvements over the pressed mats described above. These fibrilated-Teflon-bonded mats are discussed in the following section of this report.

Table 23

Electrolytic Resistance of Pressed Matrices

Specimen	Thick. (inch)	Potential (volts)	Specific Resistance (ohm cm^2)
1a	0.06	0.0567	0.066
1b	0.06	0.0593	0.081
3a	0.062	0.0582	0.075
3b	0.062	0.0586	0.078
8a	0.060	0.0607	0.089
8b	0.068	0.0604	0.087
9a	0.075	0.0596	0.083
9b	0.075	0.0606	0.089
10a	0.075	0.0780	0.187
10b	0.072	0.0712	0.094
11a	0.078	0.0758	0.175
11b	0.078	0.0730	0.159
Blank	- - -	0.0550	
Blank	- - -	0.0544	

D. Matrices Bonded by Fibrilated Teflon

This bonding function is based on the unusual tendency of Teflon 6 extrusion powder to convert to fibers under very mild shearing forces. The fibering property of Teflon 6 appears above a transition temperature at 19°C and becomes more pronounced with temperature increase. The diameter and extension of the fibers are illustrated in Figure 31, an electron micrograph prepared by E. I. duPont de Nemours Company. The fibrilation evident in this specimen was incurred entirely incidentally to the manipulation involved in mounting the Teflon powder for examination.

The technique recommended by duPont Company for exploitation of Teflon 6 properties is described as their HS-10 Process. It consists of rolling the Teflon 6 powder, or the mass containing Teflon 6 powder, to produce a flat sheet. The sheet is then folded double or triple and rolled again at right angles to the previous rolling direction. This operation is repeated until optimum bi-lateral fiber development is attained. If rolling is continued beyond the optimum condition, the fibers break and general weakening of the mat follows.

1. Mat Preparation

In adapting the HS-10 process to the making of matrices, the Teflon powder is blended with inorganic solids that are readily wetted by the prospective aqueous electrolyte and are resistant to chemical attack. The hydrophobic Teflon must be present at low concentrations so that the composite mass will absorb and retain electrolyte by capillarity.

The HS-10 process includes recommendation of a lubricant - kerosene or Stoddard Solvent - to facilitate the rolling. When these lubricants are used, the high-boiling residues left in the matrix upon drying reduce or prevent wetting by the aqueous electrolyte. Consequently, we tried to produce mats by rolling the mixture dry, on a surface at 350°F, but the mass became too intractable. We also tried to use pure isopropyl alcohol as the lubricant at room temperature, but the mass failed to develop the desired coherence. With naphthol as the lubricant and processing at about 250°F, the matrix cracked upon drying. Odorless mineral spirits was finally adopted as a satisfactory lubricant. It is a more carefully refined hydrocarbon with a relatively narrow boiling range. Matrices prepared with odorless mineral spirit and dried on the hot plate at 130°C are readily wetted by water and KOH solution. In order to ensure the expulsion of hydrocarbon residues, the matrices were first dried at 130°C and finally at 100°C in a vacuum oven.

At the start of processing, the mixture of Teflon inorganic powder and mineral spirit is very weakly coherent like moist,

Figure 31. Teflon 6 Powder and Fibers.

fine sand. With shearing and rolling action, fibers begin to develop and the mixture becomes increasingly coherent, like a pastry dough. As the fiber development proceeds, the bonding of adjacent layers becomes weaker and the matrix becomes more laminar in character. Plasticity of the mass and interlayer bonding is improved by supplying more lubricant as the rolling treatment proceeds. The operator judges the processing completed when the matrix has attained a certain "toughness".

Specifically, the steps in preparing a matrix are the following:

1. The components for a single matrix are weighed.

2. The components with mineral spirits sufficient to form a mobile slurry are mixed for about 30 seconds in a Waring-type blender.

3. The slurry is filtered in a Buchner funnel under mild suction.

4. The moist cake is placed on the hot plate (250°F) and "smeared" with a metal spatula until fibrous cohesion of the mass develops.

5. The mass is then rolled with a wood rolling pin until the fiber development is judged satisfactory. Toward the end of this operation, the rolling is increasingly directed to the formation of an approximate square sheet. During this working, mineral spirit is supplied liberally to the mass to replace evaporation losses and maintain the desired plasticity.

6. A sheet of aluminum foil is placed under the matrix mass, and with metal shim strips at either side, the matrix is rolled down to the desired wet-thickness.

7. The matrix is permitted to dry on the hot plate and is then trimmed to 9" square size.

8. The matrix is placed in a vacuum oven at 100°C for about 1 hour to expel organic residues from the lubricant.

9. The matrix is placed on a flat slab of Plexiglass and, with selected shims at either side, rolled down to the desired final thickness. The thickness is measured with a dial gage at nine locations across the surface. Some matrices cannot be suitably reduced by this cold rolling treatment and must be scrapped.

10. The matrix is trimmed to 8-inch square dimensions.

After hot-plate drying (step 7), the matrix is placed on a sheet of paper for all subsequent handling and manipulation. This prevents the matrix from being stretched or torn under its own weight - a particular danger to the very dense mats of ceria and zirconia.

In a matrix, the optimum concentration of Teflon is the minimum necessary to bind the inorganic particles. The low-density PKT requires about 5% by weight of Teflon; materials of higher density, like ceria, zirconia, and magnesia require only 1% by weight.

2. Composition of Matrices Prepared for Testing

The materials chosen for matrices were PKT, ceria, and zirconium. Matrices were also prepared with magnesia and magnesium titanate, but these efforts were entirely exploratory since there was no previous knowledge of the performance of these materials in a low-temperature alkaline cell.

Teflon concentration of 5 weight percent in PKT matrices was apparently the optimum. In the ceria and zirconia matrices, Teflon concentrations of 1% and 2% were prepared and tested. Finally, 1% Teflon was adopted as the optimum for the latter two compositions. Matrices of magnesia and magnesium titanate were bonded with 5% Teflon; these were not included in the work of Task 3.

3. Chemical Compatibility

The tests of Teflon bonded matrices (reported in Tables 24, 25, 26, 27, 28) were similar to the tests of component materials described earlier. At first, all the insolubles in the KOH were recovered by filtration, washed, dried, and weighed. Later, when it became evident that most of the new matrices could be expected to remain intact during test, the procedure was modified. The matrix specimen was removed, and the KOH solution and specimen were filtered, washed and dried separately. This permitted evaluation of the change in the specimen and the quantity of insoluble material released into the KOH solution by the specimen. The quantity of free insoluble material recovered from the KOH solution is recorded with parenthesis as percent of the original specimen weight.

At temperatures below 200°C, the matrices of ceria and zirconia remain virtually unchanged in weight. PKT generally gains weight, in a few instances, in large proportion. We can offer no tenable explanation for the very large value at 100°C 60% KOH, and 100 hours.

The PKT specimens, while still saturated with KOH solution seemed unchanged but when rinsed and dried, the specimens shrank

Table 24. Chemical Degradation Tests of PKT - Teflon Matrices

WEIGHT CHANGE OF SPECIMENS IN PERCENT

Specimens: PKT Matrix - 5% Teflon

100 Hr. / 1000 Hr.	50°C	100°C	150°C	200°C
30% KOH		+6.5 / (0.0) +6.4	+8.2 / +7.3	(0.0) +4.5
40% KOH		+7.6 / +6.3	+14.4 / +5.9	(0.0) +1.7
50% KOH		+4.2 / +6.0	+2.9 / +4.5 +5.5	(0.0) +3.4
60% KOH		+118.0 / (5.9) +29.4	+19.5 / +4.1 +3.5	(0.3) -5.6

( ) insolubles in the KOH

Table 25. Chemical Degradation Tests of Ceria - Teflon Matrices

WEIGHT CHANGE OF SPECIMENS IN PERCENT

Specimens: Ceria Matrices - 1-2% Teflon

100 Hr. / 1000 Hr.	50°C	100°C	150°C	200°C
30% KOH		-0.7 / (0.2) -1.5	-0.4 / -1.8 -6.3	/ (3.7) -1.4
40% KOH		-1.0 / -2.5	-1.0 / -1.6 -2.1	/ (97.2) -100
50% KOH		-1.2 / -1.5	-0.4 / -0.9 -1.5	/ (0.0) -2.1
60% KOH		-1.9 / (0.7) -1.7	-1.3 / -2.0 -3.4	/ -100

( ) insolubles in the KOH

Table 26. Chemical Degradation Tests of Zirconia - Teflon Matrices

WEIGHT CHANGE OF SPECIMENS IN PERCENT

Specimens: ZrO_2 - 1-3% Teflon Matrices

100 Hr. / 1000 Hr.	50°C	100°C	150°C	200°C
30% KOH		(0.1) -0.7	(0) (0.1) -0.4-0.7	(0) +0.4
40% KOH		(0) -0.4	(0.3)(0.2 -0.8 -0.8	(4.1) -3.2
50% KOH		(0) -0.5	(0) (0.2 -0.5 -0.4	(7.3) -7.2
60% KOH		(0.1) -0.6	(0.4)(0.5 -0.3 -0.8	-100

( ) insolubles in the KOH

Table 27. Chemical Degradation Tests of Magnesia - Teflon Matrices

WEIGHT CHANGE OF SPECIMENS IN PERCENT

Specimens: MgO - 5% Teflon Matrices

100 Hr. / 1000 Hr.	50°C	100°C	150°C	200°C
30% KOH		(0) +33.7	(0) (0) +33.6 +32.9	(136) -100
40% KOH		(0) +34.2	(0.4) (0) +32.0 +32.2	(132) -100
50% KOH		(0) +34.5	(1.4) (1.2) +33.4 +33.3	(132) -100
60% KOH		(1.0) +31.9	(7.4) (10.5) +24.1 +28.9	-100

( ) insolubles in the KOH
NOTE: All Mats Disintegrated

Table 28. Chemical Degradation Tests of Magnesium Titanate - Teflon Matrices

WEIGHT CHANGE OF SPECIMENS IN PERCENT

Specimens: Mg Titanate - 2% Teflon Matrices

100 Hr. / 1000 Hr.	50°C		100°C		150°C		200°C	
30% KOH			-0.6	+ 0.2 +4.8	+1.1	+9.0		
40% KOH			-0.7	-0.7	+1.6	+19.6		
50% KOH			+4.7	+18.3	+12.6	+30.8 +30.3		
60% KOH			+27.5	+ 1.7 +52.9	+51.6	+46.2 +45.3		

somewhat and became stiff and brittle. The ceria specimens were apparently unchanged. The dimensions were unchanged and the corners and edges of the specimen retained their original sharp angularity. When rinsed and dried, the ceria specimens were still flexible. The zirconia specimens were similar in this attribute to the ceria matrices.

At 200°C and 1000 hours duration, the zirconia and ceria matrices began to fail by disintegration. PKT matrices did not fail similarly, although the beginning of such failure may be indicated by the specimen weight loss in 60% KOH. When the specimens disintegrated, the Teflon fibers evidently dissolved completely in the concentrated KOH. This reaction of the Teflon was contrary to the previous test results and to the generally reported inertness of Teflon in aqueous alkaline solutions. However, these tests were of very long duration and the Teflon was in a state of extremely great surface exposure, conditions that might permit a very slow reaction to produce the observed effect.

Several short but severe tests were made of the Teflon reactivity. A matrix was prepared with calcium carbonate for the inorganic filler, and the latter was dissolved in dilute HCl, leaving a mat of fibrilated Teflon. This mat was placed on molten KOH in a platinum dish and maintained above the melting temperature for about 1-1/2 hours. The KOH slowly became golden yellow and finally black, and about 2/3 of the Teflon dissolved. After cooling, the KOH was dissolved in water, and a yellow insoluble solid was formed. Tests of the solution and the solid for fluoride were negative.

In another test, a small quantity of Teflon 6 powder was placed on the surface of molten KOH, which was then heated fairly strongly. The Teflon ignited and burned vigorously. After several repetitions of this test, the KOH (entirely black in color) was diluted and tested. Fluoride ion was present in abundance.

In the compatibility tests of matrix specimens, failure by dissolution of the Teflon fibers appeared only at 200°C. The tests of 150°C for 1000 hours revealed no significant failure of the Teflon fiber. Consequently, these tests indicate that the Teflon bonded matrices may be satisfactory for long service at 150°C, but not at 200°C. They also show that fluoride ion may be formed in the electrolyte, and that a possible adverse reaction with cell components should be considered.

4. Electrolyte Absorption and Retention

The fibrilated Teflon bonded matrices did not wet to saturation by spontaneous absorption. To ensure complete saturation of the specimens, they were vacuum impregnated with KOH solution.

Each weighed specimen was sandwiched between two layers of polyprolylene screen, and after impregnation, the excess solution was absorbed from the screen surfaces by filter paper. The specimen was then weighed to determine the quantity of solution absorbed. The specimen was then tested for electrolyte retention under 25g acceleration. The test results are summarized in Table 29.

From this data, it can be seen that the PKT mats have the greatest capacity of the four types for holding electrolyte. On a volume-to-volume basis, the advantage ofPKT is this respect is significant. On a weight-to-weight basis, the relatively low density of PKT increases its advantage even more. All the mats appeared satisfactory in retaining electrolyte after a 25g test. The main variation in this property appeared to be due to mat thickness rather than to the mat material. The 20-mil mats retained 85-90% of the electrolyte after the test; the 60-mil mats retained 93-95%.

5. Gas Permeability (Bubble Pressure)

The fibrilated Teflon matrices were tested by essentially the same procedure described previously for the pressed matrices. However, the data lacked the desired consistency. We attribute this to the fact that the hydrophobic Teflon in these specimens is so completely and intimately dispersed through the mass of inorganic particles that uniform distribution of aqueous electrolyte by capillarity alone may not occur.

As expected, the specimens show no significant gas-sealing capability until they were saturated (or nearly saturated) with electrolyte (Table 30). Several matrices did not leak gas at 15 psi differential. The 20 mil thick specimens generally leaked at a low pressure differential, but the 30 mil mats were usually very much superior.

6. Electrolytic Resistance

The fibrilated Teflon bonded matrices retain integrity and strength when saturated with electrolyte and swell only slightly. Consequently, these specimens were mounted directly between the halves of the measuring cell. The net potential developed across the specimen (with correction for the blank) reflects the electrolytic resistance of the saturated specimen.

Although these Teflon-bonded matrices will absorb KOH electrolyte spontaneously, the Teflon does reduce the absorbancy somewhat, and consequently we used vacuum impregnation to ensure complete flooding of the specimen. After clamping the dry specimen between the cell halves, the cell was evaluated, filled with electrolyte and then returned to atmospheric pressure. Usually, electrochemical cells are charged with electrolyte by this procedure.

Table 29

Electrolytic Absorption and
Retention of Teflon Bonded Matrices

Specimen	Thickness	Absorption g KOH/g of Spec.	g KOH/ cm^3 Spec.	Retention After 25 g Test
MgO 95%	0.0215 inch	1.283	0.85	89%
	.0196	1.270	.83	89
	.0592	1.430	.86	95
	.0582	1.434	.87	95
CeO_2 99%	0.0188	0.328	0.70	86%
	.0189	.304	.65	86
	.0573	.321	.78	94
	.0580	.304	.77	93
ZrO_2 99%	0.0197	0.240	0.645	87%
	.0200	.244	.605	86
	.0605	.564	.625	94
	.0613	.492	.585	93
PKT 95%	0.0200	3.13	1.317	90%
	.0189	3.11	1.574	91
	.0560	4.06	1.138	95
	.0563	3.80	1.140	95

Table 30

Gas Permeability of Teflon Bonded Matrices
(Specimen Diameter 1 inch)

Matrix Composition	Thickness inch	Electrolyte: Matrix	Bubble Pressure (psi) Specimen 1	Specimen 2
PKT 95% Teflcn 5%	0.020	dry	0.05	
		1:1	0.06	
		2:1	0.06	
		3:1 (sat'd)	2.06	
PKT 95% Teflon 5%	0.027	dry	0.90	
		1:1	0.90	
		2:1	1.51	
		3:1	15 (no leak)	15 (no leak)
PKT 95% Teflon 5%	0.060	dry	0.02	
		1:1	0.04	
		2:1	0.06	
		3:1	7.40	
		4:1 (sat'd)	9.75	
PKT 95% Teflon 5%	0.030	sat'd	13.23	
			14.00	
Ceria 95% Teflon 5%	- - -	dry	0.24	
		1:1	0.33	0.26
Ceria 99% Teflon 1%	0.020	dry	0.04	
		1:1 (sat'd)	1.42	
Ceria 99% Teflon 1%	0.030	(sat'd)	11.22	10.88
Ceria 99% Teflon 1%	0.060	dry	0.05	
		(sat'd)	6.47	
Ceria 99 3/4% Teflon 1/4%	0.070	dry	0.36	
		(sat'd)	12.0	
Ceria 99 3/4%	0.060	(sat'd)	12.0	

Table 30 Cont'd

Matrix Composition	Thickness Inch	Electrolyte Matrix	Bubble Pressure (psi) Specimen 1	Specimen 2
Zirconia 99% Teflon 1%	0.020	dry sat'd	0.04 1.96	
Zirconia 99% Teflon 1%	0.030	sat'd	15.0 (no leak)	15 (no leak)
Zirconia 99% Teflon 1%	0.060	dry sat'd	0.04 15.0 (no leak)	
Magnesia 95% Teflon 5%	- - -	dry 1:1	0.10 15.0 (no leak)	15 (no leak)
Magnesia 95% Teflon 5%	0.030	sat'd	15.0 (no leak)	15 (no leak)
Magnesia 95% Teflon 5%	0.060	dry 1:1 sat'd	0.05 4.90 5.05	

The results of these measurements should be accepted with considerable reservation, inasmuch as the blank correction is very large. The blank measurement is made with the cell halves clamped together, with no specimen in place., and the Luggin capillary orifices brought together. With zero electrolytic flux, the reference electrode current supplies are adjusted to zero potential difference between the reference electrodes. Then with a flux of 50 ASF, the potential between the reference electrodes is measured again. The blank value thus obtained was in the order of 20 mv.

The values obtained with the specimen in place are, in most instances, not greatly different from the blank value, and the net corrected potentials are very small. The accuracy of the derived value of specimen resistance cannot be confirmed by the testing of standard materials since none of this type is available. The only opportunity for a corroborative test occurred in another project. A matrix prepared for test in an acid electrochemical cell was also tested for electrolytic resistance by the procedure described above. The full matrix in the test cell had almost precisely the resistance predicted from the resistance test.

The results of the tests of the fibrilated Teflon bonded matrix specimens are recorded in Tables 31 and 32. A sample calculation is presented below:

Specimen: Ceria + 1% Teflon 0.02 inch thick
Current: 70 ma.
Potential measured across specimen: 0.0270 volts
Potential (blank determination) 0.0182 volts
Net potential for specimen 0.0088 volts

$$\text{Resistance of specimen} = \frac{0.0088 \text{ volts}}{0.07 \text{ amp}} = 0.126 \text{ ohm}$$

Diameter of specimen face = 1/2 inch
Area of specimen face = 1.269 cm^2
Unit area resistance of specimen = 0.126 x 1.269
= 0.160 ohm cm^2

Table 31 reports the tests of specimens prepared during the initial development of fibrilated Teflon bonded matrices. Specimen thicknesses conformed only very roughly with those specified for acceptable matrices. Table 32 reports the tests of specimens of the correct thicknesses.

In Table 32, the very high values of resistance for 0.06 inch thick ceria matrix are inconsistent with the other values. We believe that these specimens were not completely saturated

Table 31

Electrolytic Resistance of Preliminary Teflon Bonded Matrices

30% KOH Electrolyte, I = 70 ma.

Specimen	Thickness (inch)	Potential Diff. (volts)	Net Potential Diff. (volts)	Resistance (ohms)	Resistance (ohm cm^2)
Blank		0.0203			
A		.0200			
		.0195			
		0.0199 avg.			
B		0.0196			
		0.0217			
		0.0214			
		0.0209 avg.			
PKT - 5% Teflon	0.029	0.0276			
A		.0278			
		.0277			
		0.0277 avg.	0.0078	0.111	0.141
B	0.029	.0250			
		.0248			
		.0250			
		0.0249 avg.	0.0040	0.057	0.077
Magnesium Titanate - 5% Teflon					
A	0.024	0.0340			
		.0344			
		.0338			
		0.0341 avg.	0.0142	0.203	0.257
B	0.024	0.0372			
		.0374			
		.0373			
		0.0373 avg.	0.0164	0.234	0.296

Table 31 (Cont'd)

Specimen	Thickness (inch)	Potential Diff. (volts)	Net Potential Diff. (volts)	Resistance (ohms)	Resistance (ohm cm^2)
Ceria - 5% Teflon					
A	0.034	0.2211			
		.2200			
		.2150			
		0.2187 avg.	0.1988	2.84	3.60
B	0.034	0.1079			
		.1070			
		.1082			
		0.1077 avg.	0.0868	1.24	1.57
Ceria - 0.25% Teflon					
A	0.084	0.0683			
		.0686			
		.0678			
		0.0682 avg.	0.0483	0.690	0.824
B	0.077	0.0584			
		.0578			
		.0580			
		.0585 avg.	0.0376	0.538	0.681

Table 32

Electrolytic Resistance of Teflon Bonded Matrices

30% KOH Electrolyte; 70 ma current

Specimen	Thickness (inch)	Potential Diff. (volts)	Net Potential Diff. (volts)	Resistance (ohms)	Resistance (ohm cm^2)
Blank		0.0190) 0.0175) 0.0182 avg.			
Ceria + 1% Teflon	0.02	0.0270	0.0088	0.126	0.160
		.0256	0.0074	.106	.134
	0.03	.0256	0.0074	.106	.134
		.0210	.0024	.035	.044
	0.06	.0316	.0134	.192	2.43
		.0475	.0293	.420	5.32
PKT + 5% Teflon	0.02	0.0166	- *	-	-
		.0240	.0058	0.083	0.105
	0.03	.0236	.0054	.078	.099
		.0219	.0037	.053	.067
	0.06	.0273	.0091	.130	.165
		.0239	.0057	.081	.103
Zirconia + 1% Teflon	0.02	.0320	.0138	.197	.249
		.0284	.0102	.146	.185
	0.03	.0278	.0096	.137	.173
		.0208	.0026	.037	.047
	0.06	.0640	.0458	.655	.830
		.0650	.0468	.669	.846
Magnesia + 5% Teflon	0.02	.0330	.0148	.212	.268
		.0430	.0248	.354	.448
	0.03	.0450	.0268	.380	.481
		.0541	.0359	.513	.650
	0.06	.0385	.0203	.290	.367
		.0578	.0396	.566	.716

* Measured potential is less than blank value. No tenable explanation can be offered.

with electrolyte. In general, the values of specimens resistance correlate very poorly with thickness.

7. Fiber Structure

Although these matrices contain only a small relative amount of Teflon, the fibers are apparently the sole basis of matrix integrity. Whereas compacts of the inorganic components alone are rigid and brittle, these matrices are very flexible and can be stretched considerably before parting. Since the inorganic particles do not adhere strongly to the Teflon fiber surfaces, it is presumed that each inorganic particle is trapped in the random network of fibers.

When a specimen of matrix is carefully stretched to failure, and the specimen is examined at about 30X magnification under reflected light, fibrous composites can be seen bridging the new voids (Figure 32). Under greater optical magnification, these can be identified as strings of inorganic particles incorporated in fiber bundles. Sometimes under properly directed illumination, individual fibers (or probably fiber bundles) can be seen across the void.

8. Surface Area

Measurement of surface area of matrices by the BET method produced the values listed in Table 33. The PKT and MgO matrices are clearly of greater area than the ceria and zirconia matrices, but these differences do not correlate with properties of immediate concern in matrix performance.

9. Tensile Strength

Specimens of the Teflon fiber bonded matrices were measured with the Instron Tensile Tester. The elongation curves are presented in Figures 33, 34 and the interpretations in Table 34. The specimens were die-cut rectangles, 2 x 3 inches. They were mounted in the tester to present a gage width of 2 inches and gage length of 1 inch. Crosshead speed was 0.5 inch per minute.

The Teflon-fiber bonded matrices are all very flexible and will stretch inelastically. The low-density PKT matrices may be handled without significant danger of distortion. However, the more dense ceria and zirconia matrices, in the full size and especially in the 20-mil thickness, are much more susceptible to stretching by incautious handling. It is advisable to support these matrices on paper or cardboard.

When these matrices are saturated with electrolyte, the strenth remains virtually unchanged. However, because of the increased weight, greater handling care is required to avoid distortion of wet matrices.

Figure 32. Fibers in Teflon-Bonded Matrix.

Table 33

Surface Area of Teflon Bonded Matrices

Specimen	Area (1)	Area (2)
PKT 95%; Teflon 5%	8.52 m^2/g	8.19 m^2/g
CeO_2 99%; Teflon 1%	1.55	1.50
MgO 98% Teflon 2%	10.55	10.55
ZrO_2 98%; Teflon 2%	1.41	0.87

9	PKT	0.02"
10	"	"
11	"	0.06
12	"	"
13	ZrO_2	0.02
14	"	"
15	"	0.06
16	"	"

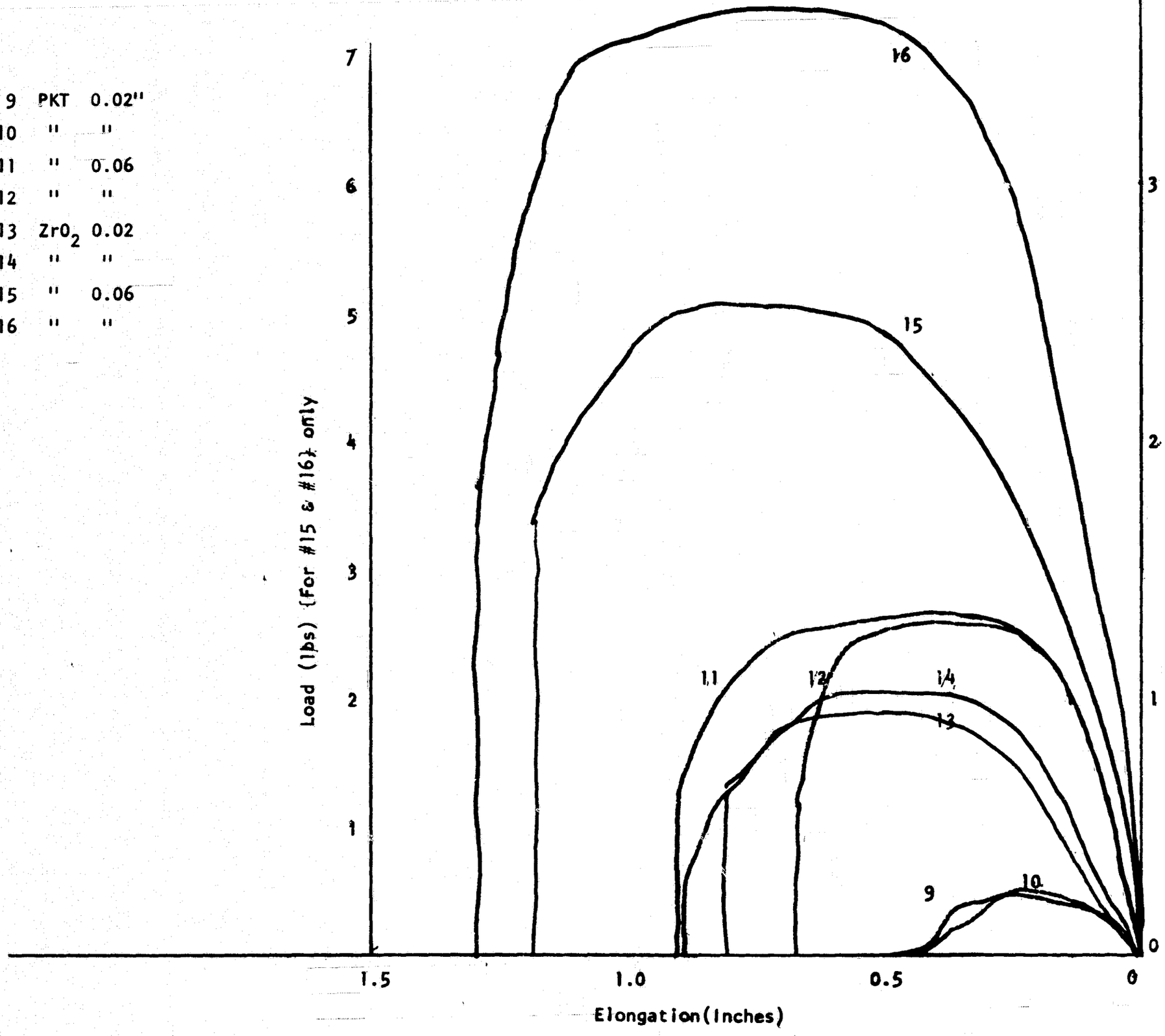

Figure 33. Tensile-Elongation Curves for Teflon-Bonded Matrices

1	MgO	0.02"
2	"	"
3	"	0.06
4	"	"
5	CeO_2	0.02
6	"	"
7	"	0.06
8	"	"

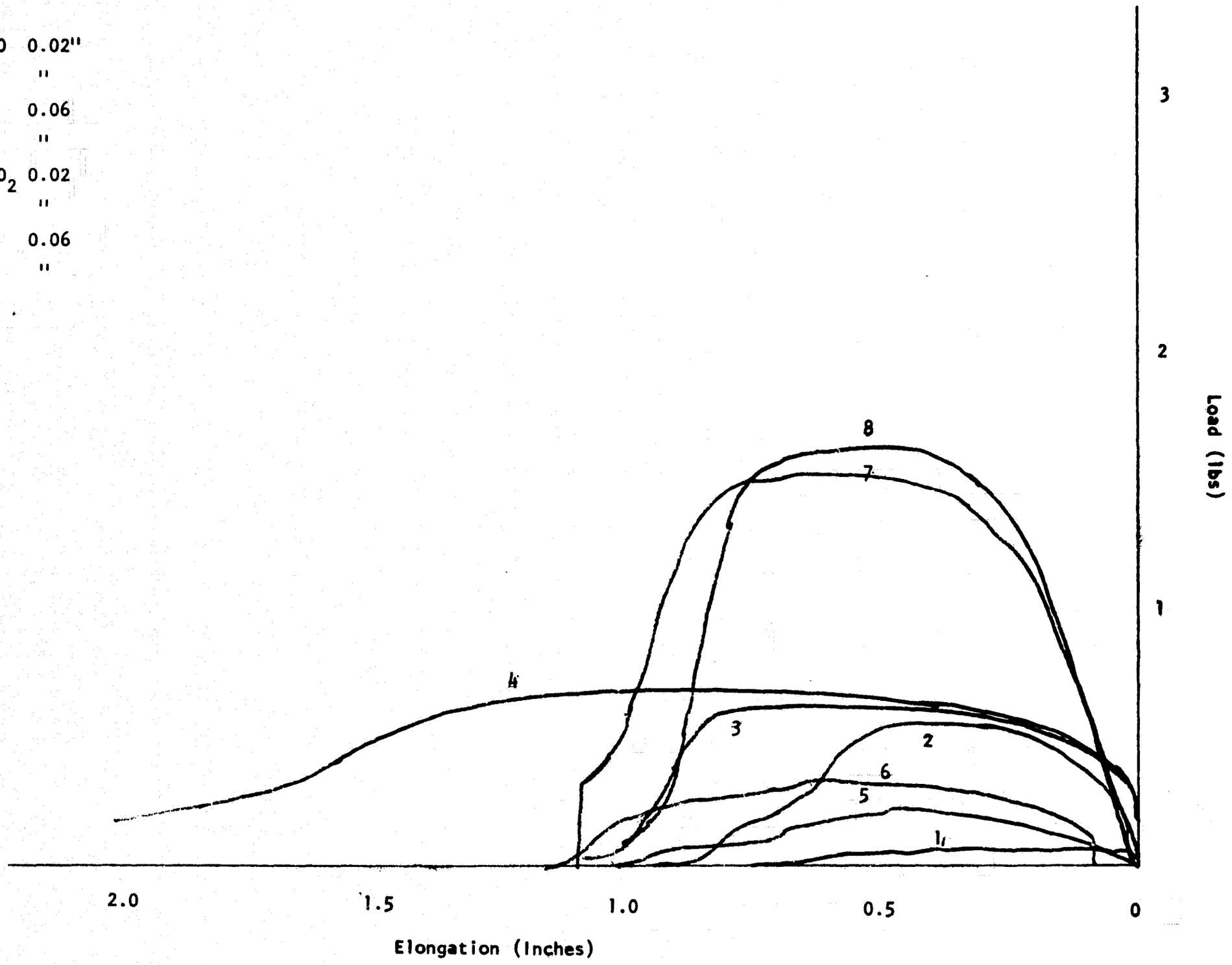

Figure 34. Tensile-Elongation Curves for Teflon-Bonded Matrices.

Table 34

Tensile Tests

Apparatus: Instron Tester
Gage Length: 1 inch; Gage Width: 2 inch
Crosshead Speed: 0.500 in/min

Specimen		Thickness (nominal) (in)	Elongation %	Load (lbs)	Tensile Strength psi
MgO	95%	0.02	-	0.30	15
		.02	62	.59	30
		.06	90	.655	10.9
		.06	152	.715	11.9
CeO_2	99%	.02	50	.203	10.
		.02	67	.345	17.2
		.06	90	1.605	28.7
		.06	80	1.715	28.6
PKT	95%	.02	30	.203	10.1
		.02	27	.265	13.2
		.06	72	1.395	23.2
		.06	57	1.360	22.7
ZrO_2	98%	.02	72	.995	49.7
		.02	62	1.075	53.7
		.06	97	5.33	88.9
		.06	112	7.74	129.0

10. Density and Porosity

The average density of a matrix is derived from the geometric volume and weight of a specimen. The percent void volume is the difference between the theoretical density and actual density, expressed as percent of the theoretical density of the matrix material. Because of the very minor contribution of Teflon to the matrix volume, the calculations are based on the inorganic component alone.

Absolute densities of PKT, ceria, and zirconia were measured in the air comparison pycnometer, with the following results:

PKT	3.426 g/cc
Ceria	6.85 g/cc
Zirconia	5.367 g/cc

The relative void volume is calculated from the relation:

$$\text{rel. void vol.} = 1 - \frac{\text{actual density}}{\text{theoretical density}}$$

The specimens measured were those prepared for the electrolyte absorption and retention tests. They were rectangular pieces 1 inch x 1/2 inch. Thickness was measured with a dial gage equipped with a 1/2 inch diameter "point" loaded only by its own weight and the light internal return spring.

The data and results from these tests are recorded in Table 35.

11. Pore Size Distribution

Matrix specimens of the Teflon fiber bonded matrices were tested by the mercury intrusion method. As expected, these specimens were compressed by the surrounding mercury before actual penetration occurred. This is manifested by the long gradual rise of the curve preceding the pronounced upward deflection (Figure 35). Although the data do not permit a quantitative description of the specimen compression, it may be concluded that the PKT and MgO matrices are much more compressible than ceria and zirconia matrices.

Penetration of the inter-particle voids is understood to begin with the upward inflection of the curve and approach completion at the limiting pressure. The curves do not indicate a significant porosity of the particles.

The numerical interpretation of the penetration curves given in Table 36 is based on arbitrary estimates of the beginning and end of the steep rise and the total penetration at limiting

Table 35

Density and Porosity of Matrix Specimens

Composition	Thickness (inches)	Weight	Geometric Density (g/cc)	% Void Volume
99% Ceric Oxide 1% Teflon	.0188	0.3941	2.46	64.1
	.0189	.4002	2.49	63.6
	.0573	1.1263	2.31	66.3
	.0580	1.1347	2.30	66.4
99% Zirconium Oxide 1% Teflon	.0197	0.4636	3.11	42.1
	.0200	.4370	2.89	46.2
	.0605	1.5450	3.37	37.2
	.0613	1.5955	3.44	35.4
95% Potassium Titanate 5% Teflon	.0200	0.0735	0.485	85.9
	.0189	.0676	0.556	83.8
	.0560	.1257	0.296	91.4
	.0563	.1350	0.317	90.7

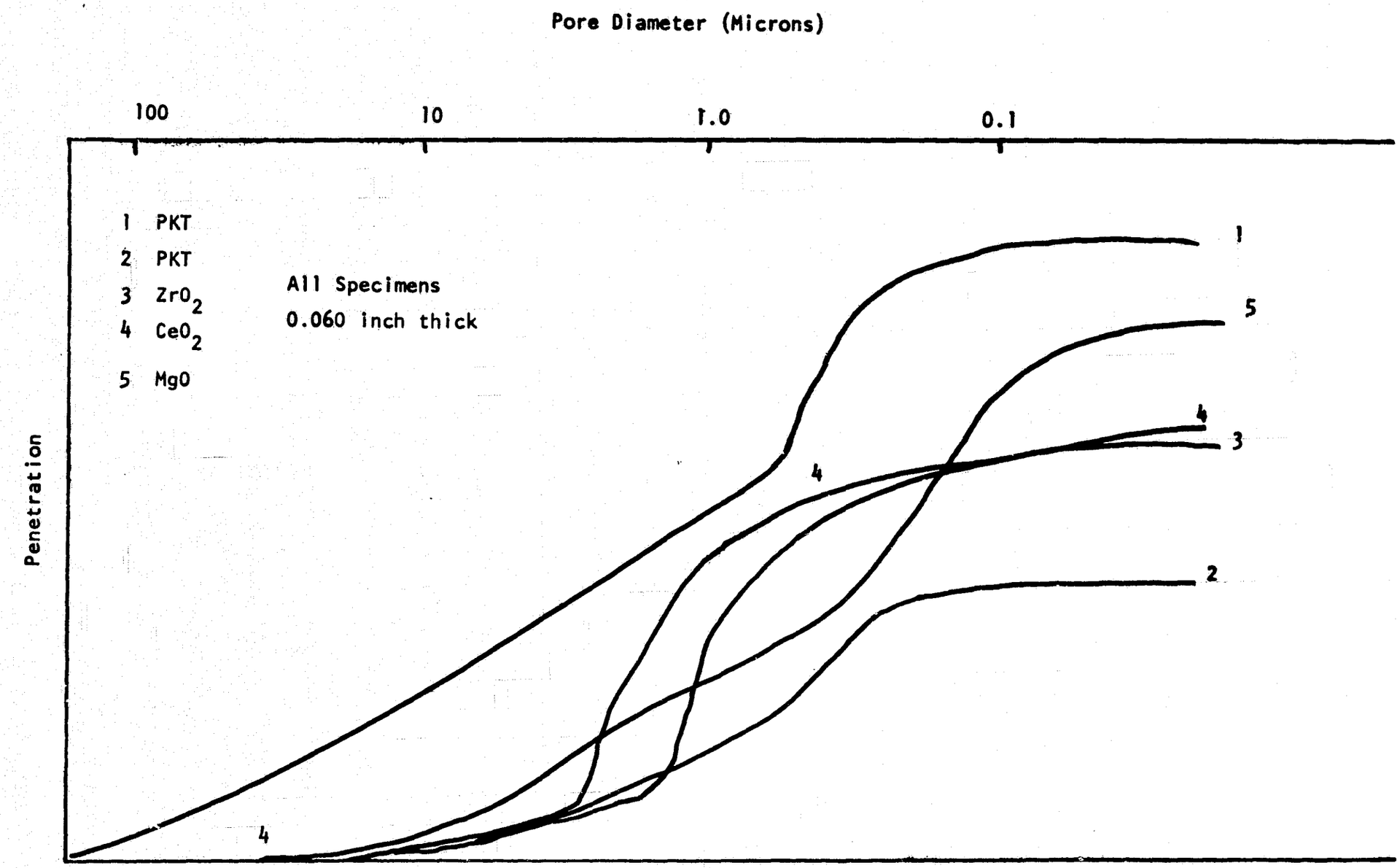

Figure 35. Pore Size Distribution of Teflon Bonded Matrices.

Table 36

Pore Size Distribution

95% PKT - 5% Teflon .060" Thick

Pore Size	Percentage
Between .73 - .32 microns	70.6%
Smaller than .32 microns	29.4%

99% CeO_2 - 1% Teflon .060" Thick

Pore Size	Percentage
Between 3.0 - 1.2 microns	61.9%
Smaller than 1.2 microns	38.1%

99% ZrO_2 - 1% Teflon .060" Thick

Pore Size	Percentage
Between 1.7 - .8 microns	58.2%
Smaller than .8 microns	41.8%

95% MgO - 5% Teflon .060" Thick

Pore Size	Percentage
Between .35 - .12 microns	72.7%
Smaller than .12 microns	27.3%

pressure. For example, the curve for PKT matrix indicates that about 70% of the penetration occurs in the pressure range corresponding with pore diameters of 0.73 and 0.32 microns and the remaining 30% involves pores of smaller diameter.

12. Electrochemical Degradation

Specimens of the Teflon-fiber bonded matrices composed of ceria, PKT, and zirconia were tested in 40% KOH at 100°C for 72 hours under a current density of 50 ASF. At 24-hour intervals and at the end of 72 hours, the electrodes remained perfectly clean, and the electrolyte remained free of impurities detectable by spectrographic technique.

E. Conclusions From Task 2A Work

1. Composites of inorganic particles with pre-formed fibers of Teflon or polypropylene are inferior to chrysotile mats in several of the properties required in a matrix.

2. By a relatively simple technique, Teflon 6 extrusion powder, present in very low concentration in a selected inorganic powder, can be converted into an integral network of very fine fibers, permeating the mass completely and forming a flexible, strong, and wettable porous matrix. These matrices are somewhat inferior to chrysotile mats in gas sealing capability and electrolytic resistance, but they are adequate in this early stage of development, and there is prospect for improvement. These new matrices are apparently suitable for long service in alkaline electrolyte at 150°C or for shorter time at 200°C.

3. Ceria and zirconia are substantially inert in KOH at the temperatures stipulated for this work. PKT reacts with KOH solution to form an insoluble higher titanate or stable hydrate; in the process, the short fiber aspect of the original PKT apparently disappears. These inorganics do not dissolve appreciably in the KOH.

4. The failure of these matrices, which occurred only in the 1000 hours tests at 200°C in 60% KOH, was due to chemical destruction of the Teflon fibers.

Supplementary tests indicate that the interaction of Teflon with KOH is accelerated by an oxidant. One might, therefore, anticipate that matrix failure will occur principally near the cathode surface in a fuel cell.

Fluoride ion, a product of the Teflon-KOH interaction, may become an agent of attack on metals of the cell structure, with

perhaps severe effects on the electrode catalysts. The fluoride ion will be electrochemically stable in the aqueous environment, but it will react primarily by forming soluble metal complexes.

5. Several other inorganics merit a more adequate examination. Magnesium titanate, a special commercial pigment, reacts slowly with KOH to form an insoluble potassium titanate and gelatinous magnesium hydroxide. The latter should significantly enhance the gas sealing capability of the matrix.

Zirconia has recently been produced in the form of hollow spheres, available in very small particle size. A matrix based on this material should be less dense and more absorptive of electrolyte than the zirconia used in this program.

XI TASK 3 - FULL-SIZE MATRICES

A. Equipment Changes and Technique Improvements

Task 3 comprised the preparation of 8-inch square matrices of three selected compositions and testing of the full size matrices to determine the best of the three. The three compositions selected for study in Task 3 were:

1.	95% PKT	5% Teflon
2.	99% Ceria	1% Teflon
3.	99% Zirconia	1% Teflon

In each case, the proportion of Teflon was chosen as the approximate minimum required to effect adequate bonding of the inorganic particles.

Six matrices were made of each of three thicknesses (20, 30, and 60 mil) and in each of the three compositions to give a total of 54 matrices. All were measured and weighed to determine the matrix density. Three matrices of each kind were saturated with 30% KOH solution by vacuum impregnation and weighed to determine electrolyte absorption. These saturated matrices were then tested for gas permeability (bubble pressure).

For the preparation of these matrices, we procured an electric hot plate with an 18 x 24 inch steel surface. The plate was then surface-ground to improve flatness, but we found that the plate bowed slightly when heated, and the desired flatness was lost. However, a final cold-rolling treatment of the matrix produced the desired uniformity of thickness.

The procedure for making the large matrices was the following: The weighed mixture for a single matrix was blended with odorless mineral spirits in an electric blender to form a mobile slurry and filtered under suction in a Buchner funnel. The moist cake was placed on the hot plate (about 250 to 300°F) and "smeared" with a spatula to start the fiber development. Mineral spirit was added to the mass, at the discretion of the operator, to produce the desired plasticity of the mass. When the mass became sufficiently cohesive, the rolling treatment was begun. As the fiber development approached the optimum, as indicated by the working properties of the mass, the rolling was controlled to produce the roughly square piece from which the matrix would be obtained.

Finally the sheet of material was placed on a sheet of aluminum foil on the hot plate and with shim strips placed at each side, was rolled to the desired preliminary wet thickness, and then permitted to dry. It was trimmed to a 9-inch square, and heated for about 30 minutes in a vacuum oven to expel any

less-volatile residues of the mineral spirits. The cooled matrix was then placed on a slab of 1/2 inch thick plexiglass and with strips of shim metal at each side, was rolled to the desired thickness. Finally, the matrix was trimmed to 8 inches square.

B. Testing of 8-Inch Square Mats

1. Thickness Variation

The matrices prepared for testing in electrochemical cells were to conform to the following thickness requirements:

0.02 inch ± 0.002 inch
0.03 inch ± 0.003 inch
0.06 inch ± 0.004 inch

Measurements were made with a dial gage equipped with a flat, one-half inch diameter foot. The spindle weight and a very light internal return spring provided the contact pressure. Since the Teflon composites matrices are not readily compressible, the light contact pressure was deemed satisfactory.

Sixteen measurements were made across the face of a specimen. If any single dimension exceeded latitude stipulated, the matrix was either rejected or re-rolled to bring it into the acceptable range.

2. Electrolyte Absorption

Three matrices of each composition and thickness were tested for electrolyte absorption and bubble pressure. To ensure complete saturation, the weighed matrices were loaded with 30% KOH solution by vacuum impregnation and weighed again. The apparatus prepared for impregnation of these large matrices is shown in Figure 36.

In terms of weight percent, the PKT matrices appear to be superior to the ceria and zirconia matrices (Table 37). However, the proportion by volume of absorbed electrolyte is revealed by the quantities absorbed by the several specimens of similar thickness. Thus compared, the three matrix types are not greatly different.

3. Bubble Pressure

The saturated matrix prepared for the electrolyte absorption test was then used for the bubble pressure test. This procedure involves a slight modification of the project specification, namely, that the absorption test be applied to three matrices and the bubble pressure test to another three. This reflects the

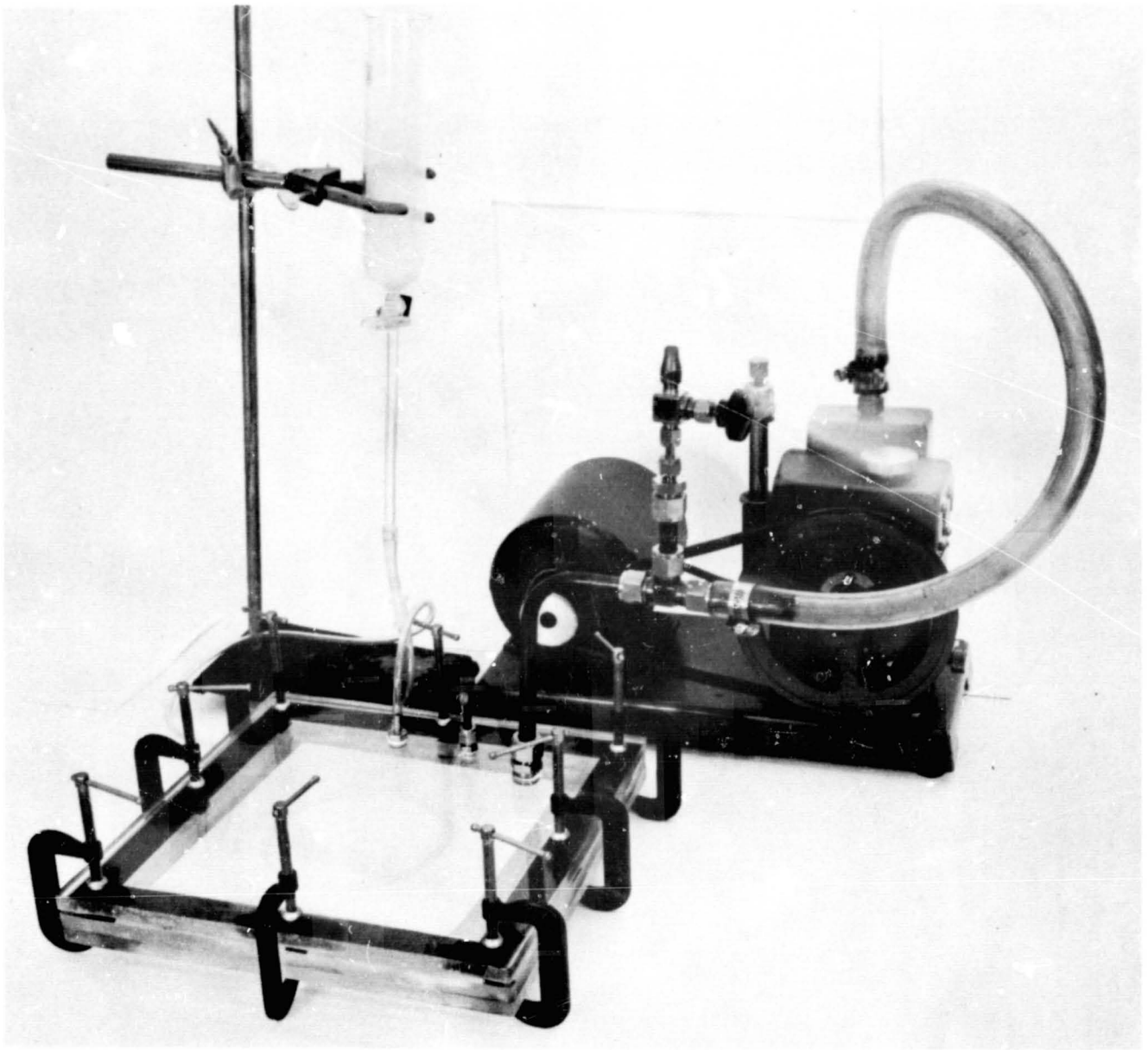

Figure 36. Apparatus for Vacuum Impregnation of 8-inch Square Matrices.

Table 37

Tests of 8-Inch Square Matrices

Spec. No.	Composition	Average Thickness (inch)	Vol. cm^3	Weight (g)	Density g/cm^3	Electrolyte Absorbed (g)	Electrolyte Matrix	Bubble Pressure: Initial (in.Hg)	Repeat (in.Hg)
1	PKT 95%	0.0209	21.94	5.0	0.23	28.6	5.7	3.2	
2	Teflon 5%	.0218	22.88	4.9	.21	29.4	6.0	1.4	
3		.0211	22.14	5.0	.23	28.5	5.7	4.0	
4		.0216	22.66	5.0	.22	28.5	5.7	9.5	
5		.0206	21.62	4.7	.22	26.1	5.5	1.8 *	
6		.0204	21.42	4.6	.22	28.0	6.1	3.8	
7		.0319	33.49	7.6	.23	31.6	4.2	6.4	
8		.0326	34.21	7.6	.22	38.9	6.7	5.5	
9		.0308	32.33	6.3	.20	41.3	6.5	6.0	
10		.0312	32.75	5.8	.18				
11		.0303	31.82	5.7	.18				
12		.0294	30.83	5.3	.17				
13		.0613	64.34	10.8	.17				
14		.0588	61.72	10.2	.16				
15		.0608	63.82	10.8	.17				
16		.0597	62.65	9.5	.15	68.2	7.2	7.4	5.2
17		.0592	62.16	10.7	.17	73.5	6.9	10.0	6.4
18		.0616	64.54	13.0	.20	81.9	6.3	7.8	6.0
19	Ceria 99%	0.0196	20.57	45.9	2.23				
20	Teflon 1%	.0210	22.04	52.3	2.37				
21		.0203	21.31	50.2	2.36				
22		.0201	21.10	49.6	2.35	23.9	0.48	7.0	6.1
23		.0190	19.94	39.8	2.00	21.2	.53	6.4	4.2
24		.0194	20.36	41.3	2.03	21.1	.51	6.0	5.4

Table 37 (Cont'd)

Spec. No.	Composition	Average Thickness (inch)	Vol. cm^3	Weight (g)	Density g/cm^3	Electrolyte Absorbed (g)	Electrolyte Matrix	Bubble Pressure Initial (in.Hg)	Bubble Pressure Repeat (in.Hg)
25	Ceria 99%	0.0306	32.12	56.1	1.75	33.0	.59	7.5	6.8
26	Teflon 1%	.0277	29.07	48.8	1.68	29.2	.60	6.2	5.8
27		.0277	29.07	45.8	1.58				
28		.0308	32.31	55.4	1.72				
29		.0301	31.65	57.3	1.81				
30		.0323	33.95	58.3	1.72	31.5	.54	7.4	6.6
31		.0616	64.66	109.3	1.69				
32		.0627	65.81	112.3	1.71	61.9	.55	8.7	
33		.0598	62.77	100.8	1.61	64.3	.64	7.6	7.2
34		.0616	64.66	105.2	1.63	53.7	.51	6.9	6.3
35		.0629	66.02	108.0	1.64				
36		.0624	65.50	102.3	1.56				
37	Zirconia 99%	0.0214	22.46	65.0	2.89				
38	Teflon 1%	.0198	20.78	63.6	3.06	15.6	0.24	Ruptured	
39		.0202	21.20	57.0	2.69	16.1	.28	6.0	3.6
40		.0185	19.42	51.0	2.63	14.6	.29	5.0	4.1
41		.0206	21.62	61.1	2.83	18.1	.30	7.0	5.5
42		.0187	19.63	50.0	2.55				
43		.0304	31.91	88.9	2.79	23.8	.27	7.1	6.5
44		.0288	30.23	82.1	2.72	25.0	.30	6.5	6.0
45		.0279	29.28	82.0	2.80	22.9	.28	7.7	6.4
46		.0302	31.70	91.0	2.87				
47		.0324	33.95	91.3	2.69				
48		.0300	31.49	86.7	2.75				
49		.0565	59.30	156.1	2.63	44.8	.30	8.0	6.6
50		.0605	63.50	156.9	2.47	53.3	.34	7.0	6.2
51		.0609	63.92	180.0	2.82	48.0	.27	9.0	7.2
52		.0583	61.19	174.5	2.85				
53		.0603	63.29	163.3	2.58				
54		.0615	64.62	161.4	2.50				

earlier experience with asbestos and asbestos composites, that the specimens used for the absorption test tend to disintegrate, and are therefore not suitable for the bubble pressure test. The new Teflon composite matrices retain integrity when saturated with KOH, and may be used for the pressure test.

The matrix is mounted in the Plexiglass holder shown in Figure 37. A shallow recess in each half of the holder is filled by a double layer of fine-mesh wire screen to support the matrix against pressure differential and to permit gas access to all parts of the specimen. Air under controlled and measured pressure is supplied to the lower specimen surface; leaked air is collected in the upper chamber and escapes through a water bubbler which serves as a detector.

In the earlier tests, we observed and recorded the pressure at which leakage first occurred. In later tests, we evaluated the matrix recovery by measuring the bubble pressure a second time after it had been permitted to rest for about five minutes under zero pressure differential. Generally, the recovery was not complete.

These saturated matrices are poorer gas seals than Fuel Cell Asbestos matrices (Table 37). However, there is a prospect that they may be improved by refinement of particle size of the inorganic component, and possibly by the addition of sealing agents.

4. Density

The geometric volume of each matrix was calculated from the face area and the average of sixteen thickness measurements across the face. Weight of each matrix was measured to the nearest 0.1g. The densities are recorded in Table 37.

C. Conclusions From Task 3 Tests

The tests revealed that no one of the matrix compositions is distinctly superior to the others. Zirconia mats have less capacity for absorbed KOH solution, but the gas sealing capabilities are comparable to the others. With the NASA project managers, we concluded that these tests were indecisive and that all three types of matrices should be prepared in quantity in Task 4 of the program for further evaluation by testing in electrochemical cells.

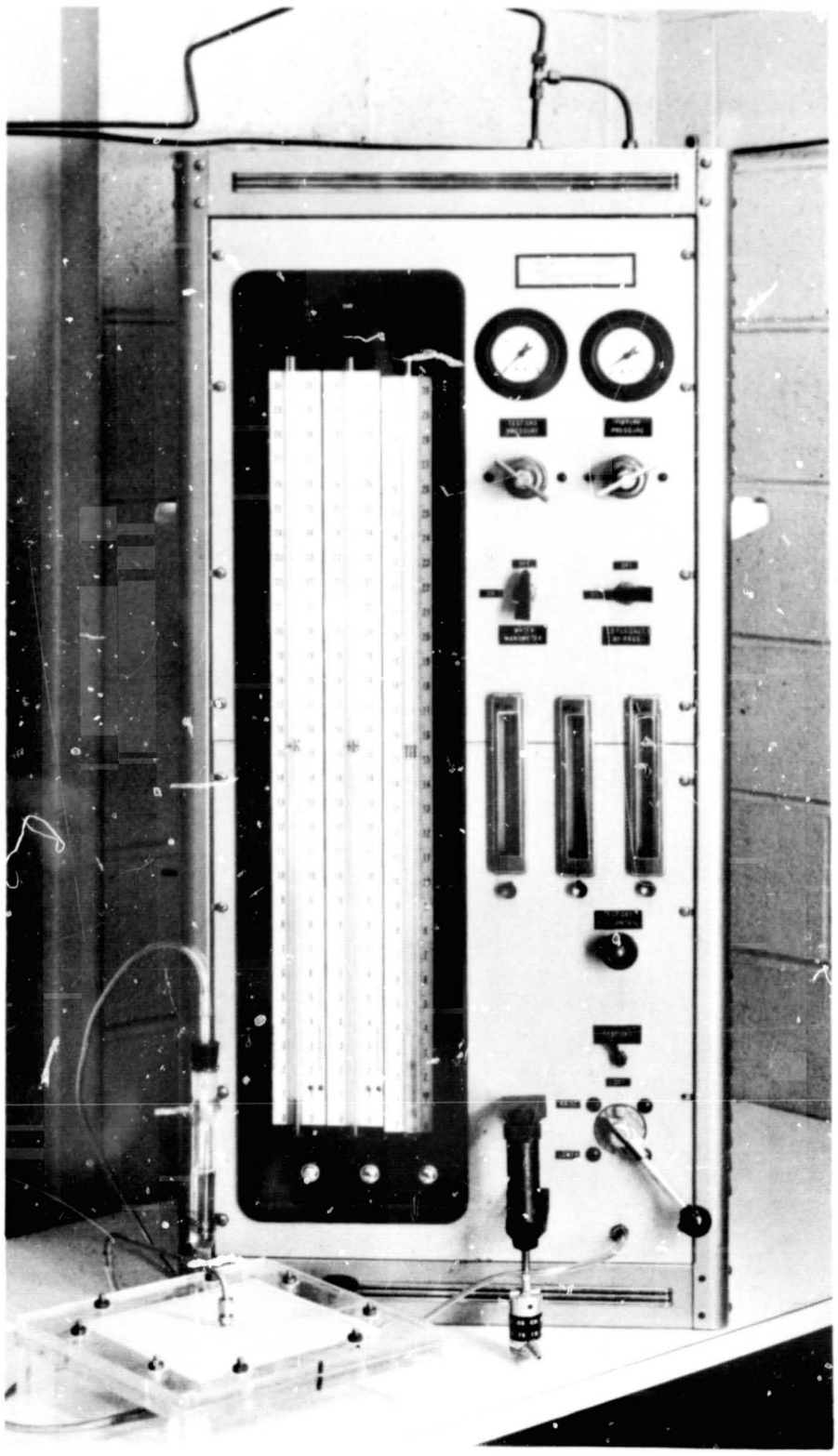

Figure 37. Bubble Pressure Apparatus for 8-inch Square Matrices.

XII TASK 4 - PRODUCTION OF FULL SIZE MATRICES IN QUANTITY

Our experience with the Teflon-bonded matrices revealed that those based on PKT, ceria and zirconia are quite similar and that the selection of the one superior composition would be most arbitrary. Evidently, cell performance test of these matrices was required before a selection could be made.

Accordingly, Task 4 was revised to require the preparation of 100 matrices of each composition - 50 to 60 mil thickness, and 25 each of 30 mil and 20 mil thickness.

The two component materials, PKT and zirconia are manufactured primarily for use as pigment and in ceramics, respectively, and particle size is therefore a matter of ordinary concern to the vendor. Ceria, on the contrary, is produced for the chemical trade, and particle size is not specified by the manufacturers or vendors. In preparing for the work of Task 4, we obtained a bulk quantity of ceria from a vendor other than the original. Although the new material was, in terms of purity specifications, superior to what we had used previously, the matrices based on this new ceria were unsatisfactory, evidently, because of the smaller particle size of the new material. Fortunately, the original vendor was able to supply our requirements of ceria for Task 4 from the single production batch of the material, thus assuring us of average uniformity of particle size for the ceria matrices.

Some consideration was given to methods of improving the speed and efficiency of production, but none seemed appropriate. Bulk weighing and dry blending of the components was rejected because of the tendency of the Teflon powder to smear and to form coherent clumps. Wet mixing in the electric blender seems more certain to achieve a thorough distribution of Teflon through the mass. We attempted to increase our production rate by stirring the heated blend (with mineral spirit lubricant) until fiber development started, but the uniformity and strength of the final rolled mat were poor.

We discovered that the entire hot rolling treatment must be performed without significant interruption, otherwise the final mat will be non-uniform and weak. This precludes the prospect of processing a large batch of mixture to some desired state of development and then taking portions for final rolling.

The matrices were therefore compounded and processed individually. The components for each mat were weighed and blended, and the entire fiber-forming process was performed without interruption. Each matrix was heated at 100°C in a vacuum oven for about 30 minutes to expel any residues of the mineral spirits. After a final cold-rolling treatment to adjust

the mat thickness, it was trimmed to the 8 inch square size. The thickness was measured with a dial gage at nine places across the surface; if any single measurement fell outside the specified range of thickness latitude, the matric was rejected.

The work statement originally specified that the weights of all matrices of a composition-thickness group must be within + 2.5% of the average of that group. This requirement was changed to specify that a matrix density must be within ± 5% of the average for its group.

The finished 8-inch square matrices were measured for thickness at 9 locations across the surface and weighed to the nearest 0.1 gram. The record of individual thickness measurements, average thickness, weight, and calculated density was attached to the envelope of each matrix. A summary of these data is contained in Tables 38, 39 and 40.

POTASSIUM TITANATE (PKT)

20 Mil Mats

No.	Thickness Mils	Weight gms	Density g/cc
1	19.3	6.4	.316
2	21.5	7.2	.319
3	20.3	6.8	.319
4	21.1	7.0	.316
5	20.7	6.4	.309
6	20.2	6.8	.321
7	19.9	6.2	.312
8	19.0	5.7	.300
9	19.4	6.5	.320
10	20.8	6.9	.302
11	20.4	6.5	.303
12	20.7	6.7	.308
13	19.7	6.3	.304
14	19.4	6.2	.304
15	19.2	6.2	.308
16	20.9	6.9	.314
17	19.4	6.2	.304
18	20.0	6.7	.319
19	19.7	6.3	.305
20	20.3	6.7	.314
21	20.3	6.6	.310
22	19.0	6.2	.311
23	19.1	6.1	.300
24	19.2	6.2	.308
25	18.9	6.2	.312

Average Density = .310 g/cc
Range @ ± 5% = .294 g/cc to .326 g/cc

30 Mil Mats

26	31.0	8.1	.249
27	31.2	8.1	.247
28	27.4	7.5	.261
29	31.8	8.3	.249
30	27.4	7.5	.261
31	28.4	7.9	.265
32	29.0	7.5	.246
33	31.2	8.6	.263
34	28.8	7.6	.251
35	30.5	8.4	.262
36	28.7	7.8	.259
37	30.0	8.2	.260
38	31.3	8.7	.265
39	27.0	7.0	.247
40	29.0	7.4	.243
41	28.1	7.4	.251
42	31.7	8.5	.256
43	31.6	8.2	.247
44	31.2	8.0	.244
45	32.7	8.8	.257
46	32.0	8.3	.248
47	31.3	8.5	.259
48	32.1	8.7	.258
49	32.6	9.1	.266
50	32.4	9.0	.265

Average Density = .255 g/cc
Range @ ± 5% = .242 g/cc to .268 g/cc

60 Mil Mats

No.	Thickness Mils	Weight gms	Density g/cc
51	61.2	14.5	.226
52	62.7	14.6	.221
53	62.6	13.8	.210
54	57.6	13.0	.215
55	61.3	13.4	.208
56	60.8	13.8	.216
57	62.6	13.6	.207
58	61.3	14.1	.219
59	57.6	12.5	.207
60	62.6	14.2	.216
61	56.2	12.2	.207
62	62.8	14.2	.216
63	58.9	13.0	.211
64	56.9	12.3	.206
65	57.8	13.4	.221
66	62.3	13.7	.210
67	62.7	13.7	.208
68	57.4	12.7	.211
69	60.7	14.1	.221
70	57.6	12.7	.210
71	62.3	13.9	.212
72	58.1	13.3	.218
73	62.1	13.7	.210
74	62.1	14.2	.217
75	61.3	13.9	.216
76	63.6	14.8	.221
77	62.1	14.7	.225
78	61.0	13.7	.214
79	61.3	14.1	.219
80	60.1	14.2	.225
81	59.1	13.3	.214
82	58.8	12.7	.206
83	60.9	13.9	.217
84	59.6	13.3	.213
85	61.0	13.5	.211
86	59.9	14.3	.227
87	60.8	14.4	.226
88	59.6	13.6	.217
89	60.7	13.8	.217
90	59.7	14.0	.223
91	63.8	15.2	.227
92	61.3	14.5	.225
93	60.4	14.3	.225
94	59.4	13.9	.223
95	58.1	12.9	.212
96	61.4	14.6	.227
97	58.0	12.9	.212
98	58.4	13.4	.218
99	60.1	13.2	.209
100	57.7	13.7	.226

Average Density = .216 g/cc
Range @ ± 5% = .205 g/cc to .227 g/cc

CERIC OXIDE

20 Mil Mats

No.	Thickness Mils	Weight gms	Density g/cc
101	21.6	60.7	2.68
102	21.6	60.5	2.67
103	21.6	64.1	2.83
104	21.6	61.5	2.71
105	20.1	56.5	2.68
106	21.7	66.8	2.93
107	21.4	65.1	2.90
108	21.8	62.2	2.72
109	21.6	65.3	2.88
110	21.3	65.3	2.92
111	21.7	67.3	2.95
112	21.8	65.3	2.85
113	21.2	63.4	2.85
114	19.8	56.7	2.73
115	21.3	63.5	2.84
116	20.2	59.0	2.78
117	18.7	53.5	2.73
118	20.9	59.8	2.73
119	21.7	65.8	2.89
120	20.8	61.9	2.84
121	20.6	61.6	2.85
122	19.6	56.7	2.75
123	21.6	65.5	2.89
124	21.6	67.0	2.95
125	20.0	57.6	2.74

Average Density = 2.81 g/cc
Range @ ± 5% = 2.67 g/cc to 2.95 g/cc

30 Mil Mats

126	28.9	74.5	2.46
127	28.6	74.4	2.49
128	28.8	74.6	2.47
129	27.6	71.7	2.48
130	31.3	79.3	2.42
131	28.7	72.9	2.43
132	30.8	82.3	2.54
133	30.8	83.2	2.58
134	29.9	77.8	2.48
135	30.4	79.1	2.48
136	30.4	79.5	2.49
137	27.4	71.2	2.48
138	29.9	79.9	2.54
139	29.4	76.6	2.48
140	31.7	85.8	2.58
141	29.6	78.9	2.54
142	27.9	73.9	2.52
143	31.3	84.3	2.56
144	31.6	86.3	2.60
145	29.6	77.1	2.48
146	29.6	79.2	2.55
147	30.1	75.8	2.40
148	31.3	80.7	2.46
149	29.4	75.6	2.45
150	30.8	79.6	2.46

Average Density = 2.50 g/cc
Range @ ± 5% = 2.38 g/cc to 2.62 g/cc

60 Mil Mats

No.	Thickness Mils	Weight gms	Density g/cc
151	60.7	153.7	2.41
152	59.6	151.3	2.42
153	59.8	158.8	2.53
154	58.9	148.7	2.41
155	60.6	163.7	2.57
156	58.2	156.3	2.56
157	57.6	146.1	2.42
158	59.9	150.9	2.40
159	58.9	161.5	2.61
160	57.2	148.0	2.47
161	63.1	174.6	2.64
162	60.4	161.3	2.55
163	60.0	162.3	2.58
164	61.8	166.2	2.56
165	62.6	167.8	2.55
166	61.4	165.5	2.57
167	61.4	169.8	2.64
168	62.1	168.0	2.58
169	62.8	171.9	2.61
170	59.8	163.9	2.61
171	63.4	170.6	2.56
172	61.1	165.8	2.59
173	61.9	168.6	2.60
174	59.8	150.7	2.40
175	56.3	143.2	2.42
176	63.0	167.9	2.54
177	61.2	167.4	2.61
178	60.8	163.7	2.57
179	62.9	171.2	2.59
180	62.4	166.8	2.54
181	60.3	167.3	2.64
182	62.0	169.0	2.60
183	62.4	164.9	2.52
184	57.2	145.6	2.43
185	63.2	170.6	2.57
186	62.4	168.1	2.56
187	56.6	155.2	2.61
188	56.6	142.6	2.40
189	56.3	141.1	2.39
190	56.3	142.0	2.40
191	61.2	167.4	2.61
192	56.9	145.6	2.44
193	61.6	154.4	2.39
194	61.2	160.9	2.51
195	56.2	141.3	2.39
196	57.2	144.6	2.41
197	58.8	154.2	2.50
198	57.3	144.9	2.41
199	58.1	146.7	2.41
200	63.6	170.6	2.55

Average Density = 2.52 g/cc
Range @ ± 5% = 2.39 g/cc to 2.65 g/cc

ZIRCONIUM OXIDE

20 Mil Mats

No.	Thickness Mils	Weight gms	Density g/cc
201	20.7	69.2	3.19
202	21.4	68.7	3.06
203	21.8	73.9	3.23
204	22.0	75.7	3.28
205	21.7	73.2	3.22
206	20.7	69.6	3.20
207	20.6	69.0	3.19
208	21.0	72.5	3.29
209	20.9	70.5	3.22
210	21.4	70.3	3.13
211	21.7	70.9	3.12
212	20.0	65.6	3.13
213	20.2	67.2	3.17
214	20.7	67.7	3.12
215	20.4	67.3	3.14
216	19.7	62.0	3.00
217	20.4	65.3	3.05
218	20.4	69.9	3.27
219	20.2	67.3	3.18
220	21.0	67.1	3.05
221	20.1	63.0	2.99
222	20.0	63.8	3.04
223	20.2	66.7	3.15
224	19.6	65.0	3.16
225	18.9	62.5	3.15

Average Density = 3.15 g/cc
Range @ ± 5% = 2.99 g/cc to 3.31 g/cc

30 Mil Mats

226	30.6	94.0	2.93
227	29.8	88.8	2.84
228	31.1	99.5	3.05
229	30.9	93.3	2.88
230	30.8	93.2	2.99
231	31.6	95.3	2.88
232	31.8	99.9	2.88
233	29.2	90.4	2.95
234	31.2	95.6	2.92
235	30.8	93.1	2.88
236	31.1	97.4	2.99
237	30.3	93.3	2.94
238	30.8	91.3	2.83
239	31.2	98.1	3.00
240	31.3	92.4	2.81
241	31.0	97.4	3.00
242	31.0	9[illegible] 9	2.86
243	30.4	9[illegible].7	2.94
244	30.3	89.7	2.82
245	30.1	92.0	2.91
246	31.3	97.5	2.99
247	30.7	91.0	2.83
248	30.3	89.6	2.82
249	30.3	92.2	2.90
250	29.7	90.6	2.91

Average Density = 2.91 g/cc
Range @ ± 5% = 2.76 g/cc to 3.06 g/cc

60 Mil Mats

No.	Thickness Mils	Weight gms	Density g/cc
251	59.0	173.4	2.80
252	60.0	178.2	2.83
253	59.0	173.6	2.80
254	59.3	176.2	2.83
255	58.9	176.4	2.86
256	59.9	180.7	2.88
257	58.8	170.7	2.77
258	59.2	169.1	2.72
259	59.4	172.3	2.76
260	58.8	171.0	2.77
261	59.1	169.2	2.73
262	58.9	170.0	2.75
263	59.7	172.5	2.75
264	59.9	174.2	2.77
265	59.6	170.1	2.72
266	58.8	166.8	2.70
267	59.3	169.7	2.73
268	58.7	167.2	2.72
269	57.7	167.0	2.76
270	58.8	173.4	2.81
271	60.3	178.4	2.82
272	60.3	172.8	2.73
273	58.9	170.5	2.76
274	59.2	169.5	2.73
275	60.0	176.8	2.81
276	60.7	182.2	2.86
277	57.4	169.1	2.81
278	60.2	178.9	2.83
279	59.6	173.5	2.78
280	59.3	170.0	2.73
281	60.0	172.3	2.74
282	60.7	177.7	2.79
283	60.3	169.7	2.68
284	59.8	176.6	2.82
285	59.6	172.3	2.76
286	60.1	168.7	2.68
287	60.4	170.1	2.68
288	59.4	169.3	2.72
289	59.4	170.4	2.73
290	57.9	168.8	2.78
291	60.2	171.5	2.72
292	58.2	169.9	2.78
293	59.4	169.6	2.72
294	59.6	172.0	2.75
295	61.1	171.9	2.68
296	59.0	165.4	2.67
297	59.1	167.5	2.70
298	59.9	170.0	2.71
299	59.7	170.1	2.72
300	58.9	170.1	2.75

Average Density = 2.76 g/cc
Range @ ± 5% = 2.62 g/cc to 2.90 g/cc

XIII CONCLUDING REMARKS

In many respects, chrysotile asbestos is ideal as a matrix material. A mat of the long, very porous hydrophyllic fibers is light and strong when dry. When wetted with electrolyte, it is an excellent gas barrier, and it has a low electrolytic resistance. Unfortunately, being a silicate, chrysotile is reactive with alkaline solutions. The asbestos fibers are destroyed in the formation of soluble silicate and gelatinous magnesium hydroxide. At low temperatures and moderate alkali concentrations, the fiber destruction is slow, but at the conditions desired for ultimate fuel cell operation, the chrysotile will not survive.

Alternative mineral fibers are generally inferior to chrysotile in both physical properties, impurity content, and prospects for survival in alkaline electrolyte. The only synthetic inorganic fiber having adequate inertness in KOH electrolyte is zirconia fiber. However, a mat of these fibers is very poor as a gas barrier and the fibers are extremely fragile. The synthetic inorganic substances having adequate resistance to attack by KOH are PKT (a very short fiber) and the granular powders ceria and zirconia. For the requisite matrix cohesion and strength, these matrices must depend on a suitable organic fiber.

Of the chemically compatible organic fibers, only polypropylene and Teflon are suitable. Of these, Teflon is distinctly superior because of its unusual ability to propagate very thin fibers under mild shear forces. By a simple rolling technique, a mixture of Teflon 6 powder with an infusible powder is converted to a flexible sheet - a matrix of powder incorporated in a network of very fine Teflon fibers. These matrices are spontaneously wettable by aqueous KOH and have a fair gas sealing capability. Chemical degradation tests show that these matrices will survive contact with 60% KOH at 150°C for at least 1000 hours; ceria matrices are apparently completely unchanged by such a treatment.

The most severe degradation tests (60% KOH at 200°C for 1000 hours) show that the Teflon fibers are attacked by alkali. It is possible, also, that the dissolution of Teflon may be faster in the persence of an oxidant. Therefore, the details concerning the upper limit of application of these mats with regard to temperature, time, KOH concentration, etc. are not yet known.

The Teflon-bonded matrices produced in this program should be regarded as preliminary. We are confident that they can be improved by several modifications such as the particle size or of particle size distribution, or the use of inorganic particle blends rather than a single species. Zirconia is now available

as a highly porous granular powder; this material should be evaluated as a way of overcoming the high density disadvantage of the zirconia mats produced in this program.

These Teflon bonded matrices are inferior to asbestos as gas seals. However they might be significantly improved by the addition of magnesia, which forms an aqueous gel filling the matrix pores. Inasmuch as the chrysotile matrices become filled with hydrated magnesia without evident loss of performance, such a magnesia treatment of the Teflon bonded matrices merits attention.

It is anticipated that evaluation of these mats in cell environments will confirm the high-temperature advantages of these separators compared to the fuel cell asbestos mats. Such cell operating experience may also uncover some other limitations of these mats. Such information can then serve as an intelligent guide for future efforts to improve even further this type of electrochemical cell separator.

XIV APPENDIX

At the beginning of Task 1, this author visited the Johns Manville development laboratories to confer with the personnel directly involved in the manufacture of Fuel Cell asbestos paper and millboard. The report of this trip, published in our First Summary Report (Dec. 28, 1966), emphasized those aspects of the technology deemed relevant to fuel cell development.

Dr. J. S. Parkinson of Johns Manville subsequently prepared an amplified description of their process for manufacturing asbestos papers and millboards for fuel cell application. Dr. Parkinson's description of the process is as follows:

PRODUCTION OF ASBESTOS FUEL CELL PAPERS AND MILLBOARDS BY JOHNS-MANVILLE

Asbestos papers and millboards for alkaline, hydrogen oxygen fuel cell diaphragms have been in limited production at the Tilton, New Hampshire plant of Johns-Manville since June 1961. These are made on machines uniquely designed for the production of high quality asbestos electrical papers and millboards. The Tilton plant site was selected to take advantage of an unusually pure source of water for these electrical papers.

The fuel cell products are made with carefully selected Arizona chrysotile asbestos. To data, standardization of the papers and boards has not been possible because customer use requirements are constantly changing. Many of the NASA evaluations were made using materials on hand at the time the sample requests were submitted. The Tilton plant's capabilities to modify these products to meet use requirements are quite extensive. Control of raw materials and product properties can be made as rigid as the economics of the product will justify. There appears to be no reason why a suitable product cannot be produced for fuel cell applications as long as the requirements do not exceed the chemical and physical capabilities of asbestos.

Raw materials used to produce the paper are water and a low iron, low calcium, low chloride, Arizona chrysotile asbestos. Only a small amount of fresh water is used after start up since there is extensive white water recycling. Although the quality of the water does vary slightly with the season of the year, there has been no need to introduce any chemical treatment or suppressant to meet finished product specifications. The fresh water used is cleaned to remove suspended solids so that it contains only trace amounts of solubles.

Stock for fuel cell paper or millboard production is prepared in equipment normally found in mills used to make fine paper. Asbestos and water are added to a pulper where the fiber is ground to reduce the size of the fiber bundles. Batch solids, temperature time, pulper rotor clearance, rotor electrical loading, and Schopper-Riegler freeness are used to control the amount of grinding. Periodic wet screen classification (McNett) of beater samples are also used as an additional check on grinding. No dry processing of fiber is carried out.

Stock from the pulper is dumped into a chest and diluted to a controlled solids content before being pumped to the stock chest. From the stock chest, the slurry goes to a consistency regulator, is diluted with white water from the paper or millboard machine, and fed to a special cleaning system. Stock finally goes to the millboard or paper machine where it is formed into the final product by normal paper making techniques.

Stock flow to the machine, and stock and white water recirculation are quite extensive. Control of stock solids, suspension and flow rates, uniformity of flow to the mold, control of liquid levels in the vat and mold, etc. are needed to form a uniform sheet. As stated before, the Tilton machines are unique in their ability to make uniform products from short fibered asbestos stocks. Sheet smoothness, density, and uniformity are also controlled by variations in machine speed, roll pressures, vacuum, and drying conditions.

Tests made by the Quality Control Laboratory depend on the paper's end use. At present, the laboratory is equipped to make the following tests on a routine basis as required;

1. Basis weight;
2. Thickness;
3. Mullen (burst strength);
4. Tensile and elongation;
5. Elmendorf tear (secondary tear);
6. Curley densometer (air permeability);
7. Williams penetrometer (resin penetration rate);
8. Organic content by ash tests;
9. Magnetic rating (related to iron in fiber);
10. Breakdown voltage;
11. Stock freeness and drainage;
12. McNett classification of stock;
13. Kerosene pick-up (saturant capacity);
14. Clark stiffness.

Normal weight and thickness tolerances on papers and millboards produced at Tilton are plus or minus ten per cent. Where required and justified by product cost, closer tolerances are maintained. Wool felts are used to carry the paper at various points in the process and these leave felt marks on the paper which can be lessening by using smoother felts and pressing or calendering the sheet during production. In no cases does the felt do more than mark the surface. It does not cause perforations in the paper. To date, papers 10, 15, and 20 mils thick, and millboards 30, 34, 40, 50, 60, and 70 mils thick have been produced. At present, efforts are made to keep the iron content of the product below 0.5 per cent, and the CaO below 1.0 per cent, the chloride content below 50 ppm Cl, and the organic content below 0.04 per cent. Chemical analysis and sheet physical property tests requiring more sophisticated equipment are made at the Johns-Manville Research Center in Manville, New Jersey.

Although there are always small variations in the properties of the sheet during a run, these are never significant after standard running conditions are established and production of the product begins.